Synthesis and Characterization of Snail Shell Based Metallic/Bimetallic Oxide Catalysts for Biodiesel Production from Spent Vegetable Oil

Shakirudeen Modupe, Abati

LCU/PG/002380

Being a MSc Thesis Submitted to the Department of Chemical Science, Faculty of Applied Sciences, Lead City University, Ibadan, Oyo State, Nigeria

In Partial Fulfillment of the Requirement for the Award of Master Degree in Industrial Chemistry

2023

Certification

This is to certify that Shakirudeen Modupe, ABATI with matriculation number LCU/PG/002380 carried out this research work titled "Synthesis and Characterization of Snail Shell Based Metallic/Bimetallic Oxide Catalysts for Biodiesel Production from Spent Vegetable Oil" in the Department of Chemical Science, Faculty of Applied Sciences, Lead City University, Ibadan, Oyo State, for the award of Master Degree in Industrial Chemistry and that this has not been previously submitted.

_____ _____

Dr. A. O. Bamisaye **Date**

(Supervisor)

_____ _____

Dr. O. M. Ighodaro **Date**

(Head of the Department)

Dedication

The entire thesis is a tribute to Almighty Allah and my dear parents, Mr. and Mrs. Abati, for their unwavering love and support throughout my life.

Acknowledgement

Without the research facilities offered by the Faculty of Applied Sciences at Lead City University in Ibadan, Covenant University in Ota, Ogun State, Climax Oil Ltd. in Ogun State, Nanomaterials Synthesis and Characterization Lab, Chemistry Dept., King Fahd University of Petroleum and Minerals in Saudi Arabia and Lighthouse Petroleum Engineering Co. Ltd. in Delta State, Nigeria, my research work could not have been completed.

If I was not properly steered, I would be like a boat that was lost in the water. I want to express my sincere gratitude to my supervisor, Dr. A. O. Bamisaye, for introducing me to the fascinating field of material science, for giving me all the necessary instructions for my experiments in great detail, and for his insightful comments on the outcomes. I want to express my gratitude to the Department's head, Professor O. M. Ighodaro, as well as to all of the lecturers in the Chemistry department. This research would not have been accomplished without the generous assistance of Dr. S. A. Ige, Dr. O. K. Oderinde and Dr. A. K. Labintan, may God richly reward them. I must convey my sincere gratitude to the laboratory staff from the Faculty of Applied Sciences.

My parents, Mr. & Mrs. Abati, have my deepest gratitude and admiration for their support and parental guidance, which I value. I want to thank my sister and brother, Fadilah and Abdul Rahman Abati in particular, for their encouragement and support. I owe a great deal of appreciation to my colleagues, especially Ms. A. Adaramaja, Dr. I. Bankole, Mr. Q. Ibrahim and Ms. A. Ogunnaike Adedoyin, for their encouragement and support.

Even though the above-mentioned institutions and persons have assisted in the process of this research work, I alone stand responsible for the errors, if any found in the work.

Abstract

The challenges associated with global climate change due to anthropogenic activities (burning of fossil fuels etc.) necessitated the development of clean alternative fuel from domestic or industrial wastes using agricultural waste as catalyst. The study investigated the synthesis of CaO, PEGylated bimetallic oxides (PEG 15%Al_2O_3/15%Fe_2O_3/CaO) and metal oxide doped snail shell-based nanocatalysts for the production of biodiesel (FAME) from spent vegetable oil through transesterification process. The catalysts were characterized using FTIR, XRD, SEM and EDX. Optimization was carried out using Box-Behnken Design using three operating parameters; temperature, time and catalyst concentration. FTIR confirms formation of new material by absorption bands disappearance and appearance. XRD showed that all the catalysts are crystalline in nature. SEM shows series of shape (flower-like, rod and spherical morphologies) while EDX reveals the elemental components of the catalysts. The calcined CaO nanocatalyst achieved 96.17% biodiesel yield with catalyst concentration of 1 wt%, reaction temperature of 48.18 °C and reaction time of 90 min, 30%Al_2O_3/CaO recorded biodiesel yield of 91.21% at 7 wt%, 40 min and 77.27 °C, 30%Fe_2O_3/CaO achieved 94.13% biodiesel yield at 9.18wt%, 40 min and 99.09 °C, 15%Al_2O_3/15%Fe_2O_3/CaO recorded biodiesel yield of 98.11% at 10 wt%, 40 min and 95.45 °C, while PEGylated 15%Al_2O_3/15%Fe_2O_3/CaO achieved FAME yield of 97.29% at 1 wt%, 40 min and 120 °C. The GC-MS and FTIR analysis confirmed the formation of biodiesel. The finding of this study shows that the synthesized biodiesel by the catalysts in order of activity; 15%Al_2O_3/15%Fe_2O_3/CaO > PEGylated bimetallic oxide> calcined SS > 30%Fe_2O_3/CaO > 30%Al_2O_3/CaO is in accordance with ASTM standards. It can be concluded that doping and PEGylation enhances the catalytic activities of the biomass based catalyst, which are cheap, eco-friendly and economically viable alternatives for the production of biodiesel.

Keywords: Biodiesel, Biomass, Transesterification, Fuel, Catalyst.

Word Count: 290

Table of Contents

List of Tables

List of Tables

List of Figures

List of Figures

List of Figures

List of Figures

List of Acronyms

Abbreviation	Meaning
AN	Artificial Neural Network
ANOVA	Analysis of Variance
AOAC	Association of Official Analytical Chemists
ASTM	American Society for Testing Materials
ATR-FTIR	Attenuated Resonance Fourier Transform Infra red Spectrophotometer
AV	Acid Value
BBD	Box-Behnken design
CN	Cetane Number
CVD	Chemical Vapor Deposition
DG	Diglycerides
EDX	Energy Dispersive X-ray
FAEE	fatty Acid Ethyl Esters
FAME	Fatty Acid Methyl Ester
FFA	Free Fatty Acid
FWHM	Full Width of Half Maximum
GC-MS	Gas Chromatogram-Mass Spectroscopy

GN	Genetic Algorithm
ICDD	International Centre for Diffraction Data
IUPAC	International Union of Pure and Applied Chemistry
JCPDS	Joint Committee on Powder Diffraction Standard
NO	Nitric Oxide
PEG	Polyethylene Glycol
RSM	Response Surface Methodology
SEM	Scanning Electron Microscopy
SVO	Spent Vegetable Oil
SS	Snail Shell
XRD	X-ray Diffraction
Y_1	Concentration of catalyst
Y_2	Transesterification time
Y_3	Reaction temperature

Chapter One

Introduction

1.1 Background to the Study

The upsurge in the world energy demand with the significant increase in global warming challenge necessitated the development of alternative and renewable clean sources of environmentally friendly energy[1]. The release of greenhouse gases, which contributes to global warming, is a serious issue with the usage of fossil fuels. Concerns regarding the supply of fossil fuel energy in the proportions required by industrialized nations have risen in social, political, and commercial contexts[2].

According to studies, conventional fossil fuels will remain the main energy source for the next 20 to 30 years[3]. However, potential replacements for diesel fuel are now being considered, such as biofuels (bioethanol, biodiesel, and biogas). Among many other alternative energy sources, biofuel is regarded as one of the best because it is safe, renewable, biodegradable, non-toxic, and environmentally friendly. There are many renewable sources from which it can be produced[4].

Fatty acid methyl ester (FAME), which makes up the majority of biofuel, has a variety of environmental advantages over fossil fuels, including low sulphur content, low toxicity, low CO_2 and CO emissions, as well as being naturally biodegradable and renewable. Additionally, due to their widespread availability and inexpensive cost, homogeneous catalysts like potassium and sodium hydroxide are now employed to synthesis biodiesel[5]. In order to improve the process conditions and reduce the overall cost of biodiesel, the kinetics of the reaction and the mass transfer of triglycerides in the transesterification reaction have been studied. However, this method is subject to important limitations, which raise the overall cost of producing biodiesel. The use of a heterogeneous catalyst in the transesterification procedure helps alleviate these

problems. The following are the main advantages of using a heterogeneous catalyst: High selectivity and activity with ease of disposal, ecologically safe, non-corrosive, and simple to separate from liquid byproducts. In contrast to the manufacture of other conventional fuels, the production of biodiesel from industrial, domestic, or biomass waste can therefore be considered to be inexpensive[5].

Biodiesel is a liquid fuel made of long-chain fatty acid esters produced from vegetable oils, animal fats, and micro- and macro-algae oil. The use of nanocatalysts is one of the most promising and cutting-edge approaches for carrying out the biodiesel synthesis process on a large scale[6]. The density, viscosity, cetane number, and acid value of these methyl esters all of which affect the type and quantity of biodiesel are mainly under their control[7].

Traditionally, both homogeneous and heterogeneous catalysts have been used to produce biodiesel. Because heterogeneous catalysts have several advantages of recyclability and reusability, basic catalyst is typically used in the transesterification process of producing biodiesel[8]. By reducing reaction time, temperatures, catalyst weight, and the ratio of alcohol to oil, nanocatalysts have become more and more crucial in improving biodiesel yield, quality, and production process. It has been found that nanocatalysts significantly increase reaction speeds without deteriorating themselves. Additionally, it greatly lowers the reaction characteristics' activation energy. Furthermore, a key element in influencing the biodiesel yield is the quantity of nanocatalyst employed[7].

Advances in the design and manufacture of nanocatalysts, such as those based on metal oxides (mixed metal oxides), hydrocalcite-based catalysts, zeolite, and other carbonaceous materials, are beneficial to numerous fields. The main characteristics of these highly developed catalysts are

their high surface area to volume ratio and their tolerance of reaction conditions. The composition of various types of nanocatalysts is greatly influenced by the nature and conditions of catalytic reactions, which vary significantly in different operating settings. With its size being monitored at the atomic level and having a larger surface area than solid acid/base based catalysts, it also acts as a bridge between homogeneous and heterogeneous catalysis[9].

When evaluating the calibre and volume of biodiesel production, physicochemical factors are also crucial. The kind of feedstock used and the pre-treatment steps it undergoes have a significant impact[10]. Pre-treatment is essential for a number of processes, including regulating moisture content, calculating free fatty acids, and creating final biodiesel products. Additionally, it will maintain the stability of biodiesel while enhancing storage and transportation[11]. Utilizing software like MINITAB and Response Surface Methodology RSM, biodiesel output is also impacted by the fine-tuning of reaction parameters including the methanol to oil molar ratio, catalyst quantity, reaction temperature, and reaction time. The output of biodiesel has increased significantly as a result of the adjusted parameters, which are easily scaled up[12].

Furthermore, due to its acceptable viscosity, boiling point, and average cetane number, methanol is used in this study[7]. Egg, oyster, crab, and snail shells, chicken dung, and animal bone have all been used as sources of CaO catalyst for the production of biodiesel from various wasted vegetable oils. One of the most promising heterogeneous catalysts is CaO, which has a high catalytic activity in the transesterification reaction, is simple to make, has a restricted solubility in methanol and biodiesel, and is inexpensive[13]. Utilizing trash as a catalyst source lowers the overall cost of biodiesel synthesis and permits the recycling of natural mineral resources, making the procedure safe for the environment.

With over 100,000 described species, snails—members of the phylum Mollusca—have the second-highest number of species on the planet after arthropods. There are a lot of freshwater snail shells in the world, which are classified as Gastropoda and Bivalvia. Because they offer food for crabs, fish, birds, and people, among others, freshwater snails are edible and important members of ecosystems. Their productivity is correlated with the numerous food chains. As environmental factors and geographic location change, so do the snail population's shell morphometry and body size. This motivated researchers to examine the features of snail shells[14]. The main issue impeding biodiesel commercialization and market competitiveness is the high cost of raw materials used in FAME production. Therefore, this necessitates the development and adoption of cost-effective and readily available feedstocks; alcohols, and catalysts to address this issue. Biodiesel production from waste, such as used spent vegetable oil and snail shell-derived CaO, is a promising alternative for low-cost, environmentally sustainable products[15]. Using spent vegetable oil and snail shell for biodiesel production has a dual benefit in that it is an effective way to reduce production cost and mitigation or eliminates the probable of environmental menace that could results from the disposal of spent vegetable oil and snail shell[16].

Determining the ideal circumstances for maximum product production involves understanding the relationship between the variables and conversion. In this study, the Response Surface Methodology technique was used to fit the quadratic surface and optimize the process variable with the experimental design. It is a statistical and mathematical method for enhancing and evaluating empirical model construction with data[17].

1.2 Statement of the Problem

There is an upsurge in the global energy demand *vis-à-vis* the global climate challenges which has been associated with the use of fossil fuel. It is therefore imperative to consider an alternative low-cost and eco-friendly source of energy in order to mitigate the probable future catastrophe that could arise. The production of FAME using nanocatalysts made of alkaline earth metal oxides, magnetic materials, zeolites, carbon, and other materials is now the subject of a significant among of researchers.

However, the advent of bimetallic nanocatalysts for the production of FAME is a revolutionary strategy that is gathering a lot of momentum in this decade. As a result, series of research has been done in this area. Thus, the adoption of bimetallic nanocatalyst for the production of FAME would expand the potential of nanomaterials and lead to the practical application of the biomass-based catalyst to reduce the manufacturing costs in the production of FAME (an alternative to fossil fuel), mitigation of environmental menace that could result from the improper management of agricultural waste and burning of traditional fossil fuel.

1.3 Justification of the Study

Biodiesel has many advantages over petro-diesel as a replacement, because it is more environmentally friendly, renewable in nature, easily accessible, higher cetane number, higher combustion efficiency, and easily biodegradable. This will mitigate the challenges associated with the use of fossil fuels, which have been labeled as harmful to the environment. More so, biodiesel is safer to handle and transport due to its higher flash point. Its excellent lubricity as a result of its higher viscosity, contributes to lowering of engine wear and extending engine life.

The quality and output of the biodiesel may be significantly impacted by a variety of catalyst properties used in the transesterification process, including surface area, particle size distribution, and surface acidity/basicity. Nanocatalyst possesses the above properties and as such, its adoption for biodiesel production will eliminate the challenges associated with the used of homogeneous acid catalysts[18].

1.4 Aim and Objectives of the Study

The aim of the study is to synthesize and characterize metallic/bimetallic oxide and PEGylated bimetallic oxide nanocatalysts using agricultural waste (snail shell) and domestic waste (spent vegetable oil), FAME can be produced by using the optimizing following operation parameters; reaction time, catalyst concentration and reaction temperature using Response Surface Methodology (RSM).

The main objectives of the study include to:

i. synthesize CaO (calcined snail shell (SS)), 30%Al_2O_3/CaO, 30%Fe_2O_3/CaO, 15%Al_2O_3/15%Fe_2O_3/CaO and PEGylated15%Al_2O_3/15%Fe_2O_3/CaO nanocatalysts from snail shell;
ii. characterize the catalysts using FTIR, XRD, SEM and EDX;
iii. determine the physiochemical properties of the spent vegetable oil;
iv. optimize reaction conditions such as reaction time, catalyst concentration and reaction temperature by using Response Surface Methodology (Box–Behnken Design) for FAME production;
v. investigate the catalytic activity of the synthesized nanocatalysts for FAME production from spent vegetable oil (SVO);

vi. characterize FAME produced from SVO with ATR-FTIR and GC-MS;

vii. compare the produced FAME's physical and chemical characteristics to the specifications for FAME fuel set out by ASTM.

1.5 Scope of the Study

Due to their distinctive physical and chemical characteristics, such as high catalytic activity as a result of their elevated surface area to volume ratio and highly reactive sites, heterogeneous nanocatalyst are currently attracting a lot of attention for their applications. This study focuses on the synthesis and characterization of CaO from snail shell, a cheap, plentiful, ecologically friendly, and reusable catalyst. CaO catalytic activity was enhanced via doping with metals and/or its oxides 30%Al_2O_3, 30%Fe_2O_3, 15%Al_2O_3-15%Fe_2O_3 and PEGylation of the bimetallic oxides. The catalyst would be utilized to produce FAME from SVO. The Response Surface Methodology would be used to optimize the process's methanol/oil ratio, catalyst concentration, time, and temperature (Box-Behnken Design). The physicochemical characteristics of the FAMEs, such as density, kinematic viscosity, acid value, saponification value, flash point, pour point, and cloud point, will be investigated in this study. The percentage yield and quality of the produced FAME will be verified by GC-MS and ATR-FTIR analyses.

In addition, PEGylating the bimetallic oxide nanocatalysts will offer a high surface area to volume ratio, boosting catalytic activity, facilitating straightforward catalyst separation and recovery as well as rapid, selective chemical transformations with outstanding FAME yields.

Furthermore, the price of the feedstock accounts for a sizable portion of the cost of producing biodiesel. The use of SVO as a feedstock and the use of a biomass-based catalyst for

transesterification will serve a dual function by easing the burdens related to the disposal of both home and agricultural waste. Therefore turning waste into wealth[19,20].

Endnotes

1. G. Enguilo, R. Romero, R. Gómez-Espinosa, A. Romero, S. Martínez & R. Natividad. *Biodiesel production from waste cooking oil catalyzed by a bifunctional catalyst.* **ACS omega,** *6*(37), 2021, 24092-24105.

2. A.R. Gupta & V.K. Rathod. *Waste cooking oil and waste chicken eggshells derived solid base catalyst for the biodiesel production: optimization and kinetics.* **Waste Manag.** 2018, 169-178.

3. N. Mansir, S. Teo, N. Mijan, & Y. Taufiq-Yap. *Efficient reaction for biodiesel manufacturing using bi-functional oxide catalyst.* **Catalysis Communications,** *149*, 2021, 106-201.

4. P.R. Pandit & M.H. Fulekar. *Egg shell waste as heterogeneous nanocatalyst for biodiesel production: optimized by response surface methodology.* **J. Environ. Manag.** 198, 2017, 319-329.

5. I. B. Laskar, K. Rajkumari, R. Gupta, S. Chatterjee, B. Paul & S. Rokhum. *Waste snail shell derived heterogeneous catalyst for biodiesel production by the transesterification of soybean oil.* **RSC advances**, *8*(36), 2018, 20131-20142.

6. S. Chozhavendhan, V. P. Singh, B. Fransila, R. P. Kumar & D. G. Karthiga. *A review on influencing parameters of biodiesel production and purification processes.* **Current Res. Green Sust. Chem.** 1–2, 2020, 1–6.

7. S. Bano. *Fabrication and optimization of nanocatalyst for biodiesel production: An overview.* **Frontiers in Energy Research,** 8, 2020, 45-98.

8. J. M. Borah, A. Das, V. Das, N. Bhuyan & D. Deka. *Transesterification of waste cooking oil for biodiesel production catalyzed by Zn substituted waste egg shell derived CaO nanocatalyst.* **Fuel,** 42, 2019, 345–354.

9. H. Pan, H. Li, H. Zhang, A. Wang & S. Yang. *Acidic ionic liquid- functionalized mesoporous melamine-formaldehyde polymer as heterogeneous catalyst for biodiesel production.* **Fuel,** 39, 2018, 886–895.

10. N. Hossain, T. M. Mahlia & R. Saidur. *Biotechnology for biofuels latest development in microalgae - biofuel production with nano-additives.* **Biotechnol. Biofuels** 12, 2019, 12-25.

11. V. Amirthavalli & A. R. Warrier. *Production of biodiesel from waste cooking oil using MgO nanocatalyst.* **AIP Conf. Proc.** 2115, 2019, 30-60.

12. A.A. Otori, A. Mann, M.A.T. Suleiman, & E.C. Egwim. *Synthesis of heterogeneous catalyst from waste snail shells for biodiesel production using Afzelia africana seed oil.* **Nigerian Journal of Chemical Research,** 23(1), 2018, 35-51.

13. M. Khatibi, F. Khorasheh & A. Larimi. *Biodiesel production via transesterification of canola oil in the presence of Na–K doped CaO derived from calcined eggshell.* **Renewable Energy**, *163*, 2021, 1626-1636.

14. K.N. Krishnamurthy, S.N. Sridhara & C.S. Ananda Kumar. *Optimization and kinetic study of biodiesel production from Hydnocarpus Wightiana oil and dairy waste scum using snail shell cao nano catalyst.* ***Renewable Energy*** 146: 2020, 280–296.

15. T. A. Degfie, T. T. Mamo, & Y. S. Mekonnen. *Optimized biodiesel production from waste cooking oil (WCO) using calcium oxide (CaO) nano-catalyst.* **Sci. Rep.** 9, 2019, 18-98.

16. T. T. Mamo. *Microwave-assisted biodiesel production from Microalgae, Scenedesmus species, using goat bone: made nano-catalyst.* **Appl. Biochem. Biotechnol.,** 2020, 12-24.

17. J. Vinoth Arul Raj. *Biodiesel production from Microalgae Nannochloropsis Oculata using heterogeneous poly ethylene glycol encapsulated ZnOMn2^{+} nanocatalyst.* **Bioresource Technology,** 282: 2019, 348–352.

18. I. B. B. Ilic, M. R. Miladinovic, O. S. Stamenkovic & V. B. Veljkovic. *Application of nano CaO-based catalysts in biodiesel synthesis.* **Renew. Sust. Energy Rev.** 72, 2017, 746–760.

19. A. Sulaiman & F. Nur. *Transition metal oxide (NiO, CuO, ZnO)-doped calcium oxide catalysts derived from eggshells for the transesterification of refined waste cooking oil.* **RSC advances** 11.35: 2021, 21781-21795.

20. E. Kurniawan & F. Perdana. *Biodiesel production of waste cooking oil catalyzed by CaO derived from snail (achatina fulica) shell waste.* **Journal of Chemical Process and Material Technology**, *1*(1), 2022, 1-7.

Chapter Two

Literature Review

2.1 Biofuels: A Source of Sustainable Energy

The final products of a biological fixation process, fatty acid methyl ester (FAME), include bio-ethanol, bio-methanol, and biodiesel among others, and are often derived using sustainable biofuels resources such as wood, cellulose, edible and non-edible things[1]. When produced on a big scale, biofuels can eliminate the requirement for fossil fuels to supply the sector's basic energy needs. Hence, reducing pollution and the ozone layer depletion. Three forms of biofuel production are distinguished based on the source of the fuel[2].

Both biomethanol and bioethanol are alcoholic substances created by either the enzymatic or chemical transformation of lignocellulosic feedstock, which goes through a number of pre-treatment steps before being hydrolyzed to create fuel-grade ethanol. Because it has more benefits than biomethanol, such as being non-corrosive, being more affordable, and requiring less energy, bioethanol is utilized on a greater scale[3].

According to reports, due to its lower emissions of dangerous gases, cheap manufacturing cost, and readily accessible raw materials, the United States and Brazil are the two countries that use bioethanol as an alternative to conventional gasoline the most. The emissions of CO_2, NO, CO, and other dangerous gases can be avoided by simply substituting it for gasoline.

Depending on its composition, biodiesel is mostly made up of various types of fatty acids. It is highly regenerative, non-poisonous, and biodegradable, and it releases fewer harmful emissions due to its low sulphur concentration[2]. It is an environmentally friendly fuel that helps to mitigate the negative consequences of fossil fuels. Biodiesel can be combined with fossil fuel to lessen

the level of pollutants and harmful emissions released by traditional fuels because it is largely produced by the transesterification of oils at a specific operating condition.

2.2 Biomass Conversion to FAME: Feedstock and Process

The majority of the feedstock is made up of oils and fats mostly derived from plants and animals. The majority of these feedstock sources are biodegradable and non-toxic for use in the transesterification procedure. The first and most crucial step in the production of biodiesel is choosing a high-quality raw material. The two primary categories of biomass obtained from plants are edible and non-edible oils. The geographical conditions of a particular region have a significant impact on the production and cultivation of feedstock[4].

Since biodiesel is mostly made from edible oils like coconut oil, palm, sunflower, and safflower, among others, biogas and bioethanol production are being researched using plant and animal waste products, lignocellulosic, cellulosic, organic waste materials and starch materials. However, it led to astronomical expenses and, as a result, a decrease in its widespread use. It also highlighted serious worries about food security and rising consumption. The ability to generate non-edible feedstock on a large scale, however, has shown to be a substantial benefit in this regard. Jojoba, rubber seed tree, Jatropa, tobacco and neem seed are among the main ingredients[5].

In addition to plants, animal fats and spent cooking oil can make promising and affordable biodiesel feedstock. These waste cooking oils with free fatty acids are finally reduced by using pre-treatment procedures and alkali-based transesterification processes since excessive fatty acid concentration causes soap production. On the other hand, different reaction parameters significantly affect the pre-treatment procedure. Free fatty acids and triglycerides are largely

esterified and transesterified to produce biodiesel, with the yield matching to the amount of free fatty acids used[6].

Algae, fungi, and microorganisms are among the bacteria that can be utilized to make biodiesel. They are primarily generated from stagnant ponds and contain both photosynthetic and non-photosynthetic microorganisms. A review of this broad feedstock will eventually increase biodiesel production on a large scale and decrease the demand for earlier materials, as shown in Table 2.1, which has a variety of feedstock types[7].

2.2.1 Spent Vegetable Oil (SVO)

The manufacture of FAME from SVO can lessen the dependency on fossil fuels and environment pollution while also replacing some fossil fuels. Because SVO is less expensive than fresh vegetable oils, making biodiesel is more affordable. The majority of the commercial restaurants and food processing businesses in the United Kingdom alone contributed about 65 000 tonnes of SVO to the collection[8].

SVO disposal is a major issue because it would otherwise contaminate the ecology and the water supply. Even though some SVO oil was used to make soap, the great majority of SVO was dumped into landfills and rivers. This study will therefore help in making biodiesel from SVO reduces both the cost of biodiesel and the environmental problems involved with disposing of SVO[8].

Table 2.1: Several feedstocks that are utilized to produce biodiesel

Edible feedstock	Non-edible feedstock	Algae based feedstock
Coconut	Jatropa	Microalgae oil
Palm oil	Jojoba	Brown algae
Sunflower	Tallow	Red algae
Canola	Waste cooking oil	Microbes
Wheat	Rubber seed	Cyanobacteria
Soybean	Animal fats	Diatoms
Rice bran	Rapeseed	
Barley	Salmon oil	
Corn	Karanja oil	

Source[8]

Table 2.2 reports the results of converting SVO into biodiesel in the presence of various catalysts. With values exceeding 96%, ZS/Si, K_3PO_4, H_2SO_4, and CaO produced the highest yields of biodiesel. With a yield of 99%, homogeneous H_2SO_4 catalyst had the highest biodiesel production. This was accomplished, nonetheless, at an unprofitable 245:1 methanol to oil ratio and a catalyst concentration of 41.8%. The ZS/Si heterogeneous catalyst, on the other hand, was more economically advantageous, generating biodiesel with a yield of 98% at an amount of catalyst of 3% and a methanol/oil ratio of 18:1 instead. Therefore, it was believed that ZS/Si was the best catalyst for converting SVO to biodiesel.

2.3 Techniques for Biodiesel Production

Biodiesel is now produced through direct mixing, pyrolysis, micro-emulsion, and transesterification. For the production of biodiesel on a wide scale, the direct blending, pyrolysis, and micro-emulsification technologies are insufficient[14]. Animal fats, vegetable oils, and other sources of biodiesel cannot be used directly due to the high viscosity and reactivity of unsaturated hydrocarbons. Different methods are being used to lessen the kinematic viscosity of such oils in order to attain the quality required for diesel engines. The most often used technique has been transesterification[15]. **Figure 2.1** schematically depicts the five biodiesel production processes and their attributes.

Table 2.2: Production of FAME from SVO in the presence of various catalysts

Catalyst	Temperature (°C)	Methanol/oil ratio	Catalyst loading (wt. %)	Time (h)	FAME conversion yield (%)	Ref.
CaO	50	8:1	1	1	96	[9]
4Mn-6Zr/CaO	80	15:1	3	3	92.1	[10]
calcined scallop shell	65	6:1	5	2	86	[8]
Waste egg shell	65	9:1	5	2.75	87.8	[11]
Waste chicken bones	65	15:1	5	4	89.33	[12]
KBr impregnated CaO	-	12:1	4	2	78.9	[13]
TiO_2-MgO	160	50:1	10	6	92.3	[8]
ZS/Si	200	6:1	3	10	81	[7]

Source: Field survey, 2022.

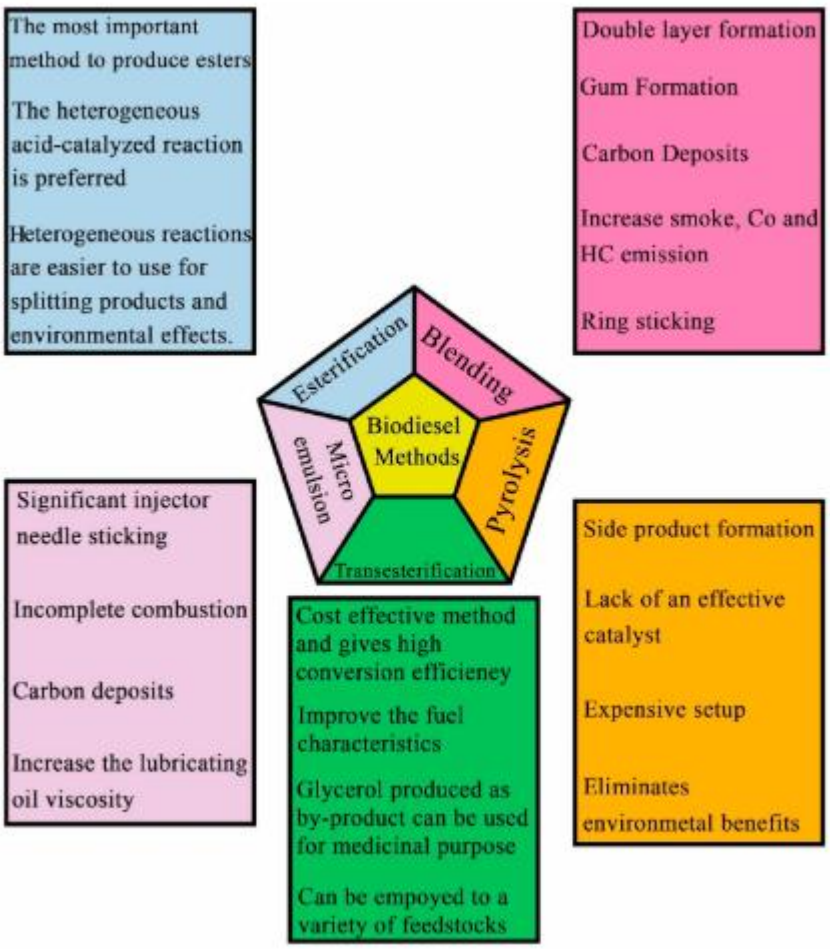

Figure 2.1: The various techniques utilized to produce biodiesel.

Source[8]

2.3.1 Direct Use of Biodiesel and Blending

You can use oil right away by preheating it to 55 °C. The viscosity of the oil is increased by preheating it, making it more comparable to oil made from petroleum. Animal fats, however, cannot be used directly as fuel for a diesel engine because of their high viscosity[21]. Vegetable oils can also be diluted with diesel, a solvent, or ethanol to make them more appropriate for

direct and indirect use in diesel engines[9]. Direct usage and blending methods for producing biodiesel have been demonstrated. In order to accomplish this, they blended conventional diesel (80%) with biodiesel made from animal fat (15%) and jet fuel (5%), creating a hybrid fuel with a 30% lower moisture content[4].

2.3.2 Microemulsion

A microemulsion, according to the IUPAC, is a system made up of water, oil, and surfactant particles that range in size from 0.001 to 0.15 mm that is thermodynamically and isotropically stable. The microemulsion method produces biodiesel that is made up of oils, surfactants, alcohols, and diesel fuel and has an adequate concentration of CN. Two of the alcohols used in this process as additives to reduce viscosity and improve the separation of oils and alkyl nitrate are methanol and ethanol. Additionally, these are used to enhance the CN[23]. This method is not only simple, but it also produces relatively little pollution. Despite the low purity of the final biodiesel, this method requires expensive equipment and high temperatures to be used[16]. The impact of microemulsion-produced biodiesel on the output of a diesel engine has been reported and studied. They offer a microemulsion with nonylphenolethoxylate as a surfactant, which was then tested in a diesel engine. Additionally, the findings suggested that the viscosity and density were higher than in petrodiesel. In addition, compared to diesel, CO and NOx were higher, and a tiny emission was lower[7].

2.3.3 Thermal Cracking (Pyrolysis)

The pyrolysis process uses heat to force chemical transformations while air or nitrogen is present. Alkanes, alkenes, carboxylic acids, alkadienes, and aromatic compounds were produced as a result of the thermal degradation of oils. Upon heat degradation, various vegetable oils experience various structural changes[17]. As an example, pyrolysis of soybean oil produces a

substance that is primarily made of hydrogen (12%), carbon (79%) and other components. The product has a low viscosity and a high cetane number concentration as compared to oil of vegetable origin. The steps used to produce biodiesel using this approach are identical to those used to produce fuel derived from petroleum, where the thermal treatment process involves oxygen exhaust that negates the environmental benefits of oils containing oxygen[18]. Additionally, this technique has drawbacks such as high viscosity, poor volatility, and instability[19].

2.3.4 Transesterification Process

The reaction between alcohol and oil to produce glycerol and methyl ester is referred to as the transesterification process. The oil viscosity falls as a result of this reaction while preserving its heating value. The CN increases as the molecular chain shrinks to just one-third as a result of this reaction[20]. Both ethanol and methanol are frequently used to synthesize biodiesel, but methanol is even more affordable, has a higher reactivity, and produces fatty acid methyl esters (FAMEs) that are more volatile than fatty-acid ethyl esters (FAEE). Contrarily, ethanol is often produced from renewable resources and is less dangerous. It is evident that there are little distinctions between the FAME and FAEE as fuels. For instance, while FAEE has slightly lower cloud points and pour points than FAME, it has somewhat higher viscosity. The dosage of the catalyst, reaction and the ratio of the reactants conditions all directly affect how effectively the reaction precedes because the process is reversible. Three moles of methanol and one mole of triglycerides are stoichiometrically required to make one mole of biodiesel. The transesterification procedure is reversible, so if you add too much methanol, you tip the scales in favor of the products and turn triglycerides into methyl esters. The cost of producing biodiesel will rise if there is too much methanol present. One way to improve the economics of the transesterification process is by the recovery of methanol[21]. When the methanol percentage is

smaller, the process takes longer to complete and produces less biodiesel. In contrast hand, glycerol's increased solubility in excess methanol makes separation difficult. However, the equilibrium shifts to the reaction's right side as a result of the glycerin that is still present in the solution, reducing the quantity of biodiesel that may be produced. Therefore, a proper amount of methanol should be used in the transesterification step[22].

Usually, catalysts are utilized to speed up the reaction and improve its effectiveness. Enzymatic, alkaline, or acidic catalysts are possible. Alkaline catalysts function substantially faster than acidic catalysts, making them a more practical option for industrial use[23]. Since the reaction is reversible, its efficiency is directly influenced by the reaction conditions, the dosage of the catalyst, and the ratio of the reactants. The chemical process that turns triglycerides into esters, which yields glycerin as a byproduct and biodiesel as the main product, is seen in Figure 2.2.

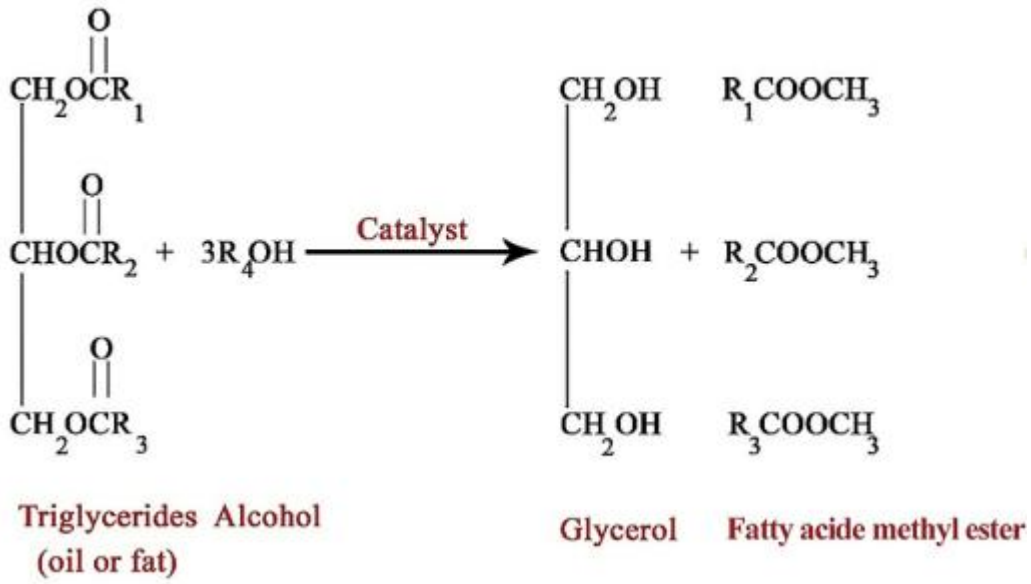

Figure 2.2: Chemical process involved in conversion of triglycerides into esters.

Source[23]

There are three sequential steps in this response:

- Glycerides formation
- Mono-glycerides formation
- Final ester (FAME or FAEE) formation as presented in **Figure 2.3**

The term "group R" refers to fatty acids with a carbon chain between 16 and 22 carbons, and either single or double bonds can be found in the chain.

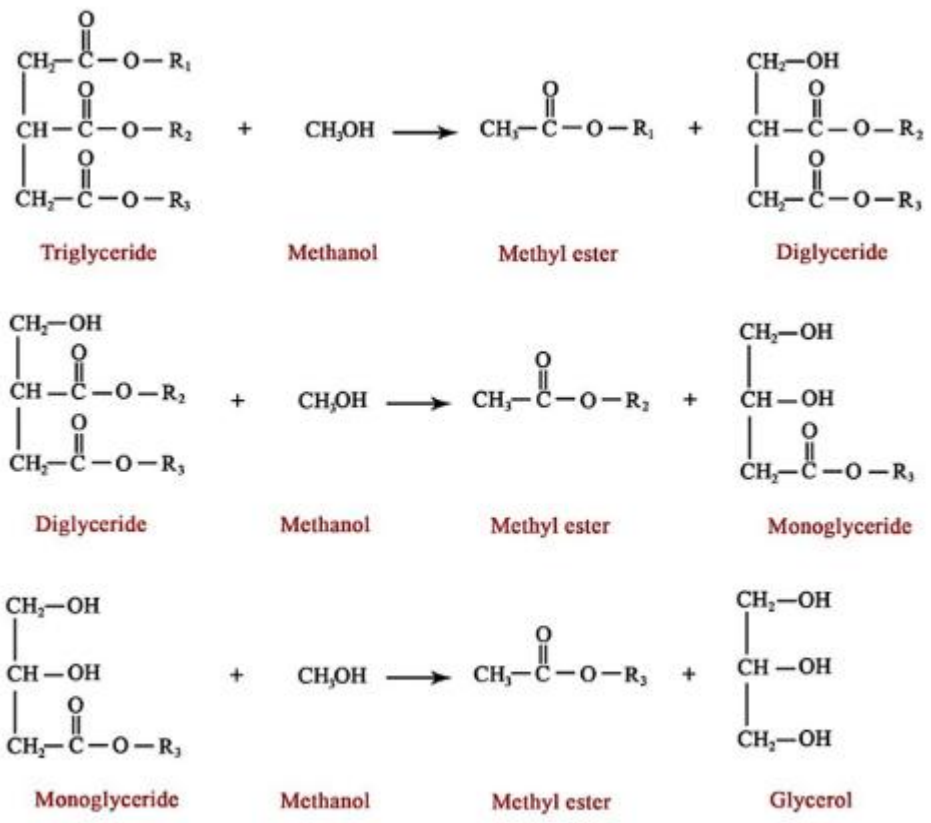

Figure 2.3: Reaction involved in formation of diglyceride, monoglyceride and final ester. Source[23]

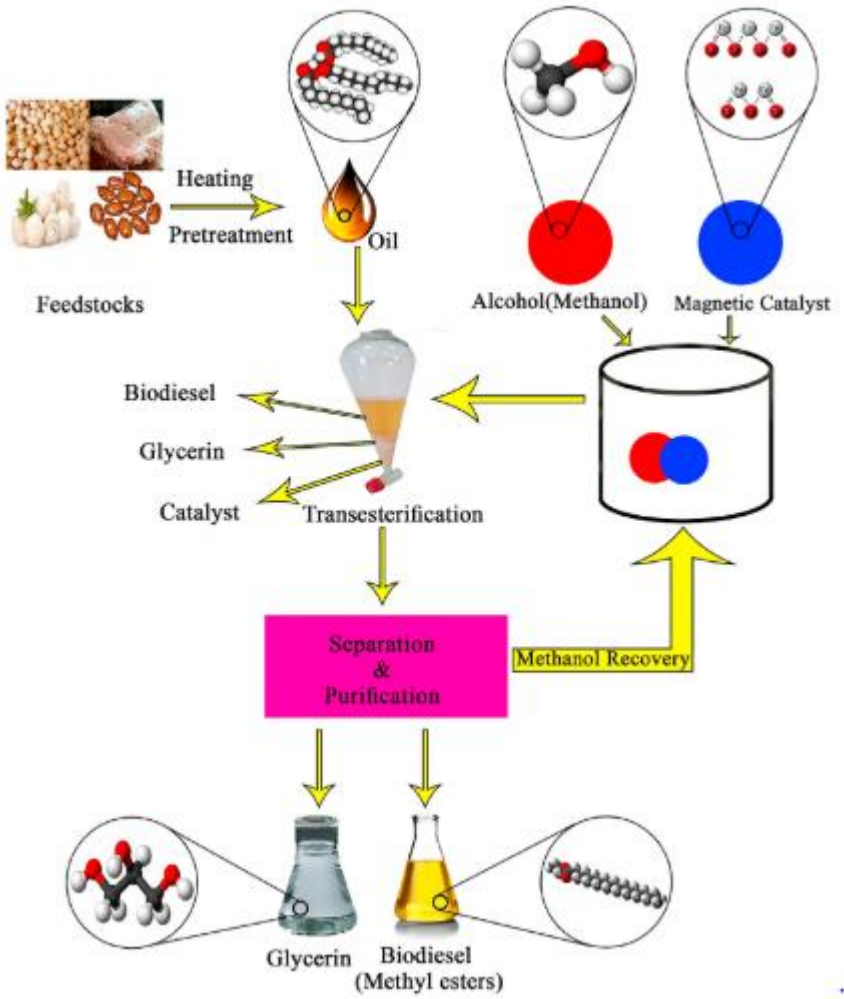

Figure 2.4: Diagram showing the transesterification process for producing biodiesel.

Source[24]

Because of its low temperature and pressure necessities, quick reaction time, high conversion yield, and straightforward and direct conversion process, the transesterification method, out of the four methods previously mentioned, offers a much more dependable and effective approach for producing biodiesel on both a laboratory and an industrial scale[26]. A generic schematic of the transesterification process used to produce biodiesel is shown in Figure 2.4. Since an ester is

produced at each conversion step, one triglyceride molecule generates three ester molecules. The transesterification reaction effectively converts a triglyceride of vegetable oil into FAME, also referred to as biodiesel, as depicted in Figure 2.5. However, the esterification reaction, a reaction between alcohols and carboxylic acids to form ester is required to convert all FFA in vegetable oil into FAME, as shown in Figure 2.6.

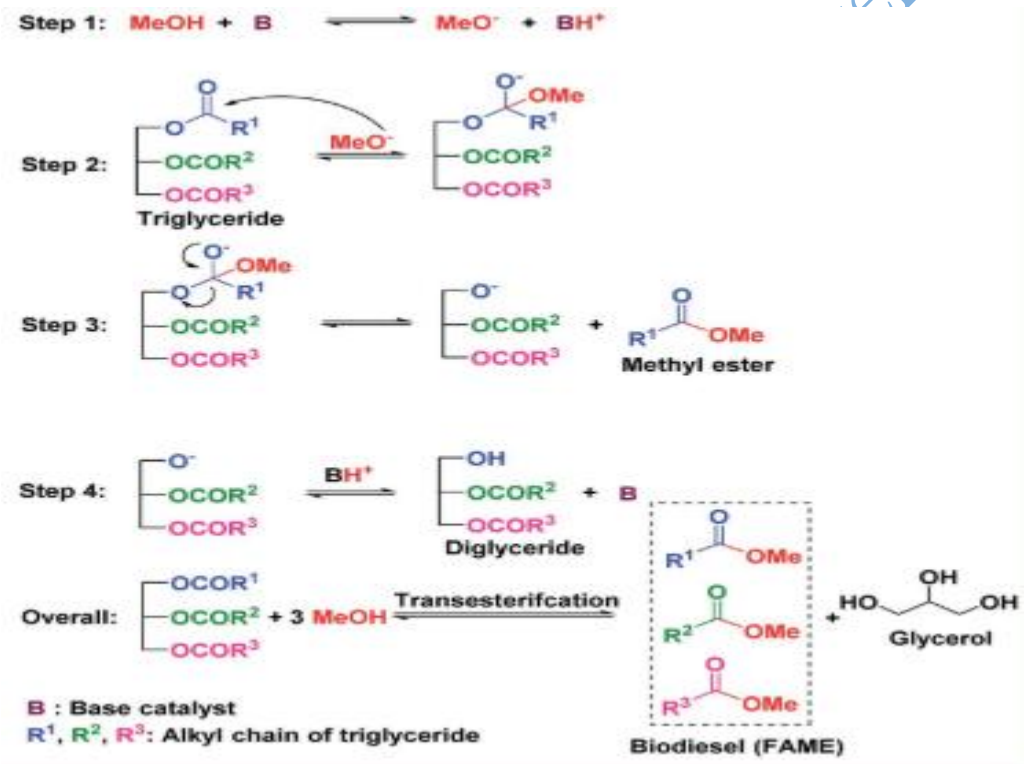

Figure 2.5: Mechanism for converting vegetable oil TGs into biodiesel by base catalysis. Source[24]

Figure 2.6: Using an acid catalyst, vegetable oil with a high FFA content is transformed into biodiesel.
Source[24]

The transesterification and esterification reactions are normally carried out using the two distinct ways. Vegetable oil with a high FFA content is typically first converted into esters (FAME) using an esterification process with an acid catalyst, and then triglycerides are converted into FAME using a transesterification reaction with a basic catalyst. It is highly desirable to transesterify processes (or concurrent transesterification and esterification) in one pot in order to convert both the triglycerides and FFA of vegetable oil (with high FFAs) to FAME in order to decrease the time and cost of manufacturing biodiesel. The various processes for manufacturing biodiesel are shown in Figure 2.7.

2.4 Catalysis in Transesterification

Separating catalysis into homogeneous and heterogeneous categories is another step. Homogeneous catalysis employs processes that are catalyzed by acids and bases. A base-catalyzed reaction proceeds far more quickly than an acid-catalyzed reaction, producing a larger yield[25].

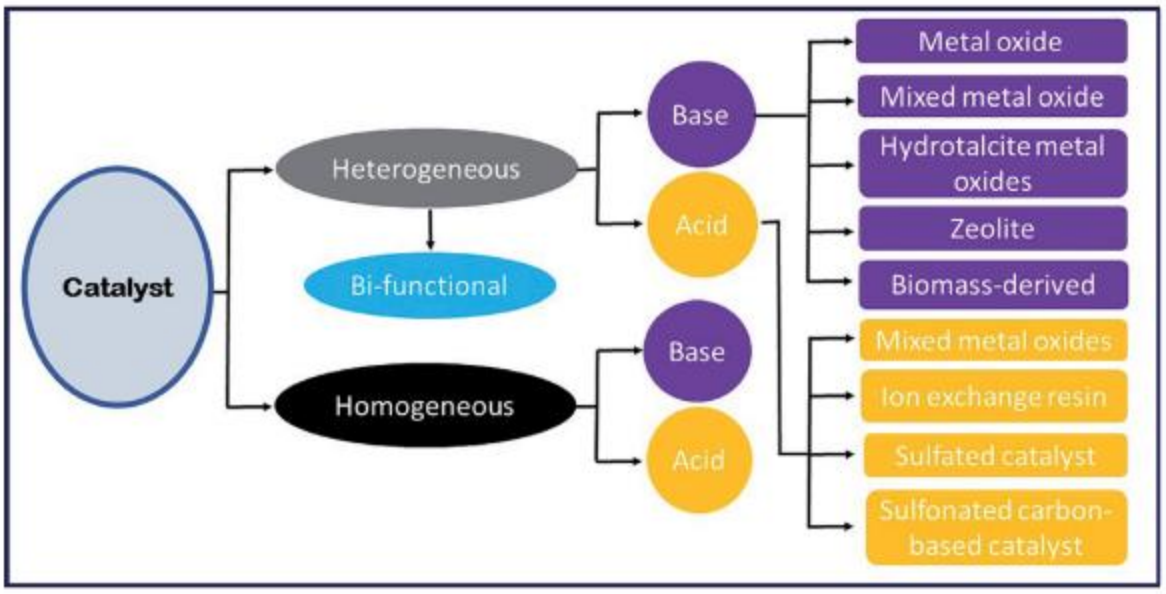

Figure 2.7: Catalyst type for the production of biodiesel.

Source[26]

The most often used catalysts are NaOH, KOH, $NaOCH_3$, and $KOCH_3$, all of which function at low temperatures and generate high yields. Additionally, it requires premium feedstock oil to lessen the saponification reaction, which raises the cost of the procedure. On the other hand, acid-catalyzed reactions demand a greater temperature and a longer reaction period. It has also been established that homogeneous catalysis achieves maximum triglyceride conversion due to high catalytic activity and reaction rate[26]. Sustainable chemistry depends on catalysis, which can increase process efficiency, lower net greenhouse gas emissions, and reduce the amount of waste that results from those emissions Figure 2.8. Green chemistry techniques also require greater use of sustainability principles, particularly in the synthesis of contemporary catalysts and in analysis procedures.

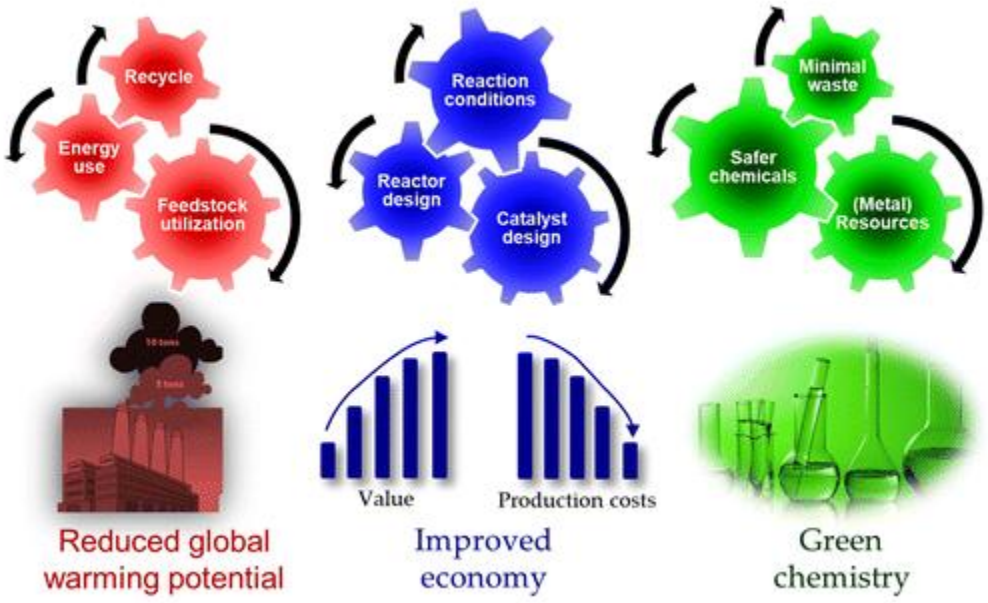

Figure 2.8: The key roles of catalysis in sustainable chemistry.

Source[26]

However, it reveals major difficulties with catalyst and product separation and purification. The more catalysts are used, the more wastewater is generated, and equipment damage occurs[27]. Heterogeneous catalysis is being studied extensively in the transesterification reaction to overcome the significant drawbacks of homogeneous catalysis. It is far more efficient and, depending on the natural catalyst, can be easily recycled. According to the type of catalyst used, heterogeneous catalysis is further divided into procedures for transesterification that rely on alkali, acid, or enzymes[28]. It is mostly influenced by the hydrocalcites, metal, acid, metal oxides, bases, and zeolites supported by the specific nanocatalyst.

2.4.1 Homogeneous Catalyst

The two categories of homogeneous catalysts utilized in the transesterification reaction are acid catalysts (hydrochloric acids and sulphuric, sulphonic and hydrofluoric) base catalysts (KOH and NaOH).

2.4.1.1 Homogeneous Base Catalyst

Homogeneous base catalysts are most frequently researched in the transesterification of vegetable oil to FAME because they are affordable and easily accessible. KOH, NaOH, and $NaOCH_3$ are a few homogeneous base catalysts that have been employed to date in the synthesis of FAME. At room temperature and pressure, the combination of NaOH and KOH as catalysts produced biodiesel with exceptional catalytic activity, a quick reaction time, and a large amount of biodiesel as a byproduct. The generation of water as a byproduct, for example, restricts the amount of biodiesel that can be produced using this process, which has some disadvantages. Since they don't create water, sodium methoxide and potassium methoxide produce better biodiesel than KOH and NaOH[20].

On the other hand, acid-catalyzed reactions demand a greater temperature and a longer reaction period. Homogeneous catalysis was also demonstrated to be the most efficient technique for converting triglycerides due to strong catalytic activity and a quick reaction rate. It does, however, highlight significant challenges in catalyst and product separation and purification. Catalyst usage increases with wastewater production and equipment damage[39].

Using the KOH catalyst, methanol was transesterified with green seed canola oil from heat-damaged seeds, managed waste fryer oil, and unmanaged waste fryer oil to create FAME. A biodiesel yield of 51–87% was discovered in the ideal reaction conditions[17]. In another study, at

the perfect reaction conditions, KOH was utilized to transform a mixture of crude palm oil and rubber oil into biodiesel with a 98% yield. Vegetable oil was first transesterified with a base catalyst, then esterified with an acid catalyst to produce a vegetable oil with a low FFA level[20].

Similar to this, 96% of soybean oil was converted into FAME using KOH as a catalyst. Additionally, roselle oil, spent olive oil, frying oil, palm kernel, rapeseed oil, and duck tallow were successfully transesterified to FAME using the KOH catalyst. Pongamiapinnata was transesterified to FAME with a 92% conversion rate using the base catalyst KOH. Interestingly, the conversion rate was increased to 95% when tetrahydrofuran (THF) was used as a co-solvent[18].

Another study found that NaOH has an unusually high activity for biodiesel generation from SVO containing high FFA, with an 89.8% conversion rate under optimal reaction conditions. A pre-esterification method using sulphuric acid lowered the high free fatty acid content of SVO[19].

2.4.1.2 Homogeneous Acid Catalyst

Base catalysts are typically preferred over acid catalysts because they are more reactive and less expensive. However, base catalysts may interact with the FFA in the feedstock during transesterification, leading to the saponification of soap, which could deplete the catalyst and impair its reactivity. Meanwhile, an acidic catalyst performs better when transesterifying or esterifying vegetable oils or fats with a high FFA content (2 wt%) since it is neutral to FFA. Most often, acid catalysts are employed to esterify WCO and animal fats in order to lower their FFA content before transesterifying them with base catalysts.

A number of acids, including hydrochloric acid, sulfonated acid, sulfuric acid, and phosphoric acid, were utilized for the transesterification of vegetable oils. The production of FAME using an

acid catalyst, however, has a number of drawbacks, including a high alcohol-to-oil molar ratio and a reaction rate that is 4,000 times slower than that of base-catalyzed esterification.

It is hence caustic and has negative environmental effects. Due to these drawbacks, acid-catalyzed biodiesel synthesis is not widely used and is only occasionally researched. Table 2.3 lists some of the findings from studies on acid-catalyzed biodiesel production that have been published.

A 90% yield for biodiesel synthesis from WCO was observed[46]. The synthesis of soybean oil to biodiesel using trifluoroacetic acid as a catalyst was investigated. The outcomes demonstrated that 98.4% of the biodiesel was synthesized under optimal reaction circumstances[53].

The catalyst achieved a high FAME yield of 98.4% under optimal reaction conditions[53]. Acid-catalyzed esterification/transesterification reactions often ask for extreme reaction conditions, such as a high M/O molar ratio, catalyst concentration, temperature, and long reaction time, in contrast to base-catalyzed transesterification reactions.

2.4.2 Heterogeneous Catalysts

Even though the homogeneous catalyst possesses its own advantages, such as high catalytic activity and low cost, there are a number of disadvantages to its usage in the synthesis of biodiesel. Examples of these faults include the poor quality of glycerol that led to the catalyst's inability to be regenerated and the time-consuming processes required for biodiesel purification. The entire procedure is therefore labor-intensive and ineffective. Because it can be tailored to specific requirements and readily recovered and reused for several cycles of catalytic reaction, the heterogeneous catalyst has attracted a lot of interest for the manufacture of biodiesel in recent years. This could result in lower labour and biodiesel costs[53].

Because heterogeneous catalysts are typically solid, as opposed to homogeneous catalysts, the reaction mixture and the catalyst are in different phases. In heterogeneous catalyzed processes, the catalyst surface serves as the main location for reaction. The use of a solid catalyst in transesterification has the following benefits that make the procedure green:

- It is possible to reuse the catalyst.
- The amount of wastewater produced throughout the procedure is quite low..
- It is significantly simpler to separate glycerol from the final mixture of glycerol, biodiesel, and catalyst.
- Glycerol with a high purity is achieved[52,53].

In comparison to homogeneous catalysts, heterogeneous catalysts provide a number of benefits, such as simplicity in separation, recyclability, and reuse. Additionally, solid catalysts require less energy, are less toxic, have less corrosion, and are more environmentally friendly. Solid catalysts hence increase the productivity and cost-effectiveness of the biodiesel production process. The two categories of heterogeneous or solid catalysts are basic and acidic catalysts. Recently, a variety of heterogeneous catalysts have been identified by researchers that can facilitate both esterification and transesterification events in the same reaction vessel (one-pot)[52].

Table 2.3: Various acidic homogeneous catalysts used in the synthesis of biodiesel

Catalyst	Feedstock	Conditions[μ]	Yield (%)	Ref.
H_2SO_4	Chicken/mutton tallow	30:1, 1.25/2.5, 50/60, 1440	99.01±0.71/93.21±5.07	19
H_2SO_4	WCO	20:1, 4, 95. 600	90	46
H_2SO_4	WCO	3.6:1, 0.1, 65, 40	79.3	19
H_2SO_4	Soybean oil	6:1, 3, 60, 2880	98	18
H_2SO_4	Zanthoxylum	24:1, 2, 60, 80	98	20
H_2SO_4	Tobacco seed oil	18:1, 1, 60, 25	91	17
$C_2HF_3O_2$	Soybean oil	20:1, 2 M, 120, 300	98.4	53

[μ]Methanol to oil molar ratio, catalyst loading (wt %), temperature (ºC), reaction time (min

Source: Field survey, 2022.

2.4.2.1 Heterogeneous Base Catalysts

Because they may be able to overcome the drawbacks of homogeneous basic catalysts and demonstrate exceptional catalytic activity under benign reaction circumstances, basic heterogeneous catalysts have drawn the most attention in recent years[21]. On the other hand, these catalysts are only suitable for biodiesel feedstocks with low FFA content; otherwise, they will react with the FFA and cause the saponification reaction, which results in the formation of soap. As a result, the production of biodiesel is reduced by the time required to separate it from glycerol. This section discusses a number of solid base catalysts that have been mentioned in the literature, including hydrotalcites, alkaline metal oxides, zeolites transition metal oxides, biomass-based catalysts and mixed metal oxides[22].

2.4.2.1.1 Alkaline Earth Metal Oxides

Alkaline earth metal oxides are one of the most extensively studied catalysts for biodiesel synthesis due to their insolubility in methanol and low toxicity. The most basic alkaline earth metal oxides are BaO, SrO, CaO and MgO. On the transesterification reaction, MgO has a very small impact.

CaO is the alkaline earth metal oxide that is most frequently employed in the production of FAME because it is strongly basic, insoluble in alcohol, non-toxic, affordable, and easily accessible. However, it is quite sensitive to the presence of FFA and loses its activity due to saponification, which also creates undesirable byproducts. Despite its high activity, SrO is rarely investigated in transesterification processes because it is very sensitive to air moisture and combines with water and CO_2 to produce $Sr(OH)_2$ and $SrCO_3$. Table 2.4 displays the activity of various alkaline metal oxides in the production of biodiesel.

Table 2.4: Under varying reaction conditions, several alkaline earth metal oxides catalyzed FAME synthesis

Catalyst	Feedstock	Conditions[µ]	Yield (%)	Ref.
CaO	Soybean oil	12:1, 8, 65, 180	95	[5]
CaO	Sunflower oil	13.:1, 3, 60, 120	94	[7]
CaO	Rapeseed oil	3.8:1. 0.7, 60, 160	90	[20]
CaO	Soybean	6:1, 3, 70, 30	95	[4]
BaO	Palm oil	9:1, 3, 65, 60	95.2	[19]

µMethanol to oil molar ratio, catalyst loading (wt %), temperature (ºC), reaction time (min).

Source: Field survey, 2022.

Under the ideal reaction circumstances, the CaO catalyst was used to study the transesterification of soybean oil, and the results showed a high biodiesel production of 95%. CaO that was calcined at 700 °C showed extremely high activity towards the generation of biodiesel from sunflower oil, yielding 94% of the target amount[20]. Additionally, the transesterification of rapeseed oil was examined. CaO was first processed with methanol to create Ca(OCH3), which served as an initiator for the transesterification reaction. Using the improved reaction conditions, a high biodiesel yield of 90% was noted[21]. Investigation into the transesterification of soybean oil by SrO demonstrated that the catalyst has outstanding activity and a high yield of 95% at 70 oC for 30 minutes. The catalyst is quite stable and can be used a further ten times[22].

2.4.2.1.2 Transition Metal Oxides

CaO is the most often used alkaline earth metal oxide in FAME synthesis because it is very basic, insoluble in widely accessible, affordable, alcohol and non-toxic. However, it is extremely sensitive to the presence of FFAs and, as a result of saponification, loses its effectiveness while producing unwanted metabolites[31,32]. Despite its high activity, SrO is rarely studied in transesterification processes due to its sensitivity to air moisture and the formation of $SrCO_3$ and $Sr(OH)_2$ when it reacts with CO_2 and water. Table 2.5 lists the many alkaline metal oxides that are active during the manufacture of biodiesel[31].

2.5 CaO as Nanocatalysts

Because they encourage extended catalytic lifetimes, high activity levels, and mild reaction conditions, solid base catalysts like CaO are chosen[4]. CaN and CaOH are typically the main basic materials utilized to make CaO. Bone, mollusk shells, and chicken eggshells are just a few examples of the calcium-rich waste products found in nature that may be used as raw materials to

make catalysts, solving the problem of waste disposal while also producing catalysts that are incredibly economical. Using a solid base CaO nanocatalyst, 93% of jatropha oil was converted to biodiesel[30]. A solid-base catalyst called CaO-KF is produced by impregnating CaO with potassium fluoride, a catalyst with high catalytic activity. During transesterification, the catalyst CaO showed great catalytic activity, but it leached off the Ca^{2+} ions that are important for the product's quality. The calcium diglyceride is hydrolyzed by moisture, which releases the Ca^{2+} ions (produced from the by-product glycerol of the unstable of CaO). Direct dissociation of CaO and the production of soluble Ca^{2+} take place during the reaction with methanol. Saponification, which results from the reaction between the leached calcium ions and the FFA in the oil, destroys the catalyst's advantageous properties[29]. The leaching of Ca active species can be stopped by using the appropriate supporting materials. The requirement for heat activation to eliminate the absorbed CO_2 and moisture is a serious drawback of employing CaO. The procedure must then be carried out in a vacuum or a nitrogen environment to prevent carbonization[29].

2.5.1 Nanocatalysts Based on Metal Oxides

The most economical metal oxides for heterogeneous catalysis are those with an Al_2O_3/Fe_2O_3-support. Metal oxides are widely accessible, affordable, and simple to produce. They are also physically, thermally, and chemically stable and have a large surface area. Main block oxides can also be created, in addition to d-block metal oxides[18]. The principal block oxides are Al_2O_3, MgO and SiO_2, whereas the d-block oxides that have been developed include TiO_2, Mn_2O_3, ZrO_2 and ZnO.

Table 2.5: Under various reaction conditions, there are varied transition metals oxide-catalyzed biodiesel synthesis yields.

Catalyst	Feedstocks	Conditions$^{\sigma}$	Yield	Ref.
α-Fe_2O_3/AlOOH	cottonseed waste oil	6:1, 3, 60, 3	95	[29]
MgO/Fe_2O_3−SiO_2	camelina oil	12: 1, 70, 4.1	99	[30]
α-Fe_2O_3/AlOOH(γ-Al_2O_3)	cottonseed waste oil	6:1, 3, 60, 3	94.3	[31]
CaO/γ-Al_2O_3	edible refined sunflower oil	9:1, 0.55, 60, 5.22	97.8	[32]
Fe_3O_4/CaO	palm oil off-grade	10:1, 1, 70, 2	90	[33]

µMethanol to oil molar ratio, catalyst loading (wt %), temperature (ºC), reaction time (min).

Source: Field survey, 2022.

2.5.2 Al_2O_3 and Fe_2O_3 as Catalyst Support

One of the most important transition alumina known is -alumina (-Al_2O_3), which is directly used in the automobile and petroleum industries as a catalyst and catalytic support[32]. The usefulness of this oxide can be attributed to a favorable interaction between its textural characteristics, such as surface area, pore volume, and pore size distribution, and its acid/base properties, which are mainly connected to local microstructure, phase composition, and surface chemical composition. However, -Al_2O_3's chemical and hydrothermal stability is still an important consideration for catalytic applications[32].

These catalysts were made using the impregnation method. Studies have shown that the amount of catalyst precursor loading on the support and the calcination temperature had an impact on the fundamental properties of the catalyst and, subsequently, the catalytic activity. Under optimal circumstances, the catalyst was created at a temperature of 718 °C with a calcium oxide precursor on alumina of 100.54%. The structural characteristics of -Al_2O_3 are extensively studied using methods like NMR spectroscopy, transmission electron microscopy, and BET adsorption, IR spectroscopy and X-ray diffraction (XRD).

For the methanol-oil transesterification, because the basic sites on the surface of the heterogeneous catalyst serve as the active centre of the reaction, CaO concentration is essential. In light of this, a catalyst's surface area is crucial. It was discovered that as the amount of CaO catalyst loaded onto Al_2O_3 declined (the loading levels were 50% and 80%), so did the yield of the biodiesel that was produced. Because the sol-gel process can be used to produce small CaO particles, the supported CaO catalyst in this study has a low concentration. For the 40% CaO/g-Al_2O_3 catalyst synthesis used in the biodiesel manufacturing process, the sol-gel technique was employed.

The most thermodynamically stable phase of iron oxide is α-Fe_2O_3. Due to its low processing costs and strong corrosion resistance, this has undergone substantial research for application as catalysts, pigments, and gas sensors.

One of the most crucial ingredients in the creation of magnetic nanocatalysts is Fe_2O_3. Fe_2O_3nanocatalysts provide a number of benefits, including a quick manufacturing process, small particle size, good performance, and a powerful magnetic characteristic[34]. Because heterogeneous magnetic nanocatalysts and catalysts have better qualities for producing biodiesel than acidic and alkaline catalysts, their employment has been greatly enhanced. A variety of magnetic particle-based catalysts are shown in **Figure 2.9**[35].

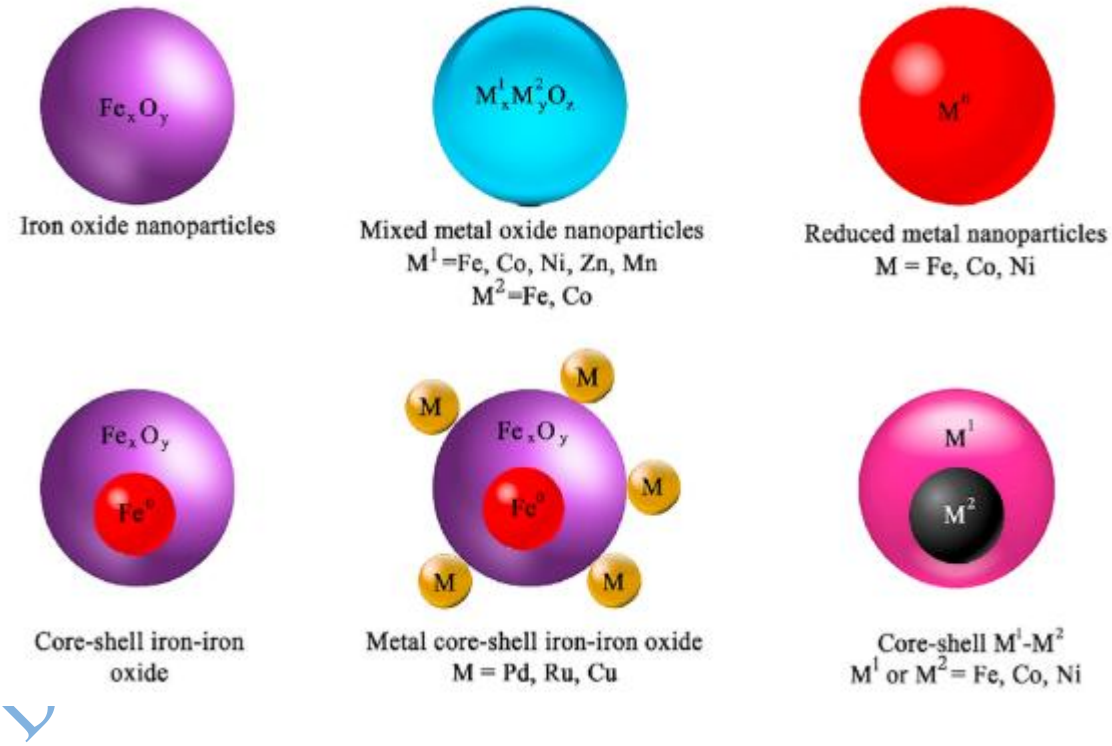

Figure 2.9: Magnetic particle-based catalysts.

Source[35]

The effectiveness of mixed metal oxide catalysts is indirectly influenced by the transfer of electrons from the metal group. Positive metal ions with Lewis acidity are produced by the binary metal oxide system, making the negatively charged oxygen ions susceptible to nucleophilic attack and serving as Bronsted bases. The catalyst's surface must have active sites in order for the (OH) bond in the methanol molecule to be easily broken down into methoxide anions and hydrogen cations during the methanolysis of oil (Figure 2.10). As seen in Figure 2.10, triglyceride and alcohol molecules interact with the methoxide anions on their surface to produce methyl ester and glycerol[36]. The alcohol used most frequently in the manufacture of biodiesel using magnetic catalysts is methanol[37]. Table 2.6 is a summary of the studies on the catalysts utilized in the synthesis of biodiesel.

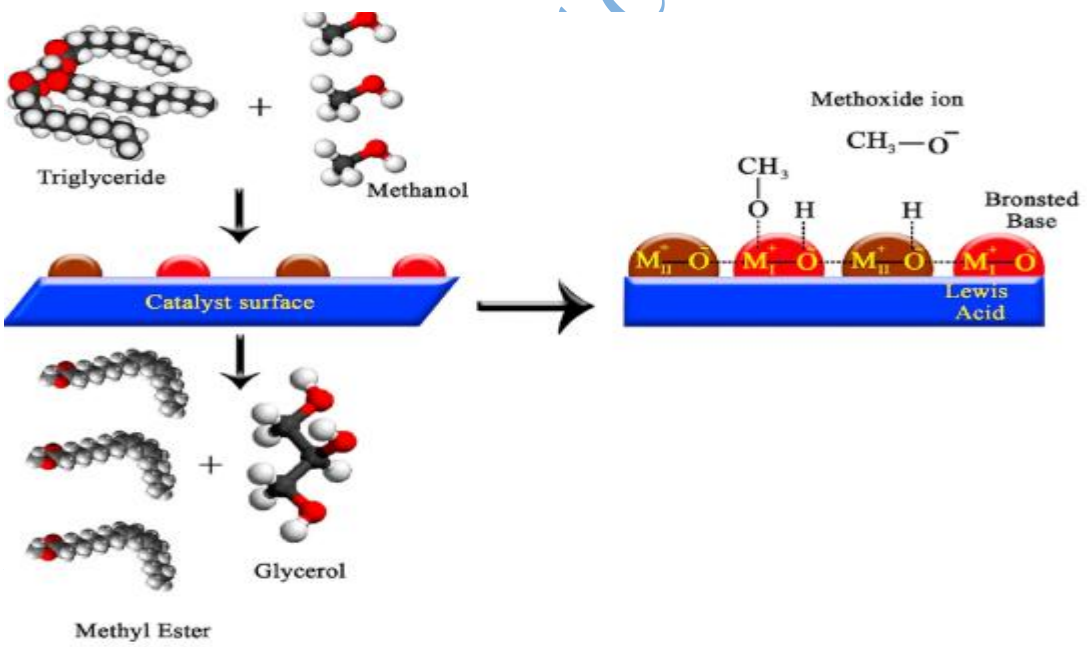

Figure 2.10: On the surface of mixed metal oxide, triglycerides and alcohol interact to create a magnetic catalyst.

Source[36]

Table 2.6: A summary of the yield of biodiesel produced using various oil sources and catalysts.

Catalyst	Feedstock	Temperature (°C)	MOR	Catalyst loading (wt. %)	Reaction time (h)	Biodiesel yield (%)	Ref.
SO_4/Mg-Al-Fe_2O_3	Waste cooking oil	95	9:1	4	5	98.5	[38]
CaO/Al/ Fe_2O_3	Rapeseed oil	-	15:1	6	3	98.71	[37]
Fe_2O_3@Li/ZnO	Rapeseed oil	35	12:1	0.8	0.58	99.8	[39]
SO_4/Fe-Al-TiO_2	Cooking oil	90	10:1	3	2.5	96	[40]
NaOH	Seed oil	60	5:1	0.13	2	70	[41]
KOH	Microalgae oil	60	12:1	2	0.2	85	[42]

Source: Field survey, 2022.

2.6 Various Methods for the Synthesis of Magnetic Nanocatalysts

There are three categories of techniques that can be used to create magnetized particles: chemical, biological, and physical techniques[43]. The chemical processes are efficient and straightforward, and by modifying the size, particle geometry, and composition of the generated magnetic nanoparticles, one may create particles with the desired properties by varying the salt, Fe_2/Fe_3 ratio, pH, and ion strength[44]. The physical processes are exact and often take place in the solid, gas, or vapour state, despite the fact that there is no control over the particle size within the nanoscale in this situation[45]. This method assumes that nanoparticles are created entirely through physical processes rather than any chemical reactions. Due to their lower cost and superior efficiency, chemistry-based synthesis methods are typically used in place of other biological approaches, with microbial culture being the most popular. Figure 2.11 shows a schematic of various production techniques coupled with an illustration of a nanocatalyst employed in earlier research activities[46,47]. Maghemite (Fe_3O_4), hematite (α-Fe_2O_3), and magnetite are a few examples of magnetic nanomaterials (α-Fe_2O_3). The three most well-known magnetic compounds are Fe, g-Fe_2O_3, and Fe_3O_4. $FeCl_3$ and FeO, two additional parts of iron, do not qualify as magnetic nanoparticles.

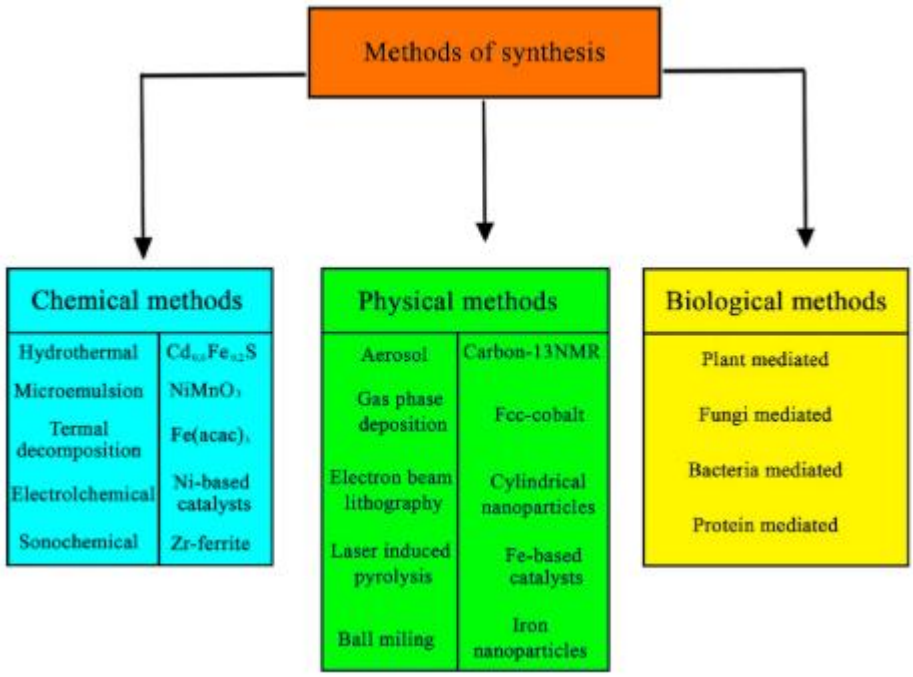

Figure 2.11: Various processes are used to synthesize nanocatalysts.

Source[47]

2.7 Characterization of Nanocatalysts

The characterization methods to be utilized are determined by the inherent properties of the nanocatalysts under investigation. The techniques employed to characterize it were utilized to look at the structures, physical appearance, shapes, electrical, sizes, mechanical and chemical properties of the generated nanomaterials[48].

2.7.1 Scanning Electron Microscope (SEM)

When an electron beam from a cathode-ray tube traverses a material in a scanning electron microscope (SEM), a scan pattern is produced. The primary electron beam interacts with the surface atoms and as a result scatters or emits electrons. For imaging and X-ray elemental analysis, SEM makes use of secondary backscattered beam effects (Figure 2.12). The quality of

the images obtained also depends on the detector type and signal processing. The form, fiber diameter, and surface morphology of nanocatalysts were investigated using SEM[48].

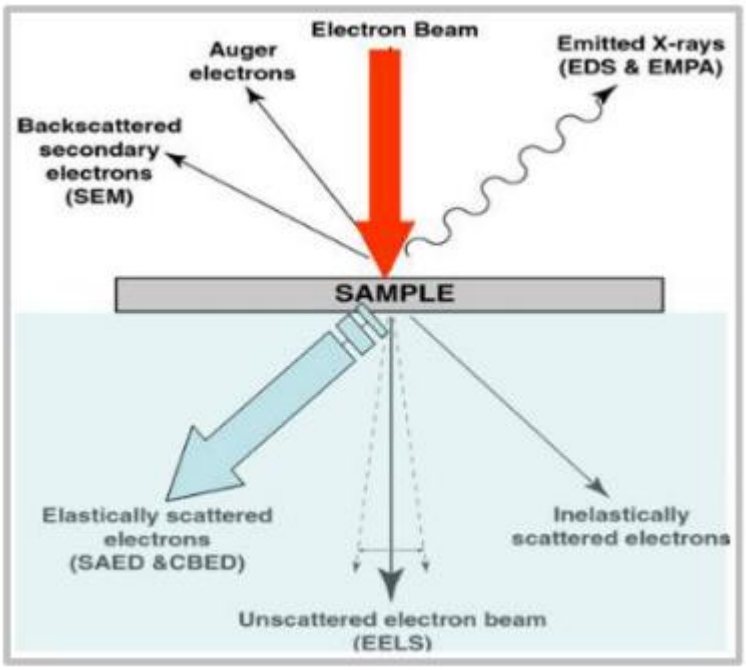

Figure 2.12: During SEM and X-ray microanalysis, the primary electron beam-specimen interaction.

Source[48]

SEM images are created when low energy secondary electrons that are leaving the material are collected. The inelastic, low energy scattered secondary electrons that originate at a depth of 1 to 50 nm contribute to the surface morphology or topography. The intensity of the secondary electron depends on the size of the beam spot, the amount of interaction and the incident angle of the beam[49].

2.7.2 XRD Crystallography

A compound's crystallinity can be ascertained using XRD. X-rays can also be reflected (diffracted) at the net plane of a sample's crystal lattice, just as electron beams (**Figure 2.13**).

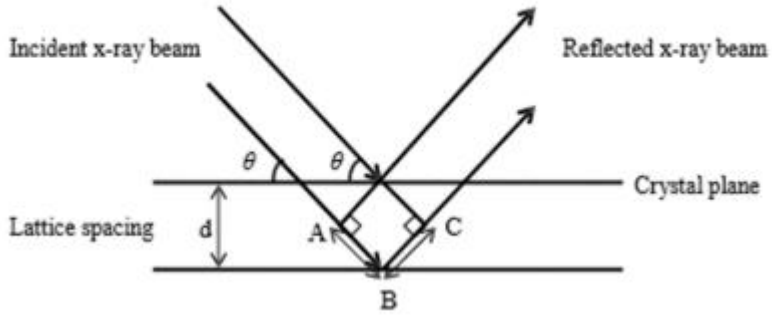

Figure 2.13: Diffraction of X-rays from a set of crystal planes.

Source[48]

When the criteria of Bragg's law, which connects the wavelength of electromagnetic radiation (λ) to the incidence angle of diffraction (θ) and lattice spacing (d) in a crystalline sample, are satisfied, Equation 2.1 can be used to calculate the particle property, d.

$n\lambda = 2d \sin \theta$ **Equation 2.1**

n is an integer

The resulting diffraction pattern is compared to recognized standard diffraction files recorded in the instrument's software, such as those from the International Centre for Diffraction Data, in order to identify the XRD pattern (spectrum) (ICDD) or the Joint Committee on Powder Diffraction Standards (JCPDS). Equation 2.2 can be used to estimate the crystallite thickness using the Debye-Scherrer equation.

$$t = \frac{0.9\lambda}{\beta \cos \theta}$$ **Equation 2.2**

Where;

θ the Bragg angle

λ is the wavelength of the X-rays (t and λ have same units),

β stands for the peak's Full-Width at Half-Maximum (FWHM), corrected for instrumental broadening, in radians.

t is the crystallite thickness

The observed particle form and d can be used to determine the volume: surface area ratio surface area and volume.

2.7.3 Fourier-Transform Infrared Spectroscopy (FTIR)

Only molecules with persistent dipole moments or phonons in crystalline materials are eligible for examination using FTIR spectroscopy. By measuring absorbance or the percentage of light transmission as a function of wave number, the FTIR spectrum was used to detect if organic functional groups and nanocatalysts were present or absent (cm^{-1}). FTIR was used to pinpoint the functional groups in PEG and doped nanocatalysts.

2.8 Physicochemical Properties of FAME

The synthesis of biofuels depends on physical-chemical property testing procedures for free fatty acid (FFA) concentration and FAME (fatty acid methyl esters). Standardized criteria outlined by European standards (EN) and ASTM (American Society for Testing Materials) play a major role in determining the quality of biodiesel. The biodiesel's quality must satisfy the requirements. The

kinematic viscosity, density, flash point, cloud point, and fire point of biodiesel synthesized with various nanocatalysts were compared to the ASTM (D6751) and EN 14214 biodiesel standards[48]. These qualities are affected by contaminants, high free fatty acid percentage and water content.

It's crucial to estimate the saponification and acid value of feedstock since these factors affect the output and purity of biodiesel. The transesterification process with conventional and ultrasonic stirring has been extensively discussed. It's interesting since it shows how the composition of the FAME as well as the provided physicochemical qualities was impacted, and a maximum production of 98.8% was attained in 120 minutes[49].

2.8.1 Measurement of Density

The process of converting mass to volume, which is necessary for the manufacture of biofuel, depends on density, which is defined as weight per unit volume. It significantly affects how well the fuel performs. Density measurements are employed to assess biodiesel fuel blends and determine the best blend formulation[50]. Although the type of oil used and the treatment technique used primarily determine the density of biodiesel, the molecular weight of the components, such as fatty acids, has an impact as well[51].

A high molecular weight equates to a high density, which has an impact on the fuel's quality. It has been widely claimed that low density fuel is of higher quality. The pycnomter is a standard test method for density measurements. Equation 2.3 shows the density measurement formula[52].

$$Density = \frac{(mass\ of\ pycnometer\ with\ biodiesel) - (mass\ of\ empty\ pycnometer)}{biodiesel\ volume} \quad \textbf{Equation 2.3}$$

Temperatures ranging from 15 to 20 °C are used to determine density, depending on the standard standards. It offers details on the fuel's uniformity and atomization[10]. The right methyl esters content of any biodiesel product can be determined accurately using theoretical density measurement utilizing the required optimization tools, in addition to experimental determination. The transesterification method can drastically lower density to meet the stipulated standard's restrictions.

2.8.2 Kinematic Viscosity

A key factor in establishing the quality of biodiesel is its viscosity. Fuel injection equipment's performance is influenced by gasoline's flowability, especially at low temperatures[53]. When fuel is atomized, high viscosity fuel causes large droplets to form, which results in operational problems like increased carbonization and, eventually, increased emissions and smoke, while fuel with too low a viscosity results in leakage and increased wear, which significantly lowers engine performance[54]. When compared to diesel fuel, biodiesel has a higher viscosity, which poses issues for process equipment and design. At a temperature of 40°C, an experimental viscosity is measured using a viscometer. According to EN 14214 and ASTM D6751, biodiesel has a kinematic viscosity of 1.9–6, 3.5–5 and 5.0 mm^2/s, respectively[54].

2.8.3 Cloud and Pour Point

The cloud point refers to the temperature upon which wax crystals becomes apparent after cooling a fuel. At lower temperatures, it makes fuel harden, which can clog fuel lines. To determine the cold point, ASTM Standards D2500, D5773, D5771 and D5772 are used[54]. It is simple to analyze the production of crystalline biodiesel using a Differential Scanning Calorimetry (DSC) curve. Eventually, increased crystallization will cause agglomeration in the fuel, which will reduce engine performance. Thickening can also lead to clogs in the engine's

fuel filters, which reduces the fuel flow capacity. The fuel's ease of crystallization is facilitated by the presence of a sizable percentage of saturated fatty acids[54].

The pour point is the lowest temperature at which fuel starts to flow. High levels of saturated fatty acids in biodiesel have a high pour point, which suggests that it has subpar fuel characteristics. The value of the pour point is significantly decreased throughout the transesterification process in order to offer superior grade fuel. The fuel characteristics are further affected by the increased fatty acid concentration that results from catalysis.

2.8.4 Flash Point

The flash point of a fuel is the temperature at which it will burn when exposed to flame. Because they have higher flash points than fuels made from petrochemicals, biodiesel fuels are safer to carry and store[54]. Low flash points indicate high volatility, and they are also helpful for categorizing fuels to reduce handling and shipping risks. Biodiesel has a greater flash point than diesel fuel. According to these specification criteria ASTM 6751 and EN14214, biodiesel must have a minimum temperature of 130°C and 120°C, respectively. It can be affected by impurities such as oil content, moisture content and unreacted alcohol. As a result, it indirectly helps to determine the quality of biodiesel fuel.

2.8.5 Acid and Iodine Values

The acid value is a crucial parameter because it affects a biodiesel's quality. This is referred to as the presence of free acids in a sample. By neutralising the sample with a certain quantity of KOH, the excess of free fatty acid that leads to soap formation and catalyst deactivation can be detected. The ideal range for feedstock acidity is 1.86 to 3.31 mg KOH/g oil. However, free fatty acid

levels in used cooking oil must be under 4 mg KOH/g in order to skip the pre-treatment stage; values under this can be employed right away in the transesterification procedure[10].

An indicator of how unsaturated a material is its iodine value. Additionally, it depends on the kind and quality of the feedstock, which has a big impact on how well the fuel oxidizes. Less than 120 g I_2/100 g of the given sample must be the iodine content of the diesel fuel. It will determine how much of a given fatty acid combination is unsaturated. Higher iodine levels are linked to worse oxidative stability. Additionally, it will provide information about the development of sludge in fuel, affect the quality of lubricants, and result in corrosion[51].

2.8.6 Saponification Value

The amount of potassium hydroxide (KOH) needed to saponify one gram of fat or oil under specific conditions is known as the saponification value. It measures the length and molecular weight of fatty acids. Crude esters have a greater saponification value than oil, ranging from 199 to 207 mg KOH/g oil[50]. Longer fatty acid chains have lower saponification values as there are fewer free carboxylic acid groups per unit amount of fat. The majority of the time, it's employed to figure out the sample's fats typical molecular weight. Contrarily, despite modest variations in average molecular weight, biodiesel and crude feedstock have similar saponification values[52].

2.9 Raw Material Optimization Parameters to Increase Biodiesel Production

The final step in choosing raw materials based on their physico-chemical properties is to modify reaction conditions before carrying out the reaction to achieve the highest yield possible. The independent and dependent variables were previously changed while just one response was being recorded at a time during optimization. This increases time consumption and increases the

likelihood of unsuccessful results because it does not involve the simultaneous interaction of several variables.

On the other hand, the development of new statistical tools and techniques would make it simple to process all of the running parameters, producing significant findings[56]. The reaction parameters were enhanced using the Taguchi approach with Response Surface Methodology, MINITAB software, fuzzy logic, design of trials, Genetic Algorithm (GN), and Artificial Neural Network (ANN) (RSM). Fuzzy logic and GNN and ANN are used in experiment design to increase biogas yield. These mathematical models have the capacity to optimize multiple reaction parameters at once. To increase yield, it can also be utilized to research reaction kinetics and microbial culture populations[33].

RSM is a significant method for examining the primary reaction parameters in the manufacture of bioethanol and biodiesel, which include molasses concentration, catalyst loading, starting pH, reaction temperature, methanol to oil ratio and reaction time[29]. As a result, it significantly increases production while reducing time, material, and cost through optimization[42].

In order to maximize the influence of key operating variables on the yield of biodiesel during the transesterification of canola oil to methyl esters (biodiesel) in the presence of the magnetic core-mesoporous shell KOH/Fe_3O_4@- Al_2O_3 nanoparticles, Response Surface Methodology (RSM) based on the Box-Behnken design (BBD) was investigated. A 97.4% biodiesel yield was achieved under optimal reaction conditions, with high concordance between anticipated and experimental data[57]. It was discovered that the key factors contributing to the best reaction conditions, specifically for transesterification, were reaction temperature and free fatty acid

content. SVO is discovered to have a significant concentration of free fatty acids because these acids cause the creation of soap.

Lowering the concentration through pre-treatment techniques, followed by an alkali-based transesterification procedure, is an important step in boosting the yield[50]. As shown by various researchers, it is also essential to keep the temperature within the boiling point range when using methanol as an alcohol source at atmospheric pressure. Although the initial methanol mixing and dispersion inhibits the reaction during the first 1–5 min, the rate of oil to methyl ester conversion improves with reaction time, and the maximum biodiesel output rises for 15 min before gradually falling. Reaction times can be greatly sped up by using contemporary heating techniques like infrared and microwave technologies. The yield of biodiesel production is significantly impacted by the following important elements.

2.9.1 Methanol to Oil Ratio

The most important factors in the production of biofuel are the kind of triglycerides and alcohol used, as well as the molar ratio of alcohol to oil. The most likely M:O ratio is 3:1 since it increases both the contact time and the oil's solubility. A high molar ratio accelerates more ester conversion[29]. To make 3 mol of fatty acids and 1 mol of glycerol, the esterification process requires 3 mol of alcohol and 1 mol of triglycerides, according to stoichiometry. High fatty acid content necessitates a sizeable amount of alcohol in order to advance the reaction because the molar ratio is heavily impacted by the type of oil and catalyst being used.

In turn, increasing the amount of alcohol used increases the production of biofuel. Alcohol consumption in excess, however, will eventually block the catalyst's active sites and favourably promote reverse reaction[55]. The main alcohols used in the transesterification process include

methanol, ethanol, propanol, and butanol. Numerous studies assert that ethanol can be utilised as well because it is environmentally beneficial and made from agricultural waste, unlike methanol, which is primarily used since it is less expensive[33].

2.9.2 Catalyst Weight (Nanocatalyst)

This is one of the important parameters influencing the production of biodiesel. The type and quantity of catalyst largely depends on whether an acidic or basic reaction is required. Additionally, it unintentionally depends on the type of feedstock used. If the feedstock is pure with typical FFA concentrations and moisture, the optimal catalyst loading is adequate to carry out the desired reaction. However, the transesterification process is actually unimportant if the feedstocks contains a lot of moisture and free fatty acids because it mostly results in soap creation and reduces the yield of biodiesel synthesis. In light of the second scenario, a greater concentration of nanocatalyst will undoubtedly enhance the synthesis of biodiesel. Therefore, a controlled optimization of the nanocatalyst depends greatly on a proper pre-treatment process for the feedstock[55].

For the best quantity of the triglycerides content, the average catalyst loading in the majority of the research was investigated in between 1 and 6 weight percent; nevertheless, it also substantially differed depending on the scale of production. Nevertheless, depending on the circumstances of the reaction, it was sometimes reported to be high. High catalyst weight has generally been found to have a detrimental effect on catalytic reaction because it limits mass transfer and lessens the contact of active sites brought on by agglomeration[58]. More addition will decrease production over the optimal level, rendering it economically inefficient.

2.9.3 Reaction Temperature

The temperature of the reaction plays a significant role in boosting biodiesel yield. Through the use of kinetics, a rise in temperature causes the reaction to proceed more quickly. The transesterification procedure frequently takes place between 50 and 60 °C, which is below the alcohol's boiling point, depending on the type of oil employed. The utilized alcohol mainly evaporates at high temperatures. Several groups claim that a 78 percent conversion is simple to achieve in 60 to 90 minutes at room temperature[33].

2.9.4 Reaction Time

Temperature and time play a role in the transesterification of oils or fatty acid esters. Fatty acid conversion is initially slow due to the oil's dispersion and mixing with methanol or alcohol, but it becomes faster over time. Due to quicker reaction kinetics, conversion occurs more frequently as the reaction approaches the threshold. The choice of catalyst considerably affects how long a reaction takes, with a mixed nanocatalyst requiring only 1-2 h. According to reports, the maximum ester conversion was achieved in 90 minutes; however, since the reaction is reversible and additional glycerol is created, adding more time has no positive impact on the yield[33].

Since these reaction parameters are the ones that are most frequently observed, numerous groups have reported the greatest yield of biofuel generation based on them. Finding the relevance between these parameters may be accomplished through techniques like ANOVA and BBD configuration as following statistical models like RSM and other models is the main approach for optimizing these parameters[51].

Initializing the interaction between parameters has been investigated to be done using a quadratic model ANOVA using a BBD design. Reaction time and catalyst loading were discovered to be the most crucial variables when the model was fitted.

According to study, the best biodiesel generation takes place at reaction temperatures of 55°C and a lower molar ratio of methanol to oil of 1:8, respectively. Additionally, it was demonstrated that glycerol becomes more soluble as methanol concentration increases, which ultimately reduces the output of completed items. A catalyst loading and reaction time of 0.6%, 80 minutes, among other significantly modified components, enable higher yields in the synthesis of biodiesel while maintaining the saponification process. Both high catalyst concentration and reaction time extremely have no discernible effects. The ideal reaction time of 80 minutes was found to have a significant impact on the highest biodiesel generation. For the given reaction temperature (55°C), molar ratio and reaction time (80 min), the ideal catalyst concentration was found to be 0.6 percent, primarily correlating that a lower catalyst amount produces a maximum yield of 92.43%[57].

Endnotes

1. E. Kurniawan & F. Perdana. *Biodiesel production of waste cooking oil catalyzed by cao derived from snail (Achatina Fulica) shell waste.* **Journal of Chemical Process and Material Technology**, *1*(1), 2022, 1-7.

2. O. Khan, A. K. Yadav, M. E. Khan & M. Parvez. *Characterization of bioethanol obtained from Eichhornia Crassipes plant; its emission and performance analysis on CI engine.* **Energy Sources, Part A: recovery, Util., Environ. Eff**., 2020, 1–11.

3. B. Thangaraj, P. Solomon, B. Muniyandi & S. Ranganathan. *Catalysis in biodiesel production.* **Current Res. Green Sust. Chem.,** 2019, 76-83.

4. J. Dantas, E. Leal, D. Cornejo, R. Kiminami & A. Costa. *Biodiesel production evaluating the use and reuse of synthesized in pilot-scale.* **Arabian J. Chem.** 13 (1), 2018, 3026–3042.

5. S. Chozhavendhan, M. Vijay, B. Fransila, R. Praveen & G. Karthiga. *A review on influencing parameters of biodiesel production and purification processes*. **Current Res. Green Sust. Chem.** 1–2, 2020, 1–6.

6. N. Jeyakumar & B. Narayanasamy. *Environmental effects optimization of used cooking oil methyl ester production using response surface methodology*. Energy **Sources, Part A Recov., Util. Environ. Eff**. 41 (19), 2018, 2313–2325.

7. A. Faisal, P. Priji, P. Unni, K. Nair & M. Kulangara. *Optimization of parameters for the production of biodiesel from rubber seed oil using onsite lipase by response surface methodology*. **Biotech.** 8 (11), 2018, 4-59.

8. B. Changmai, C. Vanlalveni, A. Ingle, R. Bhagat & S. Rokhum. *Widely used catalysts in biodiesel production: a review.* **RSC advances**. 10(68): 2020, 41625-79

9. T. A. Degfie, T. T. Mamo & Y. S. Mekonnen. *Optimized Biodiesel production from waste cooking oil (WCO) using calcium oxide (CaO) nano-catalyst*. **Sci. Rep.** 9, 2019, 18-982.

10. N. Mansir, S. Teo, I. Rabiu & Y. Taufiq-Yap. *Effective biodiesel synthesis from waste cooking oil and biomass residue solid green catalyst*. **Chem. Eng. J.** 347, 2018, 137-144.

11. Y.P. Peng, K.T. Amesho, C.E. Chen, S.R. Jhang, F.V. Chou & Y.C. Lin. *Optimization of biodiesel production from waste cooking oil using waste eggshell as a base catalyst under a microwave heating system*. **Catalysts,** 8 (2), 2018, -75-81.

12. M. Farooq, A. Ramli & A. Naeem. *Biodiesel production from low FFA waste cooking oil using heterogeneous catalyst derived from chicken bones.* **Renew. Energy** 76, 2015, 362-368.

13. S.E Mahesh, A. Ramanathan, K.M. Begum & A. Narayanan. *Biodiesel production from waste cooking oil using KBr impregnated CaO as catalyst.* **Energy Convers. Manage** 91, 2015, 442-450.

14. J. Gardy, A. Osatiashtiani, O. Céspedes, A. Hassanpour, X. Lai & A. Lee. *Applied Catalysis B: environmental A magnetically separable SO_4/Fe-Al-TiO_2 solid acid catalyst for biodiesel production from waste cooking oil*. **Appl. Catal. B Environ.** 234, 2018, 268–278.

15. M. Kirubakaran & V. Selvan. *A comprehensive review of low cost biodiesel production from waste chicken fat.* **Renew. Sust. Energy Rev.** 82 (1), 2018, 390-401.

16. B. Kayode & A. Hart. *An overview of transesterification methods for producing biodiesel from waste vegetable oils*. **Biofuels** 10 (3), 2019, 419-437.

17. Z. Duan, Q. Yin, C. Li, L. Dong, X. Bai, Y. Zhang, M. Yang, D. Jia, R. Li & Z. Liu. *Milling force and surface morphology of 45 steel under different Al_2O_3 nanofluid concentrations.* **Int. J. Adv. Manuf. Technol.** 107 (3), 2020, 1277-1296.

18. Z. Alam, C. Zhang & B. Samali. *The role of viscoelastic damping on retrofitting seismic performance of asymmetric reinforced concrete structures.* **Earthq. Eng. Eng. Vib** 19, (1), 2020, 223-237.

19. J. Zhang, J. Sun, Q. Chen & C. Zuo. *Resolution analysis in a lens-free on-chip digital holographic microscope*. **IEEE Trans. Comput. Imag** 6, 2020, 697-710.

20. Z. Wei, W. Chen, Z. Wang, N. Li, P. Zhang, M. Zhang, L. Zhao & Q. Qiang. *High-temperature persistent luminescence and visual dual-emitting optical temperature sensing in self-activated $CaNb_2O_6$: Tb3þ phosphor*. **J. Am. Ceram. Soc.** 104 (4), 2021, 1750-1759.

21. F. Trejo-Zarraga, L. Jesús, J. Chavarría-Hernandez & R. Sotelo-Boyas. *Kinetics of transesterification processes for biodiesel production. Biofuels: state of development.* **Chem. Asia J,** 2018, 149-179.

22. Y. Hu, Q. Chen, S. Feng & C. Zuo. *Microscopic fringe projection profilometry: a review*. **Opt. Lasers Eng.,** 106192 135, 2020, 106-192.

23. X. Li, R. Zhang, X. Zhang, P. Zhu & T. Yao. *Silver-catalyzed decarboxylativeallylation of difluoroarylacetic acids with allylsulfones in water*. **Chem. Asia J** 15 (7), 2020, 1175-1179.

24. W. Roschat. *The kinetic study of transesterification reaction for biodiesel production catalyzed by CaO derived from eggshells.* **Journal of Materials Science and Applied Energy** 8, no. 1: 2019, 358-364.

25. E.G. Junior, V.H. Perez, I. Reyero, A. Serrano-Lotina, & O.R. Justo. *Biodiesel production from heterogeneous catalysts based K_2CO_3 supported on extruded γ-Al_2O_3.* **Fuel,** 241, 2019, 311-318.

26. M. Ibrahim, A. Adlina, A. Islam, U. Rashid, S. Ibrahim & S. Mashuri. *Preparation of Na_2O supported CNTs nanocatalyst for efficient biodiesel production from waste-oil*. **Energy Convers. Manag.** 205, 2020, 112-445.

27. J. Gardy, M. Rehan, A. Hassanpour, X. Lai & A. Nizami. *Advances in nano-catalysts based biodiesel production from non-food feedstocks*. **J. Environ. Manag.** 249, 2019, 109316.

28. A. Marwaha, A. Dhir, S. Mahla & S. Mohapatra. *An overview of solid base heterogeneous catalysts for biodiesel production.* **Catal. Rev.** 60 (4), 2018, 594–628.

29. M. Mokhatr, M. Mohamed & H. El-Faramawy. *An innovative nanocatalyst α-Fe_2O_3/AlOOH processed from gibbsite rubbish ore for efficient biodiesel production via utilizing cottonseed waste oil.* **Fuel,** 297, 2021, 120-741.

30. T. Rahimi, D. Kahrizi, M. Feyzi, H. Ahmadvandi & M. Mostafaei. *Catalytic performance of MgO /Fe_2O_3-SiO_2 core-shell magnetic nanocatalyst for biodiesel production of Camelina sativa seed oil: Optimization by RSM-CCD method.* **Ind. Crops Prod.,** 159, 2021, 13-65.

31. M. Mohamed, W. Bayoumy, H.; El-Faramawy, W. El-Dogdog & A. Mohamed. *Novel α-Fe_2O_3/AlOOH(γ-Al_2O_3) nanocatalyst for efficient biodiesel production from waste oil: Kinetic and thermal studies.* **Renewable Energy,** 160, 2020, 450−464.

32. D.M. Marinković, M.R. Miladinović, J.M. Avramović, I. B. Krstić, M.V. Stanković, O.S. Stamenković, D.M. Jovanović & V.B. Veljković. *Kinetic modeling and optimization of sunflower oil methanolysis catalyzed by spherically-shaped CaO/γ-Al_2O_3 catalyst*. **Energy Convers. Manage.,** 163, 2018, 122−133.

33. Z. Helwani, M. Ramli, E. Saputra, B. Bahruddin, D. Yolanda, W. Fatra, G. Idroes, M. Muslem, T.M. Mahlia & R. Idroes. *Impregnation of CaO from eggshell waste with magnetite as a solid catalyst (Fe_3O_4/CaO) for transesterification of palm oil off-grade.* **Catalysts,** 10, 2020, 1-64.

34. T.T. Mamo. *Microwave-assisted biodiesel production from Microalgae, Scenedesmus Species, using goat bone: made nano-catalyst.* **Appl. Biochem. Biotechnol.,** 2020, 12-24.

35. S. Chen, M.K. Hassanzadeh-Aghdam & R. Ansari. *An analytical model for elastic modulus calculation of SiC whisker-reinforced hybrid metal matrix nanocomposite containing SiC nanoparticles.* **J. Alloys Compd.,** 767, 2018, 632-641.

36. A. Wang, P. Sudarsanam, Y. Xu, H. Zhang, H. Li & S. Yang. *Functionalized magnetic nanosized materials for efficient biodiesel synthesis via acidebase/ enzyme catalysis.* **Green Chem.** 22, (10), 2020, 2977-3012.

37. I. Ambat, V. Srivastava, E. Haapaniemi & M. Sillanpapa. *Nano-magnetic potassium impregnated ceria as catalyst for the biodiesel production.* **Renew. Energy,** 139, 2019, 1428-1436.

38. J. Gardy, E. Nourafkan, A. Osatiashtiani, A.F. Lee, K. Wilson, A. Hassanpour & X. Lai. *A core-shell SO_4/Mg-Al-Fe_3O_4 catalyst for biodiesel production*. **Appl. Catal.,** 259, 2019. 118-193.

39. A.F Kelarijani, N.G Zanjani, A.K. Pirzaman. *Ultrasonic assisted transesterification of rapeseed oil to biodiesel using nano magnetic catalysts.* **Waste Biomass Valorization** 11, 2020, 2613-2621.

40. I.B. Laskar, K. Rajkumari, R. Gupta, S. Chatterjee, B. Paul & S.L. Rokhum. *Waste snail shell derived heterogeneous catalyst for biodiesel production by the transesterification of soybean oil.* **RSC advances**, 8(36), 2018, 20131-20142.

41. J.K Efavi, D. Kanbogtah, V. Apalangya, E. Nyankson, E. Tiburu, D. Dodoo-Arhin, B. Onwona-Agyeman, A. Yaya. *The effect of NaOH catalyst concentration and extraction time on the yield and properties of Citrullus vulgaris seed oil as a potential biodiesel feedstock.* **S. Afr. J. Chem. Eng.** 25, 2018, 98-102.

42. A.P Cercado, F.C. Ballesteros, S.C. Capareda. *Biodiesel from three microalgae transesterification processes using different homogenous catalysts.* **Int. J. Technol** 4, 2018, 645-651.

43. M. Wang, M. Hu, Z. Li, L. He, Y. Song, Q. Jia, Z. Zhang & M. Du. *Construction of Tb-MOF-on-Fe-MOF conjugate as a novel platform for ultrasensitive detection of carbohydrate antigen 125 and living cancer cells. Biosens.* **Bioelectron.** 1, 42, 2019, 111-536.

44. X. Han, D. Zhang, J. Yan, S. Zhao & J. Liu. *Process development of flue gas desulphurization wastewater treatment in coal-fired power plants towards zero liquid discharge: energetic, economic and environmental analyses.* **J. Clean. Prod.** 261, 2020, 121-144.

45. Z. Alam, L. Sun, C. Zhang, Z. Su & B. Samali. *Experimental and numerical investigation on the complex behaviour of the localised seismic response in a multi-storey plan-asymmetric structure.* **Struct. Infrastruct. Eng,** 17 (1), 2020, 86-102.

46. S. Tamjidi & H. Esmaeili. *Chemically modified CaO/Fe3O4 nanocomposite by Sodium dodecyl sulfate for Cr (III) removal from water.* **Chem. Eng. Technol.** 42 (3), 2019, 607-616.

47. J. Zheng, C. Zhang & A. Li. *Experimental investigation on the mechanical properties of curved metallic plate dampers.* **Appl. Sci.,** 10 (1), 2019, 2-69.

48. Y. Huang, F. Li, G. Bao, W. Wang & H. Wang. *Estimation of kinematic viscosity of biodiesel fuels from fatty acid methyl ester composition and temperature.* **J. Chem. Eng. Data** 65, 2020, 2476–2485.

49. M.R. Abukhadra, S. M. Ibrahim, S. M. Yakout, M. E. El-zaidy & A.A. Abdeltawab. *Synthesis of Na + trapped bentonite/zeolite-P composite as a novel catalyst for effective production of biodiesel from palm oil; Effect of ultrasonic irradiation and mechanism.* **Energy Convers. Manag.** 196, 2019, 739–750.

50. E. G. Giakoumis & C. K. Sarakatsanis. *Estimation of biodiesel cetane number, density, kinematic viscosity and heating values from its fatty acid weight composition.* **Fuel**, 2018, 222, 574–585.

51. A.R Al Tawaha & V.V. Le. *Measurement and prediction of the density and viscosity of biodiesel blends.* **Internat. J. Technol. 9**, 2018, 10-15.

52. R. Karmakar, K. Kundu & A. Rajor. *Fuel properties and emission characteristics of biodiesel produced from unused algae grown in India.* **Petrol. Sci.,** 15 (2), 2018, 385–395.

53. H. C. Ong, M. Mofiju, A. S. Silitonga, D. Gumilang, F. Kusumo & T.M. I. Mahlia. *Physicochemical properties of biodiesel synthesized from Grape seed, Philippine tung, Kesambi, and palm oils.* **Energies** 13, 2020, 1319.

54. A. Bassam, M. Abatal, O. Tzuc, L. C. Pedro & C. Aguilar-uc. *Physical and chemical properties of biodiesel obtained from amazon Sailfin Catfish (Pterygoplichthyspardalis) biomass oil.* **J. Chem.,** 2019, 782-963.

55. T. Ahmad, M. Danish, P. Kale, B. Geremew, S. B. Adeloju, M. Nizami. *Optimization of process variables for biodiesel production by transesterification of flaxseed oil and produced biodiesel characterizations.* **Renew. Energy,** 139, 2019, 1272–1280.

56. J. M Borah, A. Das, .V. Das, N. Bhuyan & D. Deka. *Transesterification of waste cooking oil for biodiesel production catalyzed by Zn substituted waste egg shell derived CaO nanocatalyst.* **Fuel,** 242, 2019, 345–354.

57. A. Ghalandari, M. Taghizadeh & M. Rahmani. *Statistical optimization of the biodiesel production process using a magnetic core-mesoporous shell KOH/Fe_3O_4 @ g -Al_2O_3 nanocatalyst.* **Chem. Eng. Technol.** 42 (1), 2019, 89–99.

58. S. Kazemifard, H. Nayebzadeh, N. Saghatoleslami & E. Safakish. *Assessment the activity of magnetic KOH/Fe_3O_4 @Al_2O_3 core–shell nanocatalyst in transesterification reaction: effect of Fe/Al ratio on structural and performance.* **Environ. Sci. Pollut. Res.** 25, 2018, 32811–32821.

Chapter Three

Methodology

3.1 Materials

3.1.1 Spent Vegetable Oil (SVO) and Snail Shell (SS) Used

In this research, SVO and SS were utilized basically for FAME production. SVO was collected from some cafeteria, Ibadan after being used for cooking. The snail shell was collected from Oyingbo market in Lagos, Nigeria.

3.1.2 Chemical/Reagents Used

Analytical grade Methanol and ethanol (99%), Potassium hydroxide (KOH) pellets (ACS reagent, ≥ 85%), Aluminum chloride hydrated (97%), $FeCl_3$, phenolphthalein, Isopropanol alcohol (99%) Iodine, bromine, glacial acetic acid, $Na_2S_2O_3$, starch indicator, concentrated hydrochloric acid, granulated aluminum from BHD, London.

3.1.3 Instruments Used

Electronic balance, magnetic stirrer hotplate, heating mantle, reflux condenser, SEM, TEM, XRD, muffle furnace, FTIR, GC-MS.

3.2 Methods

3.2.1 Pretreatment of SVO

The SVO were pretreated to remove certain degree of moisture and other contaminants which could impede a high FAME yield.

3.2.1.1 Particulate Removal from SVO

Wasted vegetable oils are made up of solid items like sticks and fish (the kind and nature of the impurities depend on what the oil was used for). The container's bottom was permitted to collect large particles, which sedimentation eventually sedimented out. A 70 m pore diameter industrial sieve was used to filter out the small particles that were present in the oil.

3.2.1.2 Removal of Water from SVO

The process of transesterification exclusively used anhydrous chemicals and materials. Any water in the catalyst will interact with the FAME synthesized during hydrolysis to create free fatty acids. To allow the vaporization of the water in the treated SVO into the atmosphere, the oil was heated in an oven to 120 °C for 20 minutes. The oil's surface was scraped clean of any remaining soap droplets. To get rid of any suspended particles that might have been present, the filtration procedure was repeated. Waste oil that might be used for transesterification was produced in a clear, brilliant color.

3.2.2 Preliminary Studies of SVO

3.2.2.1 Acid Value and FFA in SVO Analysis

The amount of FFA in the oil is determined by the acid value, which is also used to establish the precise quantity of catalyst required to generate biodiesel. The ASTM D664 standard contains instructions for standardizing the titrant. In order to dissolve the FFA in the SVO, 1g of SVO was added to 50 mL of isopropyl alcohol in a 250 mL Erlenmeyer flask. The mixture was then vigorously shaken.

A few phenolphthalein indicator drops were added before titrating the mixture with 0.1N KOH solution. It was reported that the end result was a pale pink coloration. A simple titration method

was used to calculate the acid value of the SVO after measuring the quantity of KOH required neutralizing the acid in the SVO according to Equations 3.1 and 3.2

$$\text{Acid value} = \frac{Vol.\,titrant\ (ml) \times normality\ of\ KOH\ (N) \times 56.1}{Mass\ of\ waste\ cooking\ oil} \qquad \textbf{Equation 3.1}$$

= mgKOH/g of oil

$$\%\text{FFA} = \frac{Acid\ value}{2} \qquad \textbf{Equation 3.2}$$

3.2.2.2 Saponification Value of SVO Analysis

British Standards Institute's approach was used to determine the saponification value. With 25 mL of a 0.5 M methanol KOG solution, a 250 mL conical flask containing 2g of SVO was filled. Using an attached reflux condenser and a water bath, the flask's contents were refluxed for 30 minutes while being continuously whirled. The excess KOH was titrated with 0.5 M HCl using a heated phenolphthalein indicator. The saponification value was calculated under the identical circumstances as a blank determination with Equation 3.3.

$$\text{Saponification value} = \frac{(VB - VS) \times 28.05}{Weight\ of\ oil} \qquad \textbf{Equation 3.3}$$

Where;

VB= Blank titre

VS= Sample titre value

3.2.2.3 Determination of Iodine Value of SVO

250 mL conical flask containing 1g of SVO was then filled with 30 mL of Hanus solution before the flask stopped flowing. The mixture was put in the drawer for exactly 30 min after being stirred. The flask was filled with KI solution (10ml of 15% w/v), which was used to wash out

any iodide that might have been on the stopper. The solution was then titrated against 0.14M of $Na_2S_2O_3$ till light yellow was achieved. After adding starch indicator, the titration was continued until blue color vanished. The same conditions were used for a blank determination. The iodine value was calculated once the titre value was reported using Equation 3.4.

$$\text{Iodine value} = \frac{(VB-VS)-M\ of \text{Na2S2O3} \times 12.69}{weight\ of\ oil} \qquad \textbf{Equation 3.4}$$

Where;

VB= Blank titre

VS= Sample titre value

3.3 Synthesis of the Catalysts

The SS was thoroughly cleansed with tap water to get rid of the dirts and was broken into pieces. It was further washed with distilled water to remove unwanted materials and the other impurities and dried in an oven at 100 ºC for 12 h. The SS was then ground into extremely fine powder using a mortar and pestle with an outside diameter of 4 inches and a height of 3 inches, then sieved with a mesh size of 125–250 m. In order to convert $CaCO_3$ into CaO, the resultant particles were calcined for two hours at 800 °C in a muffle furnace.

3.3.1 Preparation of Metallic/Bimetallic Oxide Snail Shell Based Catalyst

The wet impregnation approach was used to synthesize the metallic/bimetallic oxides snail shell based nanocatalysts, which were then calcined. Aluminum chloride hydrated and ferric chloride was synthesized with a final weight percentage of 15 wt% using the wet impregnation process. Aluminum chloride hydrated and ferric chloride precursors weighing 0.15 g each were added to 70 g of CaO (SS) powder after being dissolved in distilled water. The mixture solution was then

continuously agitated for 2 hours at 60 °C until a paste was formed. The resulting paste was then dried for 3 hours at 120 °C in an oven before being calcined for 2 hours in a furnace at 800 °C. The same method was used to synthesize 30% Al_2O_3/CaO and 30% Fe_2O_3/CaO, respectively, using 0.30 g of aluminum chloride and iron chloride.

3.3.2 Synthesis PEGylated Bimetallic Oxide SS Based Catalyst

The PEGylated bimetallic oxide nanocatalyst were synthesized by gradual mixing the PEG with calcined 15%Al_2O_3/15%Fe_2O_3-CaO at 60 °C for 1 hr. The mixture was first dried in an oven at 120 °C for 1 hour and then calcined for 2 hours at 800 °C.

3.4 Characterization of Nanocatalysts

Using FTIR, XRD, SEM and EDX, the morphology and structure of the nanocatalyst were investigated.

3.4.1 Fourier Transform Infrared Spectroscopy (FTIR)

The sample structures were characterized by FTIR spectroscopy (Thermo Nicolet 6700 FT-IR spectrophotometer, United States).

3.4.2 X-ray Diffraction (XRD)

Using a Cu Ka radiation source (= 1.542) and a nickel filter in the 2ϴ range of 3°-80°, the XRD patterns of all the precursor and calcined samples were captured on a Rigaku Ultima IV, Kuraray Co. ltd. Japan (40 kV, 30 mA) X-ray diffractometer.

3.4.3 EDX and SEM Analysis

Using a JSM-6619LV, Scanning Electron Microscope, JEOL, United States device operating at 15 kV, EDX and SEM investigations were carried out to examine the morphology, size, and

elemental makeup of the produced catalyst samples. The range of magnification was 5000–70,000. Carbon glue was used to evenly distribute the catalyst powder on an aluminum sample holder prior to examination. To prevent the induction of electric current, the sample was subsequently coated with gold using a sputter coater.

3.5 Optimization of FAME Production with Box-Behnken Design (BBD)

To maximize the yield of FAME production, the response surface methodology was used to select the suitable transesterification process parameters (RSM). Creating linear regression models and optimizing responses that depend on various variables are the objectives of RSM. It makes it possible for researchers to quickly and correctly adapt for the best results[1,2].

In this study, 15 experiments were obtained utilizing a three-level, three-factor Box-Behnken Design (BBD) to examine the combined impacts of the three components and improve the transesterification parameters. The factors include the concentration of catalyst (Y_1), transesterification time (Y_2) and temperature (Y_3). The molar ratio of methanol to spent vegetable oil is constant (6:1 mol/mol). Each variable varies between a range of: Y_1 (1.0-10.0 % wt), Y_2 (40-90 min) and Y_3 (30-120 °C) as shown in **Table 3.1.** MINITAB 19 is a programme used for creating FAMEs, plotting response surfaces, and creating optimal conditions for statistical analysis of variance (ANOVA) of the response model.

Regression analysis was performed on experimental data before being put into a quadratic model (second-order model), as shown in Equation 3.5[3].

$$Y = \beta_0 + \sum_{i=1}^{k} \beta_i X_i + \sum_{i=1}^{k} \beta_{ii} X_i^2 + \sum_{i=1}^{k-1} \sum_{j=i+1}^{k} \beta_{ij} X_i X_j,$$

Equation 3.5

Table 3.1: Box-Behnken design factors for optimizing biodiesel production (BBD)

Factors	Units	Level		
		Low	Middle	High
Catalyst concentration (Y_1)	%wt	1.0	5.5	10.0
Reaction time (Y_2)	Min	30	75	120
Reaction temperature (Y_3)	°C	40	65	90

Source: Field work, 2022

Where Y is the response parameter or dependent variable; β_0, β_i, β_{ii} and β_{ij} is the regression coefficient for an intercept; k; is the number of parameters utilized; and X_i and X_j; are factors A number of response values, including the p-value, R^2, adeq accuracy, and lack of fit, provide evidence for the effectiveness of the model that was used.

The three levels of the three elements were taken into consideration during the experimental study: catalyst concentration (1.0 – 5.5 – 10 %wt), reaction time (30 – 75 – 120 °C) and the reaction time (40 – 65 – 90 min) in **Table 3.2**.

3.6 FAME Production

The following conditions were used for laboratory-scale transesterification: a hotplate with a magnetic stirrer spinning at 400 rpm, a methanol to spent vegetable oil molar ratio of 6:1, catalyst loading of 1.0, 5.5, and 10%wt, reaction times of 30, 75, and 120 min, and temperatures of 40, 65, and 90 °C. The temperature was regularly monitored with a thermometer.

The flask's contents were then transferred to a separating funnel where they were divided into the biodiesel and glycerol layers according to differences in density and solubility. The separating funnel was used to decant the glycerol. To get rid of the excess methanol that was present, the crude biodiesel was heated. The following equation 3.6 was used to calculate the biodiesel yield:

$$\text{Biodiesel yield} = \frac{wieght\ of\ biodiesel}{weight\ of\ oil} \times 100 \qquad \textbf{Equation 3.6}$$

Table 3.2: BBD design of experiments interpretation

Experimental Run	Catalyst Concentration (%wt) Y_1	Time (min) Y_2	Temperature (°C) Y_3
1	1	30	65
2	5.5	30	90
3	5.5	75	65
4	1	75	90
5	5.5	30	40
6	1	75	40
7	10	75	40
8	10	30	65
9	10	120	65
10	5.5	75	65
11	5.5	75	65
12	1	120	65
13	10	75	90
14	5.5	120	90
15	5.5	120	40

Source: Field work, 2022

3.7 Physicochemical Properties Determination

The density, acid value, cloud point, flash point, saponification value, kinematic viscosity, pour point, iodine value and moisture content of FAME were all assessed in the fuel testing labs of Climax Oil Ltd, Ogun State, and Lighthouse Petroleum Engineering Co. Ltd, Delta State, Nigeria, the analysis was completed in accordance with ASTM D6751 Standards.

3.7.1 Density Measurement

At room temperature (29–29.6 °C), the specific gravities of the materials were calculated using a hydrometer of the fisher brand. The sample was measured in a 250 mL measuring cylinder using a hydrometer with an accuracy of 0.001%. The biodiesel temperature of each sample as well as the hydrometer values for the lower meniscus were recorded. The reading was converted in line with ASTM D4052 using a conversion table with a 15/4 °C setting.

3.7.2 Kinematic Viscosity Measurement

Kinematic viscosity was measured by measuring the flow of samples between two specified locations on an Ostwald viscometer positioned vertically in the viscometer tube at a constant temperature of 40 °C. The viscosity was then calculated by dividing the flow duration by an Ostwald viscometer with continuous calibration.

Ostwald series 100, F5432, 150, F882, and 5263 viscometers are employed; their respective constants are 0.014770, 0.03772, 0.033268, and 0.10628.

3.7.3 Flash Point

The biodiesel sample in the cup was examined using an automated Pensky Martens closed cup tester with stirrer and thermometer ranging from 30 °C to 20 °C. The test fuel was heated and rotated constantly while being exposed to a flame. The vapour will ignite when it reaches the

flash point temperature, and a clear flash will be visible[4]. All the above was done according to ASTM D93

3.7.4 Determination of Pour Point

As with cloud point, pour point is determined. The test tube containing the sample was carefully put into a thermometer with a range of 30 °C to 20 °C. The test tube was then placed in a freezer, and the temperature was monitored frequently. Before removing the test tube, the sample was kept horizontal for a brief length of time without flowing. According to ASTM D5853, the temperature was recorded at 5 °F for the other thermometer and 3 °C above the solid point on the Celsius thermometer.

3.7.5 Determination of Cloud Point

By inserting a thermometer through the cork closing the test tube's mouth and heating a sample of biodiesel to a temperature range of 30 °C to 20 °C, the cloud point was identified. The thermometer was only 2 mm lower than the test tube's bottom prior to being placed in a refrigerator. The temperature was monitored until wax started to form at the bottom of the test tube from the biodiesel sample. There, clouds start to develop.

3.7.6 Determination of Saponification Value

The saponification value was determined using the British Standards technique. A 0.5 M methanol potassium hydroxide solution was added to 25 mL in a 250 mL conical flask containing 2 g of FAME. An attached reflux condenser was used to continually spin the contents of the flask as they were refluxed on a water bath for 30 minutes. The excess potassium hydroxide was titrated with 0.5 M hydrochloric acid using a heated phenolphthalein indicator.

The saponification value was calculated under the identical circumstances as a blank determination with Equation 3.7.

$$\text{Saponification value} = \frac{(VB - VS) \times 28.05}{Weight\ of\ Sample} \qquad \textbf{Equation 3.7}$$

Where;

VB= Blank titre

VS= Sample titre value

3.7.7 Determination of Iodine Value

A 250 mL conical flask containing 1 g of FAME was then filled with 30 mL of Hanus solution before the flask stopped flowing. The mixture was put in the drawer for exactly 30 min after being stirred. The flask was filled with KI solution (10 mL of 15% w/v), which was used to wash out any iodide that might have been on the stopper. The solution was then titrated against 0.14 M of $Na_2S_2O_3$ till light yellow was achieved. After adding starch indicator, the titration was continued until blue color vanished. The same conditions were used for a blank determination. The iodine value was calculated once the titre value was reported with Equation 3.8.

$$\text{Iodine value} = \frac{(VB - VS) - M\ of \text{Na2S2O3} \times 12.69}{weight\ of\ oil} \qquad \textbf{Equation 3.8}$$

Where;

VB= Blank titre

VS= Sample titre value

3.8 Characterization of Biodiesel

The functional group and composition of the FAME produced with all the synthesized nanocatalyst was assessed using FTIR and GC-MS.

3.8.1 Attenuated Resonance Fourier Transform Infrared Spectrophotometer (ATR-FTIR)

The catalysts were analyzed and FAME was analyzed using ATR-FTIR Perkin Elmer RXI FT-IR spectrophotometer. The samples were put into the sample holding chamber and between 600 cm^{-1} and 4000 cm^{-1} of space was scanned. It took place in a lab at Covenant University.

3.8.2 GC-MS Analysis of FAME Produced

The biodiesel samples are analyzed in order to determine the fatty acid methyl ester content using GC-MS instrumentation at the multi-purpose laboratory at Covenant University (CU), Ogun State.

Endnotes

1. O. Okonkwo, P. Chinwe, V.I.E. Ajiwe, M.C. Obiadi, C.C. Odidika & M. Okwu. *Kinetics and transesterification of the oil obtained from Cussonia bateri (Jansa Seed) as a step in biodiesel production using natural heterogeneous catalyst.* **American Journal of Applied Chemistry,** 9(5), 2021, 164-171.

2. S. Ozkan J. F. Puna, J. Gomes, T. Cabrita, J. V. Palmeira & M. T.Santos, M.T. *Preliminary study on the use of biodiesel obtained from waste vegetable oils for blending with hydrotreated kerosene fossil fuel using calcium oxide (CaO) from natural waste materials as heterogeneous catalyst.* **Energies,** 12(22), 2019, 4306.

3. H. C. Nguyen, M. L. Nguyen, C. H. Su, H. C. Ong, H. Y. Juan & S. J. Wu. *Bio-derived catalysts: a current trend of catalysts used in biodiesel production.* **Catalysts,** 11(7), 2021, 8-12.

4. H. C. Ong, M. Mofiju, A. S. Silitonga, D. Gumilang, F. Kusumo and T.M. I. Mahlia. *Physicochemical properties of biodiesel synthesized from Grape seed, Philippine tung, Kesambi, and palm oils.* **Energies,** 13, 2020, 13-19.

5. N. Nurun, R. Mostafizur, A.I. Muhammaad, M.H. Farhad, B. Peter, N.R. William, T. John, D.R. Zoran, J.B. Richard. *Fuel characterization, engine performance, combustion and exhaust emissions with a new renewable Licella biofuel*. **Energy Convers. Manage.** 96, 2015, 588–598.

Chapter Four

Results and Discussion of Findings

4.1 Synthesis and Physical Examination of SS-Based Catalyst

From **Figure 4.1**, the physical appearance shows dark brown colour after impregnating Ferric chloride into the SS. After calcination at 800 °C, the appearance turns to light dark brown as presented in **Figure 4.4** (I). **Figure 4.2** shows the synthesis of snail shell doped with Aluminum chloride hydrated by wet impregnation. A whitish colour appears after synthesizing and calcination. **Figure 4.3** shows how the snail shell are being converted from $CaCO_3$ to CaO and the final product of SS (CaO) doped with Aluminum Chloride hydrated and Ferric Chloride. **Figure 4.5** shows biodiesel separation phase of unsettled biodiesel after transesterification reaction and after 24 hrs separation showing the FAME at top layer and the glycerol with catalyst at the bottom layer.

Figure 4.1: Preparation of SS doped with Ferric chloride by wet impregnation.

Source: Field work, 2022.

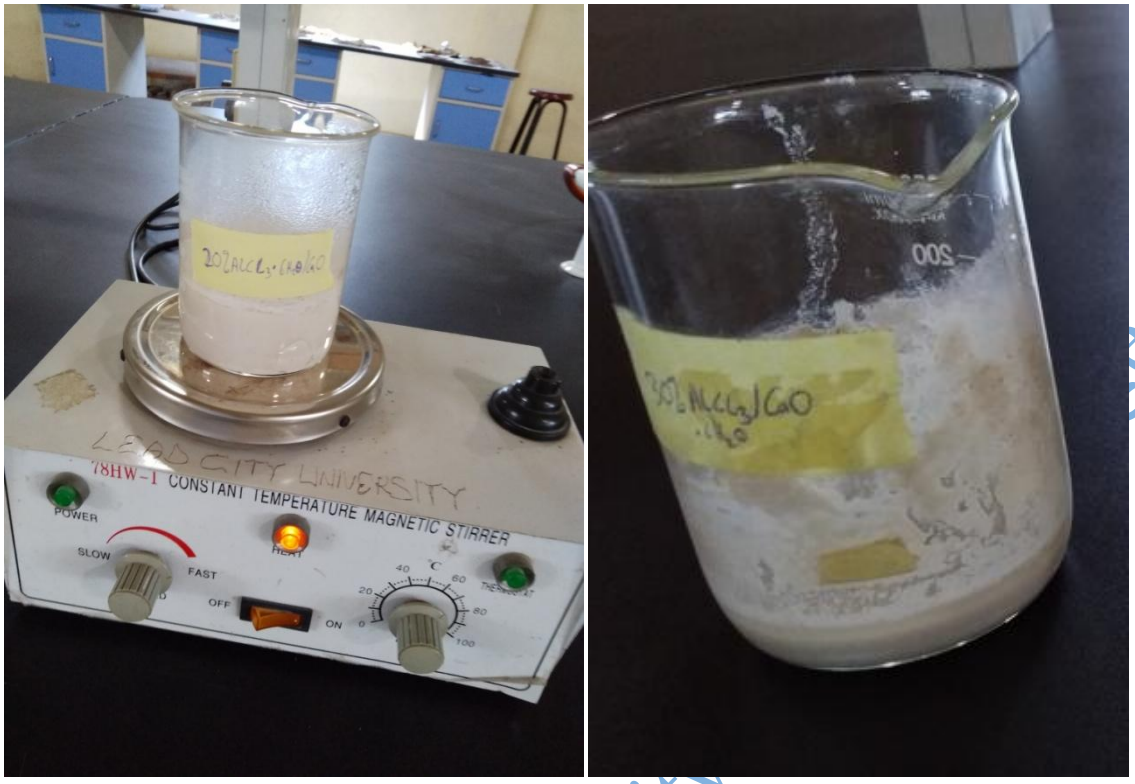

Figure 4.2: Preparation of SS doped with Aluminum chloride hydrated by wet impregnation.

Source: Field work, 2022.

Figure 4.3: Nanocatalyst samples: (A) SS (B) SS powder (C) calcined SS (D) SS doped with Aluminum Chloride hydrated and Ferric Chloride (E) SS doped with Aluminum chloride hydrated

Source: Field work, 2022.

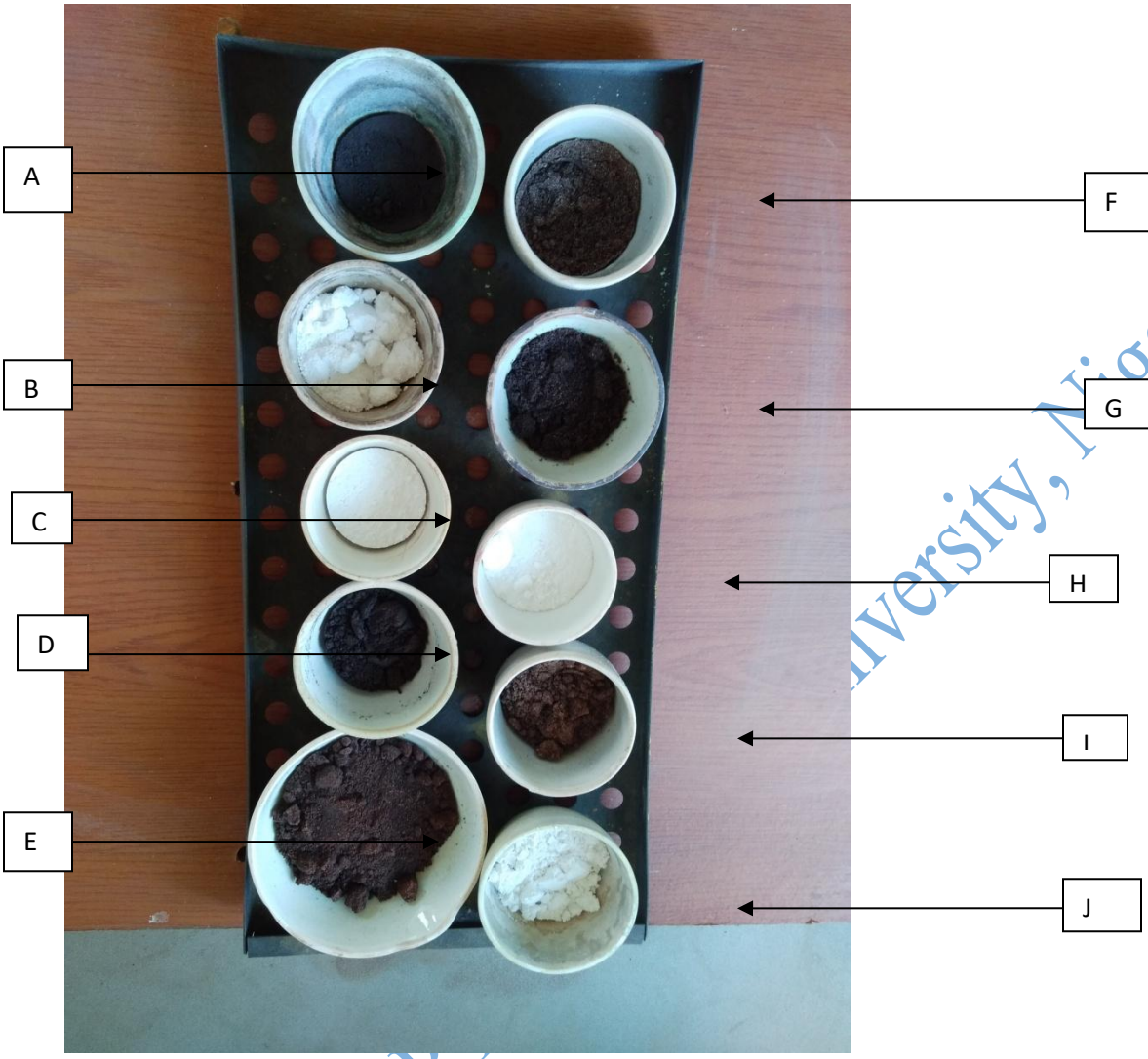

Figure 4.4: Different nanocatalysts after calcination at 800 °C; (A, D and E are bimetallic PEGylated catalysts), (B and J are calcinedSS-Al_2O_3), (C and H are calcined SS), (F and G are SS-15% Al_2O_3-15% Fe_2O_3) and (I is SS-Fe_2O_3).

Source: Field work, 2022.

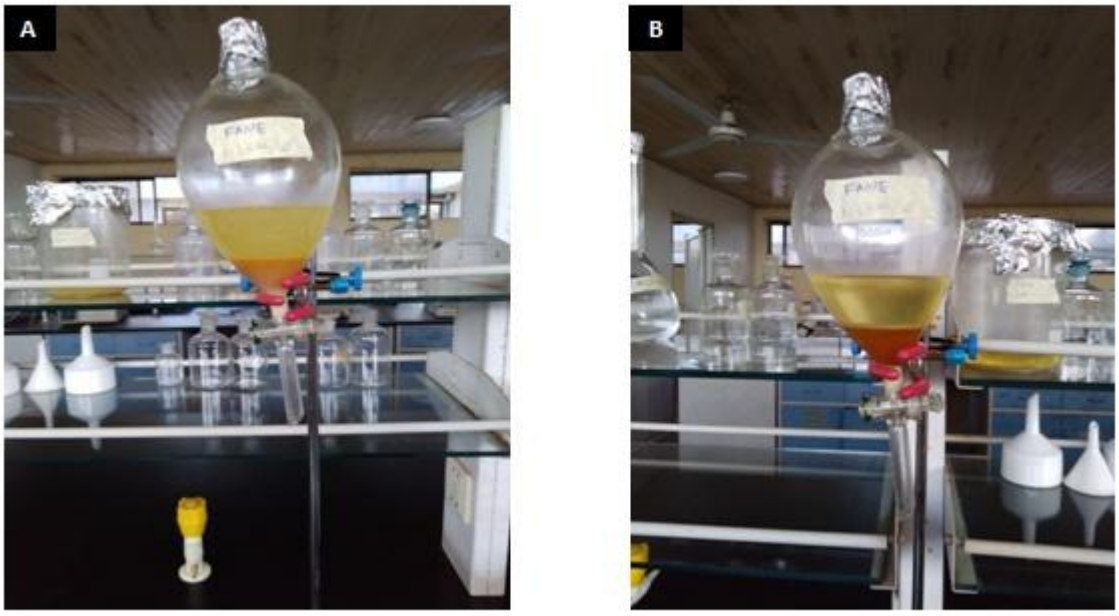

Figure 4.5: FAME separation phase; (A) unsettled FAME after transesterification reaction (B) After 24 hrs separation showing the FAME at top layer and the glycerol with catalyst at the bottom layer.

Source: Field work, 2022.

4.2 Properties of Spent Vegetable Oil (SVO)

Table 4.1: Properties of spent vegetable oil

Parameters	Method	SVO	ASTM Standards
Density @ 15 °C (g/cm^3)	ASTM D1298	0.9185	0. - 0.90
Kinematic viscosity (mm/s^2@40 °C)	ASTM D445	39.64	1.9-6.0
Flash point (°C)	ASTM D93	106	100-170 min
Acid value (mg KOH/g)	ASTM D974	2.32	≤ 0.5
FFA (%)	-	1.16	-
Saponification value (mg KOH/g)	ASTM D464	178.398	-
Iodine value (I_2/g)	ASTM D2500	107.8	-
Water content (%)	ASTM D97	0.03	0.05 max

Source: Field work, 2022

The physicochemical characteristics of the spent vegetable oil (SVO) are depicted in Table 4.1. The oil's density and kinematic viscosity both meet ASTM requirements. SVO was observed to record a flash point value of 106 °C, making it safe for use in extremely hot (climatic) conditions. In Table 4.1, the FFA content was 1.16%, which is a little bit higher than the ASTM standard. According to studies, high FFA lowers catalyst efficiency and biodiesel production yield; as a result, it is has been reported that the FFA content of SVO should not be greater than 1 wt%. Contrarily, studies have shown that heterogeneous catalysts can be used in the transesterification process of oil with a high FFA values (6–15%) without the need for pretreatment. High yield (90%) utilizing SVO has been demonstrated in prior reports under comparable reaction conditions (65 °C, 1h, 6:1, 1.1 catalysts loading). The fatty acid composition, which affected the iodine concentration, resulted in somewhat greater iodine content (107.8). The saponification value of SVO was 178.398, which is within the ASTM standard[1].

4.3 Surface Chemistry of Catalysts

4.3.1 FTIR Analysis

FTIR spectroscopy was used to determine the functional groups on the surface of the catalysts. The wave number values and the characteristic of absorption of all the catalysts are presented in Table 4.2 while Figure 4.6 showed the FTIR spectra of CaO, 30% Al_2O_3/CaO, 30% Fe_2O_3/CaO, 15%Fe_2O_3/15Al_2O_3/CaO and PEGylated catalysts accordingly. CaO is hygroscopic in nature. After calcining SS, the emergence of $Ca(OH)_2$ spectra is therefore confirmed and supports the conversion of $CaCO_3$ to CaO. Sharp peaks were observed in the absorption range value of 3600 – 3620 cm^{-1} which is a characteristic absorption of O-H. These could be observed in the catalyst analyzed as presented in Table 4.2.

Table 4.2: The FTIR absorption value of the catalysts and their assignments

Wave number (cm^{-1})	Calcined SS	30% Al_2O_3/CaO	30% Fe_2O_3/CaO	15% Al_2O_3/ 15%Fe_2O_3/CaO	PEGylated	Functional group
3630-3600	3639	3643	3637	3644	3648	O-H (stretch)
3500-3100	-	-	3449	3415	-	N-H (stretch)
3000-2850	2978	2977	-	2976 & 2893	2977 & 2892	C-H (stretch)
2250-2100	-	-	2151	-	-	C=C
1810-1775	1793	1795	1797	-	1793	C=O (stretch)
1680-1600	-	-	1623	1629	-	C=C
1300-1000	1249, 1161 & 1072	1249, 1155 & 1073	-	1251, 1073 & 1153	1251& 1074	C-O
900-690	868& 707	840	866	828	871 & 702	C-H (out of plane bend)

Source: Field work, 2022

Characteristic absorption range value of 3000 – 2850 cm^{-1} is attributed of alkyl C-H stretch due to organic matter of the of the catalyst. While the characteristic Fe-O vibration bond absorption bands were seen at approximately 537, 538, and 550 cm^{-1} from 30% Fe_2O_3/CaO and 15%Fe_2O_3/15Al_2O_3/CaO, and PEGylated bimetallic catalyst, respectively[2]. The appearance and disappearance of wave numbers of the catalysts when compared with the calcined SS as well as absorption band as recorded in Table 4.2 suggest surface modification.

Furthermore, the comparative study of the surface modification between calcined SS and 30%Al_2O_3/CaO in which a difference in C-O, C=O, O-C, -H and O-H spectra of the two material. These shifts are due to the structural change resulting from the reaction of Al_2O_3, the dopant with SS (CaO). From Figure 4.6, some certain absorption bands was noticed in calcined SS and was found to have disappeared in 30%Fe_2O_3/CaO while a shift was also observed. These phenomena are due to the structural change resulting from the reaction of Fe_2O_3, the dopant with SS (CaO). Also, the doping of CaO with Al_2O_3-Fe_2O_3 to yield Al_2O_3/Fe_2O_3/CaO catalyst complex are recorded in Figure 4.6 while the comparative study of SS with Al_2O_3/Fe_2O_3/CaO complex modified with PEG 400 resulting to the formation of PEGylated Al_2O_3/Fe_2O_3/CaO catalyst complex presented in Figure 4.6 is in accordance with the other prepared studies in which surface restructuring of the SS was noted due to the reaction with the oxides of Fe and Al at constant ration of 15% respectively. Studies have shown that the introduction of PEG known as PEGylation is to improve the surface of the catalyst through size reduction of the PEGylated material[3]. This phenomenon was observed and confirmed in the shift in the absorption band and disappearance of certain peaks when SS is compared to Al_2O_3/Fe_2O_3/CaO and PEG Al_2O_3/Fe_2O_3/CaO respectively as shown in Figures 4.6.

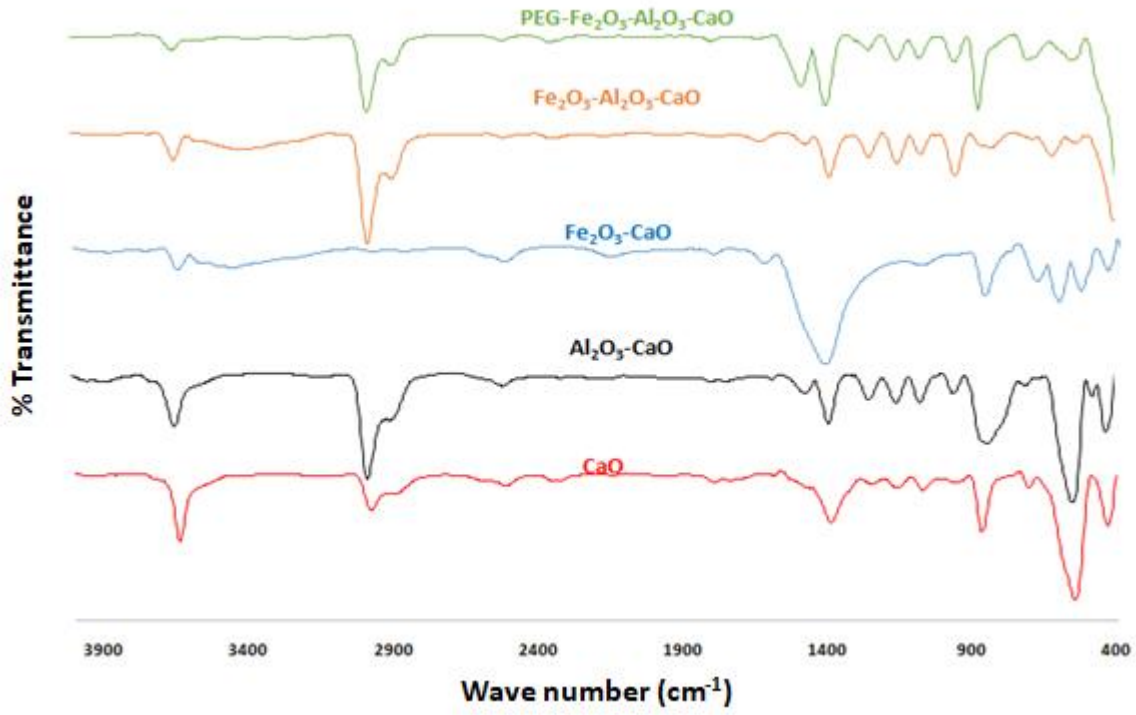

Figure 4.6: ATR-FTIR spectra of CaO, 30%Al_2O_3/CaO, 30%Fe_2O_3/CaO, 15%Fe_2O_3/15Al_2O_3/CaO and PEGylated catalysts.

Source: Field work, 2022

4.3.2 Crystallinity Study of the Catalysts

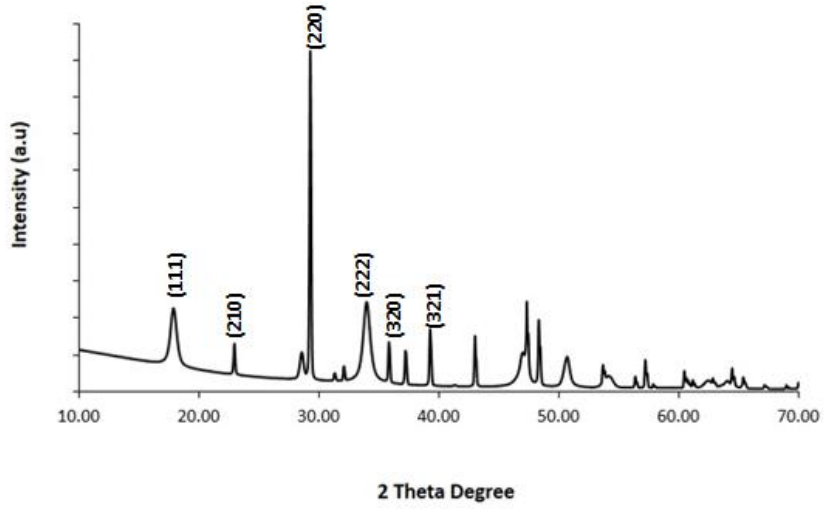

Figure 4.7: Crystallogram of calcined snail shell catalyst.

Source: Field work, 2022

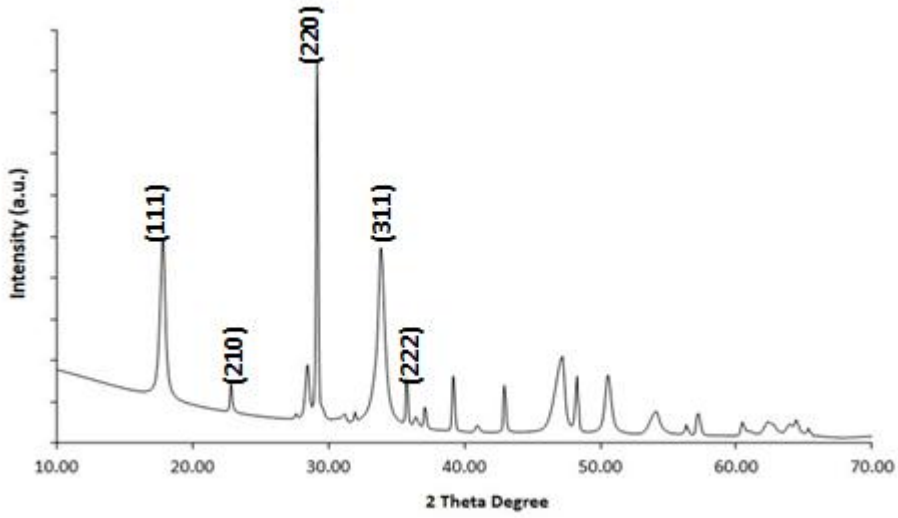

Figure 4.8: Crystallogram of 30%Al_2O_3/CaO catalyst

Source: Field work, 2022

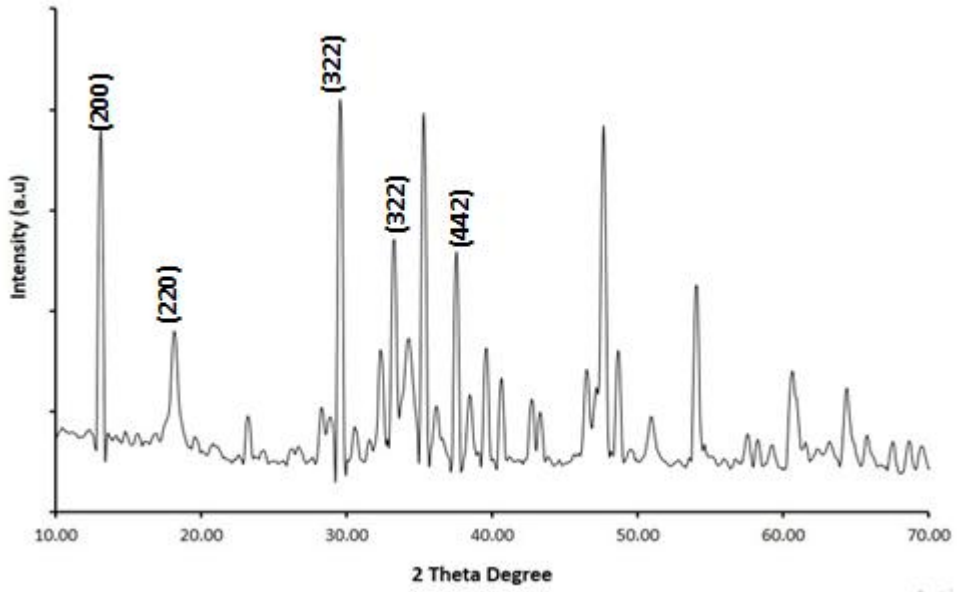

Figure 4.9: Crystallogram of 30%Fe_2O_3/CaO catalyst.

Source: Field work, 2022

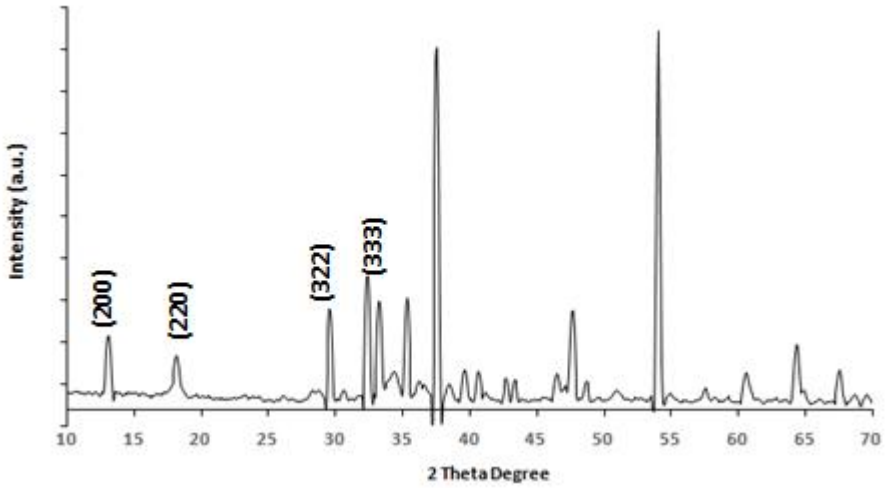

Figure 4.10: Crystallogram of 15%Al_2O_3/15% Fe_2O_3/CaO catalyst.

Source: Field work, 2022

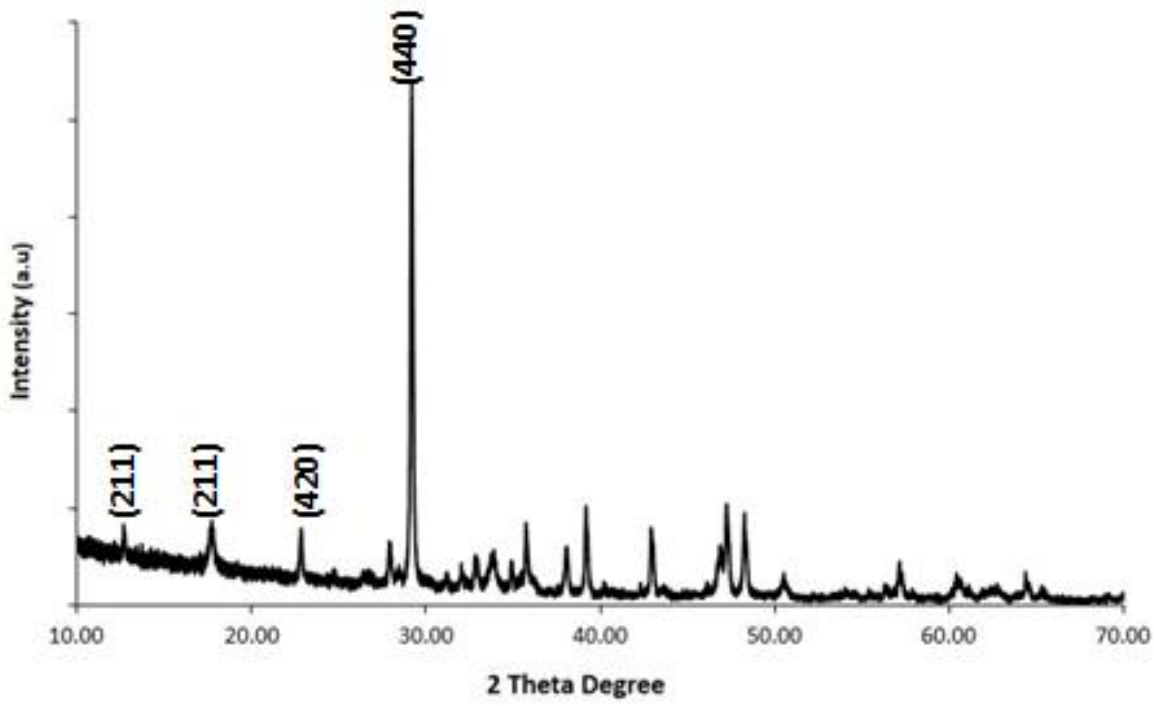

Figure 4.11: Crystallogram of PEGylated catalyst.

Source: Field work, 2022

The crystalline nature of the catalysts was examined using XRD. Figures 4.7 - 4.11 depicts the XRD patterns of the calcined SS, 30%Al_2O_3/CaO, 30%Fe_2O_3/CaO, 15%Al_2O_3/15%Fe_2O_3/CaO and PEGylated nanocatalysts. The primary components of quicklime, $Ca(OH)_2$ and $CaCO_3$, were entirely converted to CaO (JCPDS #371497) after being calcined at 800 °C for 2 hours. The sharpness of the peaks and intensity are the parameters that are used to determine the crystallinity or amophoric nature of any material. The reported data suggested that the ideal temperature to convert $CaCO_3$ and $Ca(OH)_2$ from snail shells, quicklime, and egg shells to CaO

is 800 °C[4]. However, the calcined SS (CaO) mainly consist of CaO as shown by several peaks at 2Θ about 17.83°, 22.19°, 29.26°, 35.82°, 37.20°, and 39.27° indexed as 111, 210, 220, 222, 320, and 321 planes respectively, which was in good agreement with previous studies[5]. The recorded XRD data for 30%Al_2O_3/CaO with 2θ values of 17.82°, 22.83°, 29.17°, 33.83° and 35.71° corresponds to the 111, 210, 220, 311 and 222 planes, respectively. A shift in the 2θ values of SS when compared with 30%Al_2O_3/CaO is as a result of modification of SS with Al_2O_3. As illustrated in Figure 4.8, this suggests an effective impregnation with improved crystallinity. Furthermore, the recorded XRD data for 30%Fe_2O_3/CaO with 2Θ values of 13.03°, 18.18°, 29.48°, 33.14°, and 37.50° corresponds to the 200, 220, 332, 333 and 442 planes respectively. A shift in the 2θ values of SS when compared with 30%Fe_2O_3/CaO is as a result of modification of SS with Fe_2O_3. As shown in Figure 4.9, this suggests an effective impregnation with enhanced crystallinity. The results are consistent with the research that was reported[6]. From Figure 4.10, 15%Al_2O_3/15%Fe_2O_3/CaO, the diffraction peaks identified at 2Θ = 13.13°, 18.28°, 29.67°, and 33.33° correspond to the (200), (220), (332), and (333). A shift in the 2θ values of SS when compared with 15%Al_2O_3/15%Fe_2O_3/CaO is as a result of modification of SS with Al_2O_3 and Fe_2O_3, suggesting an effective impregnation with improved crystallinity as shown by Figure 4.4. The XRD results are in good agreement with a related prior report on calcium oxide powder made from eggshell that was synthesized[7]. The recorded XRD data for PEGylated nanocatalyst with 2θ values of 12.66°, 17.70°, 22.82°, and 29.17° corresponds to the 211, 222, 420 and 440 planes, respectively. A shift in the 2θ values of SS when compared with PEGylated nanocatalyst is as a result of modification of SS with Al_2O_3, Fe_2O_3 and PEG. As depicted in Figure 4.11, this suggests an effective impregnation with improved crystallinity.

4.3.3 Morphological Characterization and Mapping of Catalysts

The morphology of the catalysts which include SS (CaO), 30% Al_2O_3-CaO, 30%Fe_2O_3-CaO, 15%Al_2O_3-15%Fe_2O_3-CaO and PEGylated 15%Al_2O_3-15%Fe_2O_3-CaO were determined using SEM. While EDX examined the existence of the metal(s) utilized as a dopant and its percentage composition (mapping) in each of the components. The SEM micrograph of SS is shown in Figures 4.12a & b thus revealing a well-organized crystalline aggregate. The crystallite surface might offer the catalyst's accessible active sites[8,9]. While the EDX shows the percentage composition of the metals that make up the catalyst. This therefore confirms the formation of Ca-O which is the major composition with higher calcium concentration than oxygen expected for calcined SS shown Figure 4.13.

The SEM and EDX micrographs of 30%Al_2O_3-CaOpresented in Figures 4.14a & b shows aggregates of spherical and cubic shaped particles, while the EDX results show the chemical mapping of the 30% Al_2O_3-CaO confirming the presence of Aluminum, Calcium and higher concentration of oxygen. This shows and ascertains the formation of oxides of aluminum coupled with CaO.

SEM micrographs of 30%Fe_2O_3-CaO shown in Figures 4.16a & b shows a flower-like morphology which is a characteristic associated with iron nanoparticles as reported[10]. This is therefore corroborating the formation of iron complex with CaO thus corroborating the results observed in EDX micrograph confirming the doping of CaO with Fe_2O_3 as presented in Figure 4.17. More so, the concentration of oxygen as shown by the EDX reveals that higher concentration of oxygen is noted according to EDX chemical mapping results.

Research has shown that PEGylation enhances the surface characteristics of particles which necessitated the modification of the bimetallic oxides of SS comprising ratio 1:1 of Al_2O_3 and Fe_2O_3 with PEG 400. The micrograph presented in Figure 4.18a and b shows aggregates particles comprising of rod-like and spherical particles compared with the cubic crystal structure of calcium oxide. With decreased Al and Fe concentrations compared to CaO. High PEG particle dispersion may be the cause of the irregular size distribution of sphere and rod-like formations. While Figure 4.19 shows that PEGylated nanocatalyst has a higher Ca content than oxygen, aluminum, and iron.

The morphological restructuring observed in the doped catalyst when compared with the CaO (SS) is attributed to the presence of the dopants which in alignment with the disappearance and appearance in the absorption bands of the catalyst recorded in the FTIR vis-à-vis XRD crystallographic studies of the catalyst. The results of this study suggest the confirmation of the morphological restructuring and transformation of the catalyst due to modification of SS with the dopants. The finding is in agreement with earlier reported studies[11].

4.3 Biodiesel Yields Obtained from Transesterification Reaction

The results of the FAME obtained from the transesterification of calcined CaO, 30%Al_2O_3/CaO, 30%Fe_2O_3/CaO,15%Al_2O_3/15%Fe_2O_3/CaO and PEGylated bimetallic nanocatalysts (under the same experimental conditions) are shown in Table 4.3. Higher FAME yields were obtained with 15%Al_2O_3/15%Fe_2O_3/CaO nanocatalyst when compared to the yield from the other nanocatalysts (15%Al_2O_3/15% Fe_2O_3/CaO > PEGylated > calcined SS > 30% Fe_2O_3/CaO > 30% Al_2O_3/CaO) experimental runs, under the same conditions.

Spent vegetable oil FAME yield for experimental run for using 15%Al_2O_3/15%Fe_2O_3/CaO, PEGylated, calcined CaO, 30%Fe_2O_3/CaO and 30%Al_2O_3/CaO catalysts separately were 98.11%, 97.29%, 96.17%, 94.13% and 91.21% respectively. 15%Al_2O_3/15%Fe_2O_3/CaO nanocatalyst has the highest percentage yield followed by PEGylated and calcined SS respectively. The other experimental runs showed tendencies that were comparable to these.

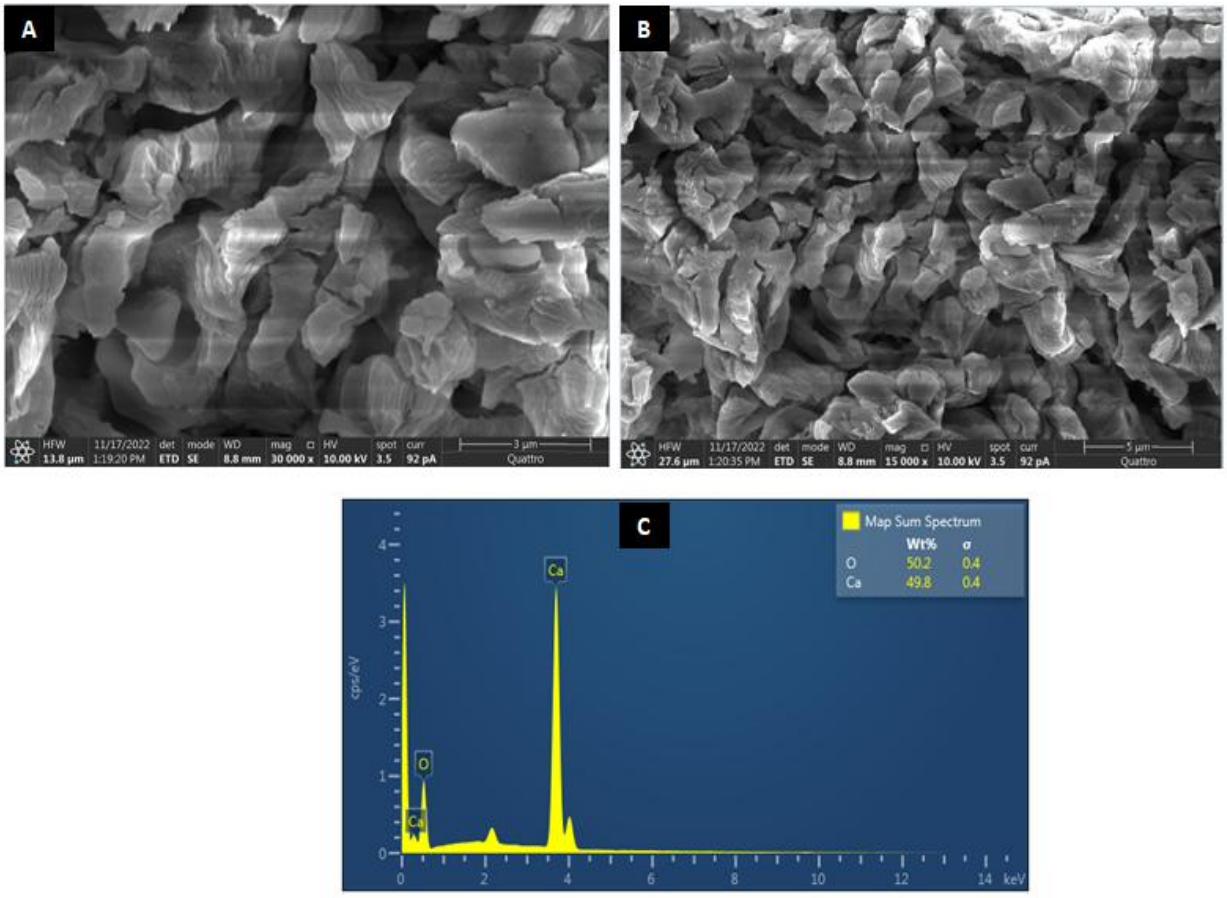

Figure 4.12: SEM micrographs of CaO at (a) 30,000x (b) 15,000x and (c) EDX chart of the elemental composition of catalyst.

Source: Field work, 2022

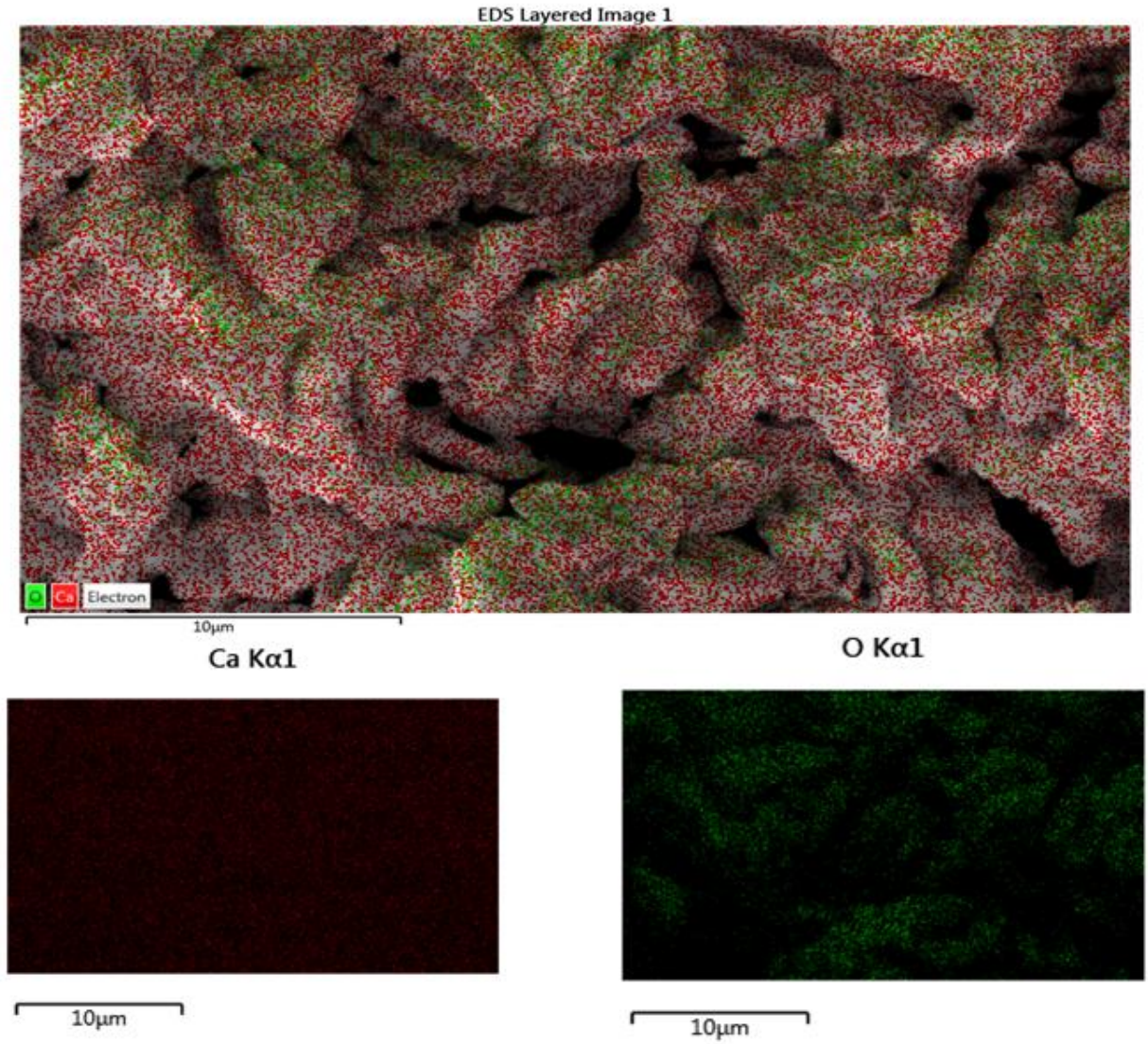

Figure 4.13: Chemical mapping of CaO catalysts.

Source: Field work, 2022

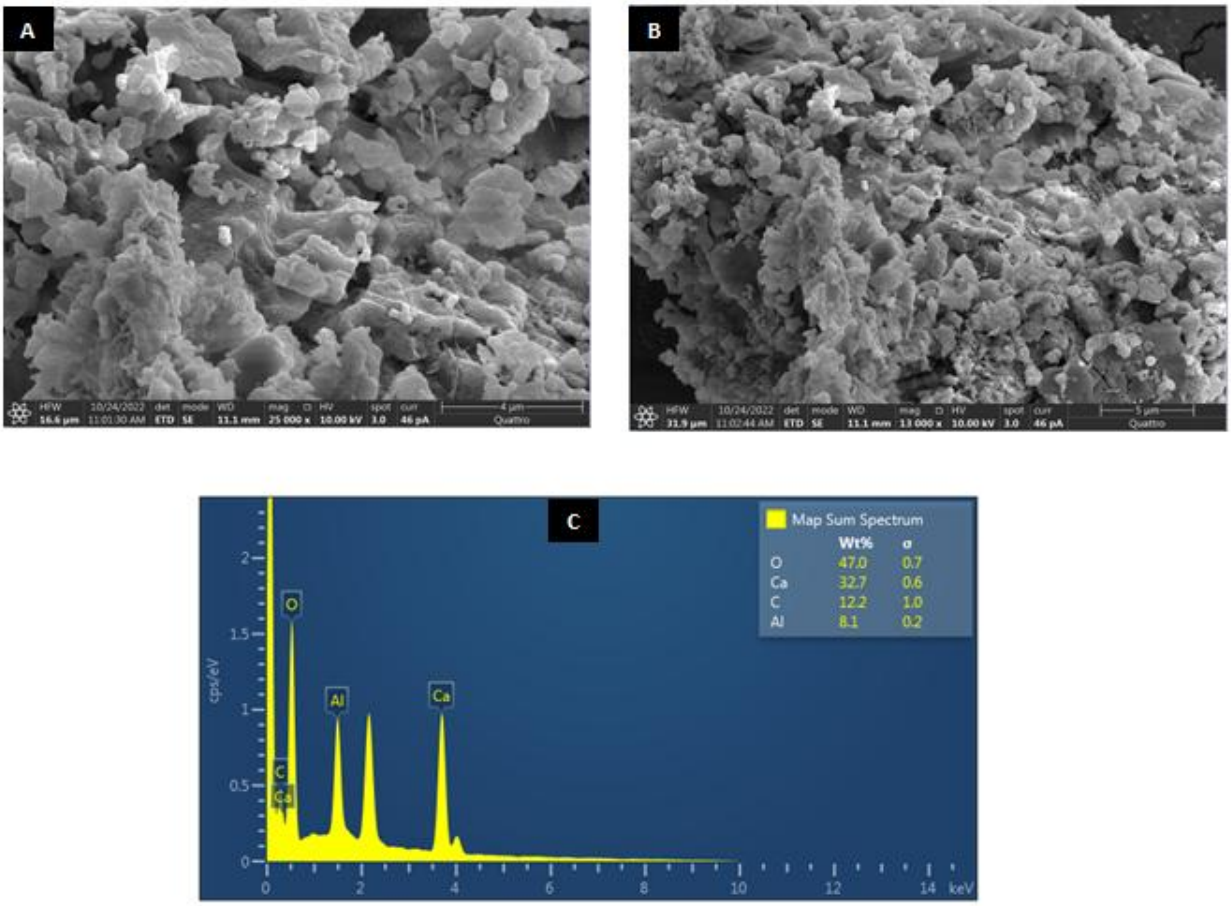

Figure 4.14: SEM micrographs of 30%Al_2O_3/CaO at (a) 30,000x (b) 15,000x and (c) EDX chart of the elemental composition of catalyst.

Source: Field work, 2022

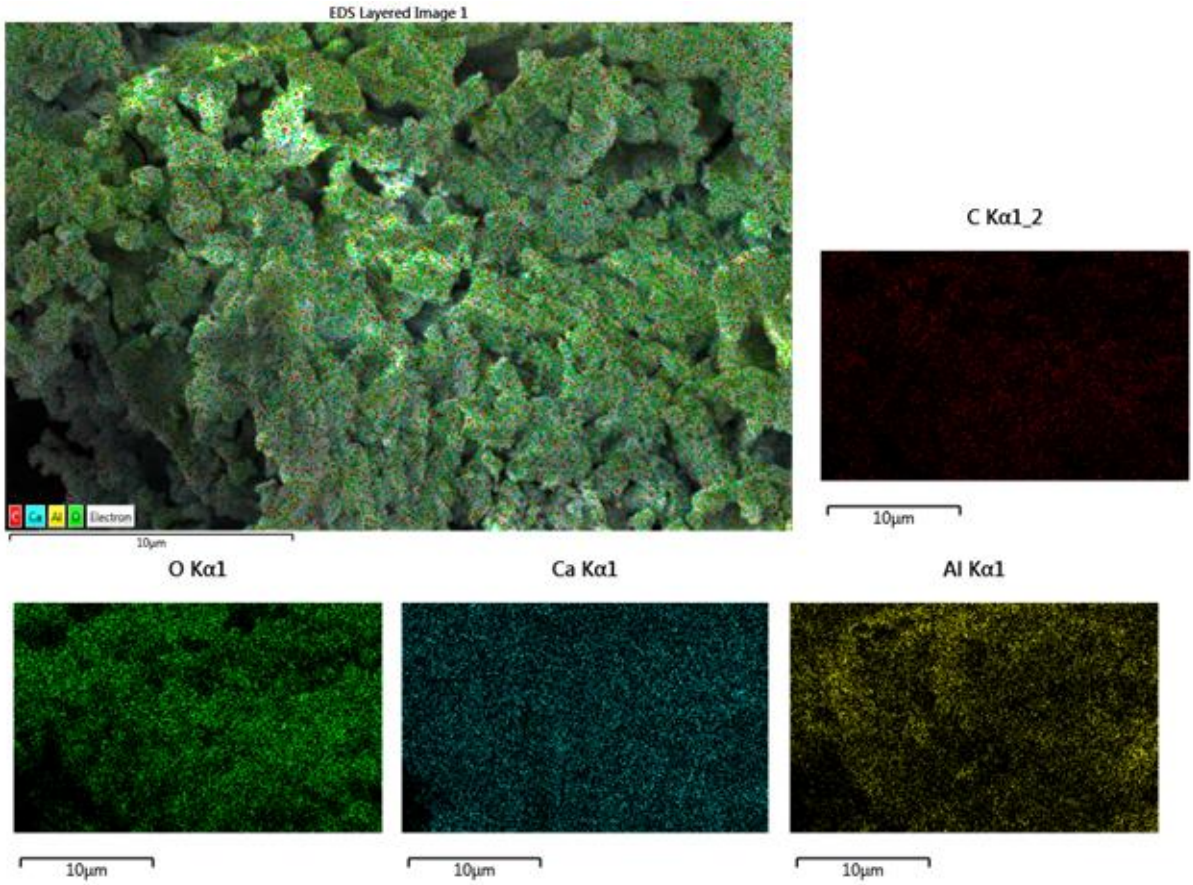

Figure 4.15: Chemical mapping of 30%Al_2O_3/CaO catalyst.

Source: Field work, 2022.

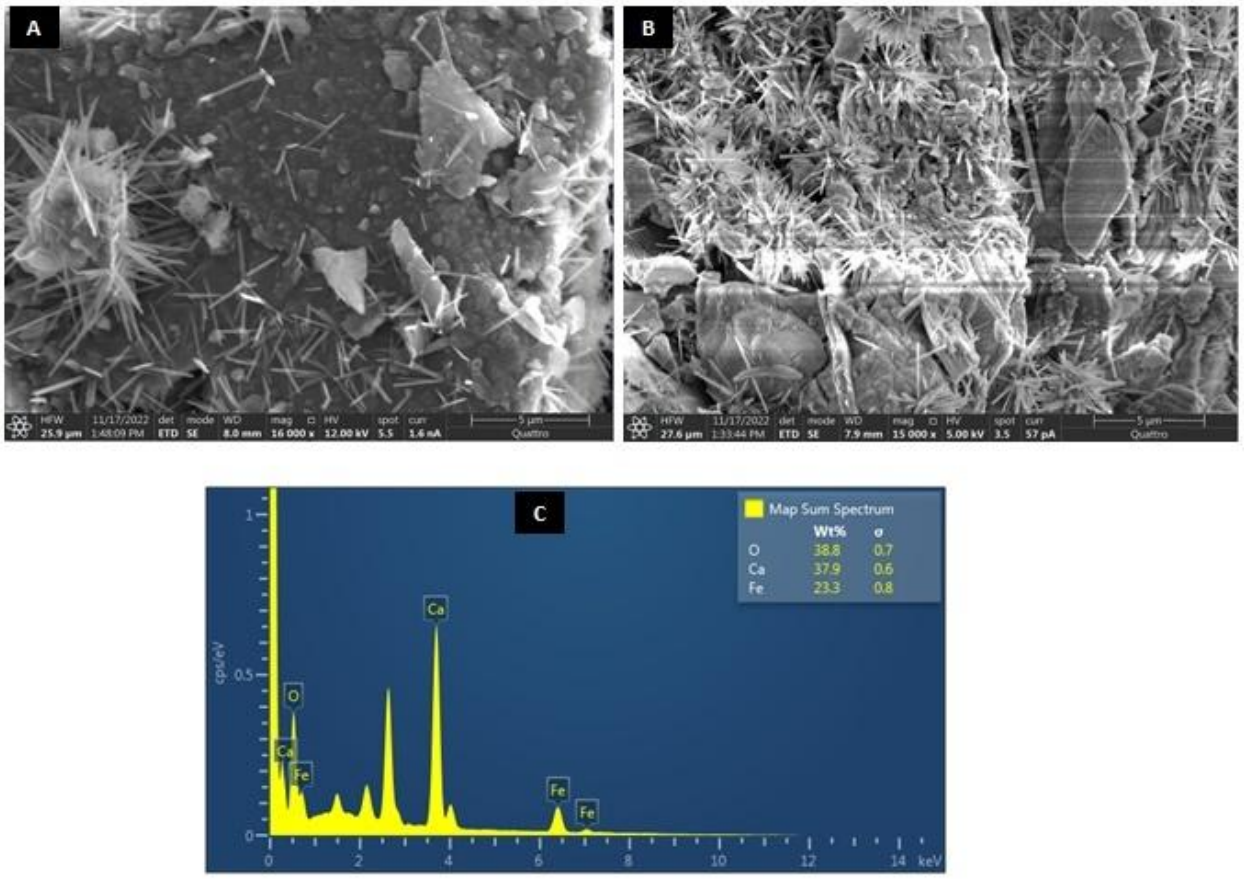

Figure 4.16: SEM micrographs of 30%Fe_2O_3/CaO at (a) 30,000x (b) 15,000x and (c) EDX chart of the elemental composition of catalyst.

Source: Field work, 2022.

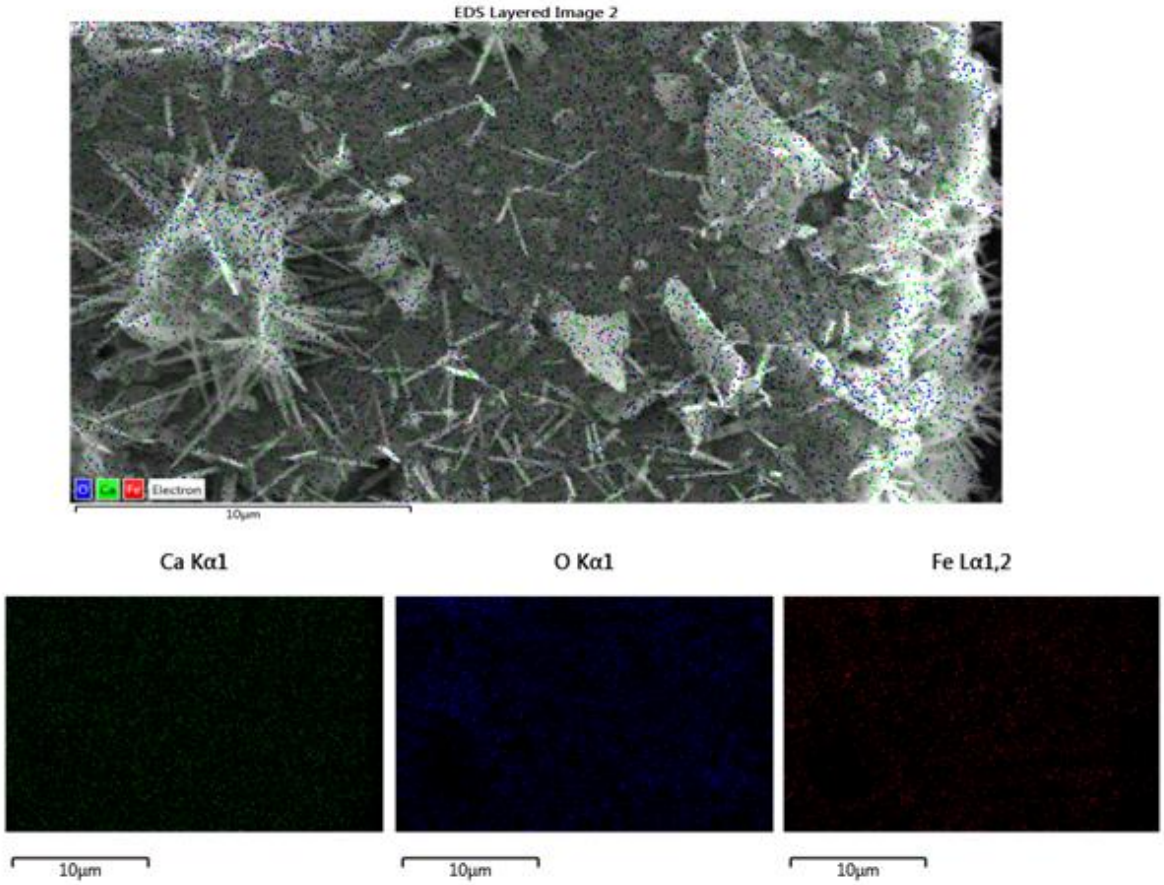

Figure 4.17: Chemical mapping of 30%Fe_2O_3/CaO catalyst.

Source: Field work, 2022.

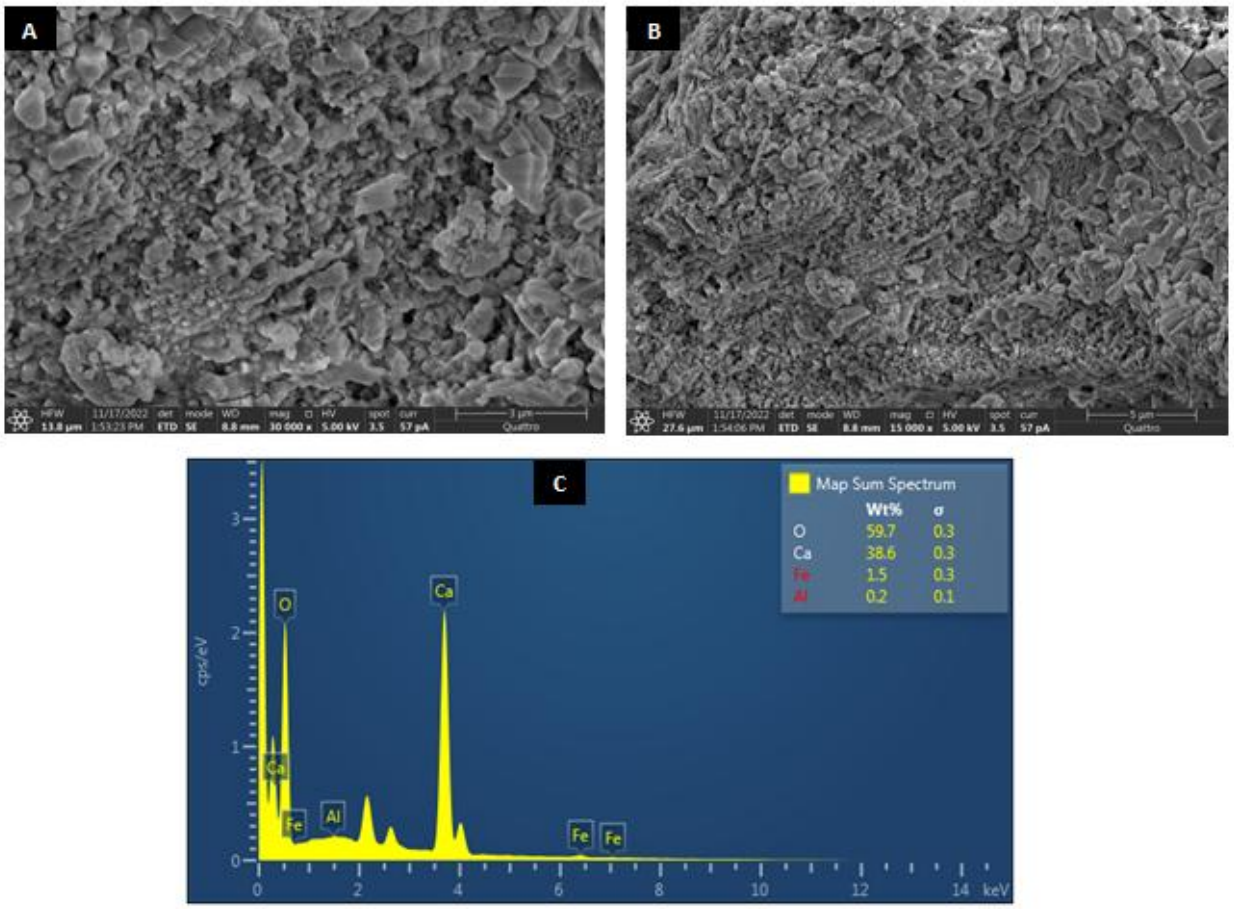

Figure 4.18: SEM micrographs of PEGylated catalyst at (a) 30,000x (b) 15,000x and (c) EDX chart the elemental composition of catalyst.

Source: Field work, 2022.

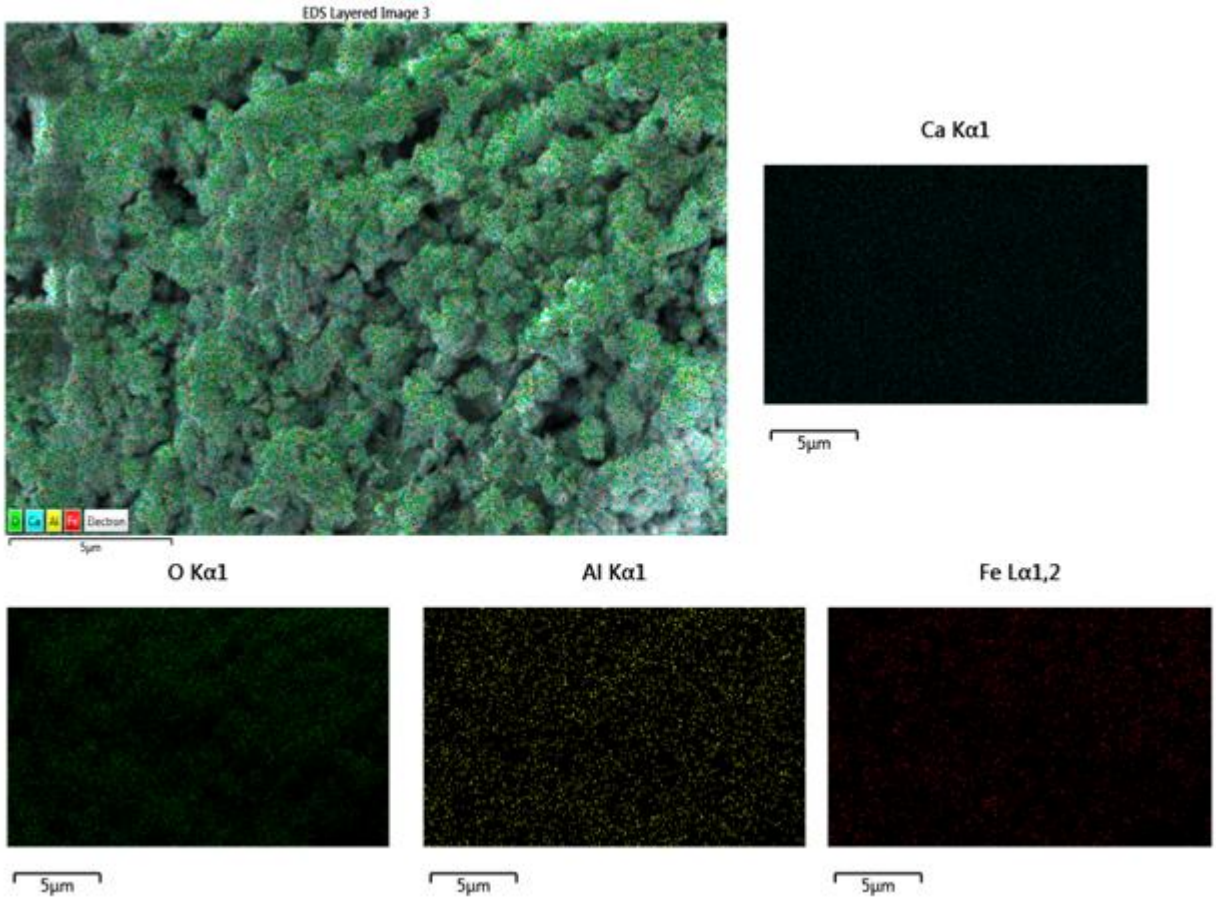

Figure 4.19: Chemical mapping of PEGylated catalyst.

Source: Field work, 2022.

Table 4.3: FAME yield obtained with different catalysts.

Experimental Run	CaO	30% Al_2O_3/CaO	30% Fe_2O_3/CaO	15% Al_2O_3/15Fe$_2O_3$CaO	PEGylated
1	92.54	82.27	76.43	91.21	94.66
2	91.81	84.32	80.22	90.72	95.66
3	93.44	89.54	86.75	94.53	96.23
4	94.43	90.01	88.33	94.89	97.97
5	93.95	89.92	90.84	96.76	95.77
6	90.11	87.32	80.11	89.01	94.72
7	91.23	87.06	84.46	90.53	93.76
8	93.79	86.99	90.33	92.43	97.11
9	90.32	87.62	82.32	91.22	93.33
10	93.22	90.52	91.22	93.38	94.65
11	90.07	89.23	88.33	90.21	92.11
12	94.22	91.11	90.66	92.98	96.22
13	95.17	90.11	90.77	93.01	97.42
14	93.33	88.22	89.08	90.33	94.53
15	91.22	89.23	90.33	92.11	96.11

Source: Field work, 2022.

Response Surface Methodology is used to optimize the transesterification reaction for the synthesis of FAME; the three factors used are (Y_1, catalyst concentration; Y_2, reaction time and Y_3, reaction temperature). To determine the coefficient of the second-order polynomial regression model for three variables, this optimization employs the Box-Behnken Design (BBD) by repeating the centre point three times. In order to achieve the best biodiesel production utilizing the transesterification reaction, 15 experimental designs were produced after inputting each factor's value in the MINITAB 19 and choosing BBD, as shown in Table 4.3. Table 4.4 also displays the yield of biodiesel produced by the transesterification reaction in actual and expected amounts. Also, a formula that may be used to forecast the biodiesel production for any given variable is found. The biofuel output equation is shown in the quadratic model equations as follows (Equations 4.1 to 4.5) based on the experimental design that has been conducted:

$$\text{CaO yield (\%)} = 101.36 + 0.405\ Y_1 - 0.254\ Y_2 - 0.0383\ Y_3 - 0.0586\ Y_1{*}\ Y_1 + 0.00198\ Y_2{*}\ Y_2 - 0.000879\ Y_3{*}\ Y_3 - 0.0152\ Y_1{*}Y_2 + 0.01651\ Y_1{*}\ Y_3 + 0.001185\ Y_2{*}Y_3$$

*R-sq = 66.34%*66.34% *R-sq (adj) = 5.76%* **Equation 4.1**

$$30\%Al_2O_3/\text{CaO yield (\%)} = 88.5Y_1 + 1.42 - 0.298\ Y_2 + 0.185\ Y_3 - 0.0896\ Y_1{*}\ Y_1 + 0.00169\ Y_2{*}\ Y_2 - 0.001661\ Y_3{*}\ Y_3 - 0.0091\ Y_1{*}Y_2 + 0.0026\ Y_1{*}\ Y_3 + 0.001353\ Y_2{*}\ Y_3$$

R-sq = 68.17% *R-sq (adj)= 10.87%* **Equation 4.2**

$$30\%Fe_2O_3/\text{CaO yield (\%)} = 79.7 + 2.91\ Y_1 - 0.221\ Y_3 + 0.096\ Y_2 - 0.146\ Y_1{*}\ Y_1 + 0.00113\ Y_3{*}\ Y_3 - 0.00055\ Y_2{*}\ Y_2 - 0.0087\ Y_1{*}\ Y_3 - 0.0060\ Y_1{*}\ Y_2 + 0.00167\ Y_3{*}\ Y_2$$

R-sq = 57.94% *R-sq (adj) = 0.00%* **Equation 4.3**

$15\%Al_2O_3/15\%Fe_2O_3/CaO = 101.96 + 1.740\ Y_1 - 0.403\ Y_2 + 0.058\ Y_3 - 0.1537\ Y_1 * Y_1 + 0.00331\ Y_2 * Y_2 - 0.001942\ Y_3 * Y_3 - 0.0292\ Y_1 * Y_2 + 0.02663\ Y_1 * Y_3 + 0.001161\ Y_2 * Y_3$

R-sq = 70.12% *R-sq (adj) = 16.33%* **Equation 4.4**

$PEGylated\ yield\ (\%) = 87.9 + 0.27\ Y_1 + 0.041\ Y_2 + 0.004\ Y_3 + 0.0069\ Y_1 * Y_1 + 0.00018\ Y_2 * Y_2 + 0.000672\ Y_3 * Y_3 + 0.0006\ Y_1 * Y_2 - 0.0052\ Y_1 * Y_3 - 0.000775\ Y_2 * Y_3$

R-sq = 42.26% *R-sq (adj) = 0.00%* **Equation 4.5**

4.4 Modeling of Biodiesel Yields

To find important variables and their interactions that have a substantial impact on FAME yield, ANOVA was used. Table 4.5 presents the ANOVA analyses findings. P-value of less than 0.0512,13 indicates the presence of a significant factor influencing FAME yield. It is clear from Table 4.5 that the quadratic model has an F-value of 1.10, indicating that it is significant. The probability that this F-value is noise-related is less than 0.01%. A significant model term is indicated by a p-value less than 0.05. In the meantime, the model's suitability is evaluated using the lack of fit. A p-value > 0.05 indicates that the lack of fit is not statistically significant. The negligible lack of fit proves that the model is plausible and reliable[13].

Table 4.4: Results and experimental plans for transesterification reaction with BBD in the manufacturing of biodiesel

Nanocatalysts	Y_1(wt %)	Y_2(min)	Y_3(°C)	Yield (%)		
				Actual	Predicted	Residual
CaO	1.0	90	48.1818	95.87	95.59	0.28
30% Al_2O_3/SS	7.0	40	77.2222	91.53	92.19	-0.66
30% Fe_2O_3/SS	9.1818	40	99.0909	94.03	95.36	-1.33
15% Al_2O_3/15 Fe_2O_3/SS	10.0	40	95.9191	95.91	99.14	-3.23
PEGylated	1.0	40	120	96.11	95.89	0.22

Source: Field work, 2022.

The ANOVA for the quadratic model are presented in Table 4.5 (CaO), Table 4.9 (30%Fe_2O_3/SS) and Table 4.13 (PEGylated). The model F- value of 1.10, 0.77 and 0.41 indicates high significance of the model respectively. An F-value this large might happen owing to noise only 0.01% of the time. Additionally, "Prob > F" values less than 0.0500 show that the model terms are important[14]. It is evident from Tables 4.5 (CaO), 4.7 (30%Fe_2O_3/SS), and 4.17 (PEGylated) that all model terms (linear, square, and two-way interaction) for Y_1, Y_2, and Y_3, as well as Y_1* Y_1, Y_2* Y_2, and Y_3* Y_3, all have non - significant effect (p-values > 0.05) on FAME yield, indicating that the factors are less impactful. Additionally, the lack of fit from each of the aforementioned tables has a negligible impact (p = 0.064, 0.112, and 0.087 > 0.05), demonstrating the validity and logic of the model[15].

To analyze the actual data from the applied parameters, Table 4.6 (CaO), Table 4.10 (30%Fe_2O_3/CaO), and Table 4.14 (PEGylated) each contain a statistical model. Squared term coefficients, interactive term coefficients, constants and linear coefficients for independent variables are used to express model coefficients. After that, the model's fit can be assessed using the determination coefficient (R^2), adjusted coefficient of determination (adj-R^2), and anticipated coefficient of determination (pred-R^2). The model's R^2 value is 0.6634 for CaO, 0.5794 for 30% Fe_2O_3/SS, and 0.4226 for PEGylated, meaning that it accounts for 66.34%, 57.94%, and 42.26% of the variability in responses, respectively (experimental values). An excellent relationship between predicted and experimental response values is indicated by a high R^2 value, which means that the model is highly reliable at forecasting the FAME output. The model is appropriate because the adjusted R^2 values, which are 0.5760, 0.0000, and 0.0000, respectively, are reasonable in comparison to the predicted R^2 values, which are all 0.0000, with some of the values not having a difference of more than 0.5[16]. This demonstrates that the model is effective

and may enhance the link between processing parameters in reaction, enabling the application of the optimization model.

Table 4.11's yield of the catalyst mixture (15% $Al_2O_3/Fe_2O_3/CaO$) illustrates that the catalyst concentration (Y_1), time (Y_2), and temperature (Y_3) all have an insignificant effect ($p > 0.05$) on the yield of FAME, indicating that the factors are less important for the production of FAME. The quadratic model can also access and examine how each parameter interacts with one another. The interaction between catalyst concentration and catalyst concentration (Y_1Y_1), temperature and temperature (Y_3Y_3), and time and time (Y_2Y_2) did not have any significant effects on the yield of FAME manufacture ($p > 0.05$), respectively. The catalyst concentration and temperature (Y_1Y_3) showed a significant effect (p 0.05) in the two-way interaction, whereas the catalyst concentration and transesterification time (Y_1Y_2) and the time and temperature (Y_2Y_3) showed insignificant effects ($P > 0.05$), indicating that these factors have less of an impact on the production of biodiesel. Since the model's lack of fit was unimportant ($p = 0.283$), it was safe to infer that the model accurately represents the data. This demonstrates that the primary transesterification reaction variables that influence the formation of FAME yield are Y_1Y_1, Y_3Y_3, and Y_1Y_3.

The most significant interaction between catalyst concentration and time will be produced by optimization. Due to the fact that certain variables have a significant or deciding impact, the two-way interaction models and square are well-designed. This demonstrates that the model is capable of accurately predicting any set of independent variables that fall within the scope of this study and can serve as a guide for future research on the production of FAME via the transesterification reaction.

The actual data from the applied parameters can be evaluated using the statistical model in Table 4.12. After that, the model's fit can be assessed using the coefficient of determination (R^2), adjusted coefficient of determination (adj-R^2), and anticipated coefficient of determination (pred-R_2). This model is typically deemed appropriate when the value is p 0.05, there is no lack of fit ($p > 0.05$), and $R^2 > 0.9$. This is done by maximizing the adjusted R^2 and the projected R^2 [7]. The model obtained from Table 4.4 has an R^2 value of 0.7012, which means that it accounts for 70.12% of the variability in responses (experimental values). An excellent correlation between experimental and predicted response values is indicated by a high R^2 value, which means that the model is highly reliable at forecasting the FAME output. The model is appropriate since the adjusted R^2 value, which is 0.1633, is within acceptable bounds with a predicted R^2 value of 0.0000, where the value does not differ by more than 0.1. This demonstrates that the model is effective and may enhance the link between process parameters in response, enabling the application of the optimization model.

ANOVA was used to investigate the model's validity and the importance of the variables and their interactions; the findings are shown in Table 4.7 (30%Al_2O_3/CaO). Except for temperature (Y_3), which has a substantial impact on biodiesel yield (p-value 0.05), none of the model terms are significant ($p > 0.05$). The model is rational and valid because the lack of fit is small ($p = 0.23$) and the effect is not substantial[17]. The derived model has an R^2 value of 0.6817, which means that it accounts for 68.17% of the variability in responses (experimental values). The modified R^2 value, which is 0.1087, is reasonable in comparison to the anticipated R^2 values, which are 0.0000, and some of the values do not differ by more than 0.1, proving that the model is appropriate[16]. This implies that the model is effective and may enhance the link between process parameters in response, enabling the application of the optimization model.

Table 4.5: ANOVA of quadratic model to evaluate relevant variables using BBD (SS)

Source of variation	DF	Adj SS	Adj MS	F-Value	P-Value	
Model	9	26.3030	2.9226	1.10	0.486	**
Linear	3	11.2420	3.7473	1.40	0.344	**
Y_1	1	6.1403	6.1403	2.30	0.190	**
Y_2	1	2.2705	2.2705	0.85	0.399	**
Y_3	1	4.7435	4.7435	1.78	0.240	**
Square	3	6.0299	2.0100	0.75	0.566	**
Y_1* Y_1	1	3.3009	3.3009	1.24	0.317	**
Y_2* Y_2	1	3.1951	3.1951	1.20	0.324	**
Y_3* Y_3	1	4.9120	4.9120	1.84	0.233	**
2-Way Interaction	3	17.3370	5.7790	2.17	0.211	**
Y_1* Y_2	1	5.7961	5.7961	2.17	0.201	**
Y_1* Y_3	1	11.4824	11.4824	4.30	0.093	**
Y_2* Y_3	1	8.1926	8.1926	3.07	0.140	**
Error	5	13.3436	2.6687			
Lack-of-Fit	4	13.3194	3.3299	137.60	0.064	**
Pure Error	1	0.0242	0.0242			
Total	14	39.6466				

Source: Field work, 2022.

Table 4.6: ANOVA summary and fitting statistics (SS)

Fit statistics	Result
S	1.90499
R^2	0.6634
Adjusted-R^2	0.5760
Predicted-R^2	0.0000

Source: Field work, 2022.

Table 4.7: ANOVA of quadratic model to evaluate relevant variables using BBD (30%Al_2O_3/CaO)

Source of variations	DF	Sum of squares	Mean square	F-Value	P-Value	
Model	9	55.7125	6.1903	1.19	0.447	**
Linear	3	49.5375	16.5125	3.17	0.123	**
Y_1	1	0.4061	0.4061	0.08	0.791	**
Y_2	1	0.0692	0.0692	0.01	0.913	**
Y_3	1	46.2471	46.2471	8.89	0.031	*
Square	3	19.3035	6.4345	1.24	0.389	**
Y_1* Y_1	1	7.7341	7.7341	1.49	0.277	**
Y_2* Y_2	1	2.3281	2.3281	0.45	0.533	**
Y_3* Y_3	1	17.5232	17.5232	3.37	0.126	**
2-Way Interaction	3	12.5610	4.1870	0.80	0.543	**
Y_1* Y_2	1	2.0673	2.0673	0.40	0.556	**
Y_1.* Y_3	1	0.2861	0.2861	0.05	0.824	**
Y_2* Y_3	1	10.6720	10.6720	2.05	0.212	**
Error	5	26.0174	5.2035			
Lack-of-Fit	4	25.5372	6.3843	13.30	0.203	**
Pure Error	1	0.4802	0.4802			
Total	14	81.7300				

Source: Field work, 2022.

Table 4.8: ANOVA summary and fitting statistics (30%Al_2O_3/CaO)

Fit statistics	Result
S	2.28112
R^2	68.17%
Adjusted-R^2	10.87%
Predicted-R^2	0.00%

Source: Field work, 2022.

Table 4.9: ANOVA of quadratic model to evaluate relevant variables using BBD ($30\%Fe_2O_3/CaO$)

Source of variations	DF	Adj SS	Adj MS	F-Value	P-Value	
Model	9	186.707	20.745	0.77	0.658	**
Linear	3	130.659	43.553	1.61	0.300	**
Y_1	1	13.299	13.299	0.49	0.515	**
Y_3	1	0.047	0.047	0.00	0.968	**
Y_2	1	111.503	111.503	4.11	0.098	**
Square	3	35.634	11.878	0.44	0.736	**
Y_1* Y_1	1	31.659	31.659	1.17	0.329	**
Y_3* Y_3	1	1.514	1.514	0.06	0.823	**
Y_2* Y_2	1	3.767	3.767	0.14	0.725	**
2-Way Interaction	3	33.913	11.304	0.42	0.749	**
Y_1* Y_3	1	2.978	2.978	0.11	0.754	**
Y_1* Y_2	1	4.618	4.618	0.17	0.697	**
Y_3* Y_2	1	14.806	14.806	0.55	0.493	**
Error	5	135.531	27.106			
Lack-of-Fit	3	125.254	41.751	8.13	0.112	**
Pure Error	2	10.276	5.138			
Total	14	322.238				

Source: Field work, 2022.

Table 4.10: ANOVA summary and fitting statistics ($30\%Fe_2O_3/CaO$)

Fit statistics	Result
S	5.20635
R^2	57.94%
Adjusted-R^2	0.00%
Predicted-R^2	0.00%

Source: Field work, 2022.

Table 4.11: ANOVA of quadratic model to evaluate relevant variables using BBD

(15%Al_2O_3/Fe_2O_3/CaO)

Source of variations	DF	sum of squares	Mean square	F-value	p-value	
Model	9	42.5776	4.7308	1.30	0.404	**
Linear	3	15.7126	5.2375	1.44	0.335	**
Y_1	1	10.7279	10.7279	2.96	0.146	**
Y_2	1	0.1287	0.1287	0.04	0.858	**
Y_3	1	9.7107	9.7107	2.68	0.163	**
Square	3	31.4165	10.4722	2.89	0.142	**
Y_1*Y_1	1	22.7283	22.7283	6.26	0.054	*
Y_2*Y_2	1	8.9463	8.9579	2.47	0.177	**
Y_3*Y_3	1	23.9463	23.9463	6.60	0.050	*
2-Way Interaction	3	35.8119	11.9373	3.29	0.116	**
Y_1*Y_2	1	21.2708	21.2708	5.86	0.060	**
Y_1*Y_3	1	29.8604	29.8658	8.23	0.035	*
Y_2*Y_3	1	7.8658	7.8658	2.17	0.201	**
Error	5	18.1550	3.6290			
Lack-of-fit	4	17.4837	4.3709	6.61	0.283	**
Pure Error	1	0.6613	0.6613			
Total	14	60.7226				

Source: Field work, 2022.

Table 4.12: ANOVA summary and fitting statistics (15%Al_2O_3/Fe_2O_3/CaO)

Fit statistics	Result
S	1.90499
R^2	0.7012
Adjusted-R^2	0.1633
Predicted-R^2	0.0000

Source: Field work, 2022.

Table 4.13: ANOVA of quadratic model to evaluate relevant variables using BBD (PEGylated)

Source of variations	DF	Adj SS	Adj MS	F-Value	P-Value	
Model	9	18.9721	2.10801	0.41	0.886	**
Linear	3	1.1559	0.38530	0.07	0.971	**
Y_1	1	0.1809	0.18090	0.03	0.859	**
Y_2	1	0.8118	0.81182	0.16	0.709	**
Y_3	1	0.1054	0.10539	0.02	0.892	**
Square	3	5.2477	1.74924	0.34	0.800	**
Y_1* Y_1	1	0.0454	0.04539	0.01	0.929	**
Y_2* Y_2	1	0.0278	0.02783	0.01	0.944	**
Y_3* Y_3	1	2.8639	2.86385	0.55	0.491	**
2-Way Interaction	3	4.9121	1.63738	0.32	0.814	**
Y_1* Y_2	1	0.0087	0.00873	0.00	0.969	**
Y_1* Y_3	1	1.1595	1.15952	0.22	0.656	**
Y_2* Y_3	1	3.5022	3.50219	0.68	0.449	**
Error	5	25.9177	5.18353			
Lack-of-Fit	4	25.8295	6.45737	73.21	0.087	**
Pure Error	1	0.0882	0.08820			
Total	14	44.8898				

Source: Field work, 2022.

Table 4.14: ANOVA summary and fitting statistics (PEGylated)

Fit statistics	Result
S	2.27674
R^2	0.4226
Adjusted-R^2	0.0000
Predicted-R^2	0.0000

Source: Field work, 2022.

4.5 Contour Plots of FAME Yields

Minitab 19 software was used to provide graphical representations of the impacts of operational parameters (catalyst concentration, reaction time, and reaction temperature) on the yields of FAME for CaO, 30%Al_2O_3/CaO, 30%Fe_2O_3/CaO, 15%Al_2O_3/15%Fe_2O_3/CaO and PEGylated for each.

The maximum SVO biofuel yields discovered using contour plots are represented in Figures 4.20 –4.25 for various catalyst concentrations, reaction times, and reaction temperatures.

4.6 Graphical Interpretation and RSM Parameter Interaction

The major effect and interactions of various parameters on the response in the form of FAME yield produced by the transesterification of SVO with all the manufactured nanocatalyst were examined in this work using a contour plot. A contour plot represents the regression equation graphically by highlighting two parameters while keeping the other factors constant. This contour graphic was created using the quadratic model's regression Equations 4.1 to 4.5. The effects of the catalyst concentration (Y_1), time (Y_2) and temperature (Y_3), are depicted in this plot and are shown in Figures 4.20 - 4.25.

Figures 4.20A, 20B, and 4.20C show the contour plots of the calcined SS for FAME yield conversion against the Y_1Y_2, Y_3Y_2, and Y_1Y_3 variables (Figure 4.20C). Figure 4.21A, 4.21B, and 4.21C show contour plots of 30% Al_2O_3/CaO biodiesel yield conversion against each of the three Y values (Figure 4.21C). Figure 4.22A, 4.22B, and 4.22C show contour plots of 30% Fe_2O_3/CaO FAME yield conversion over Y_1Y_2, Y_2Y_3, and Y_3Y_2 (Figure 4.22B).

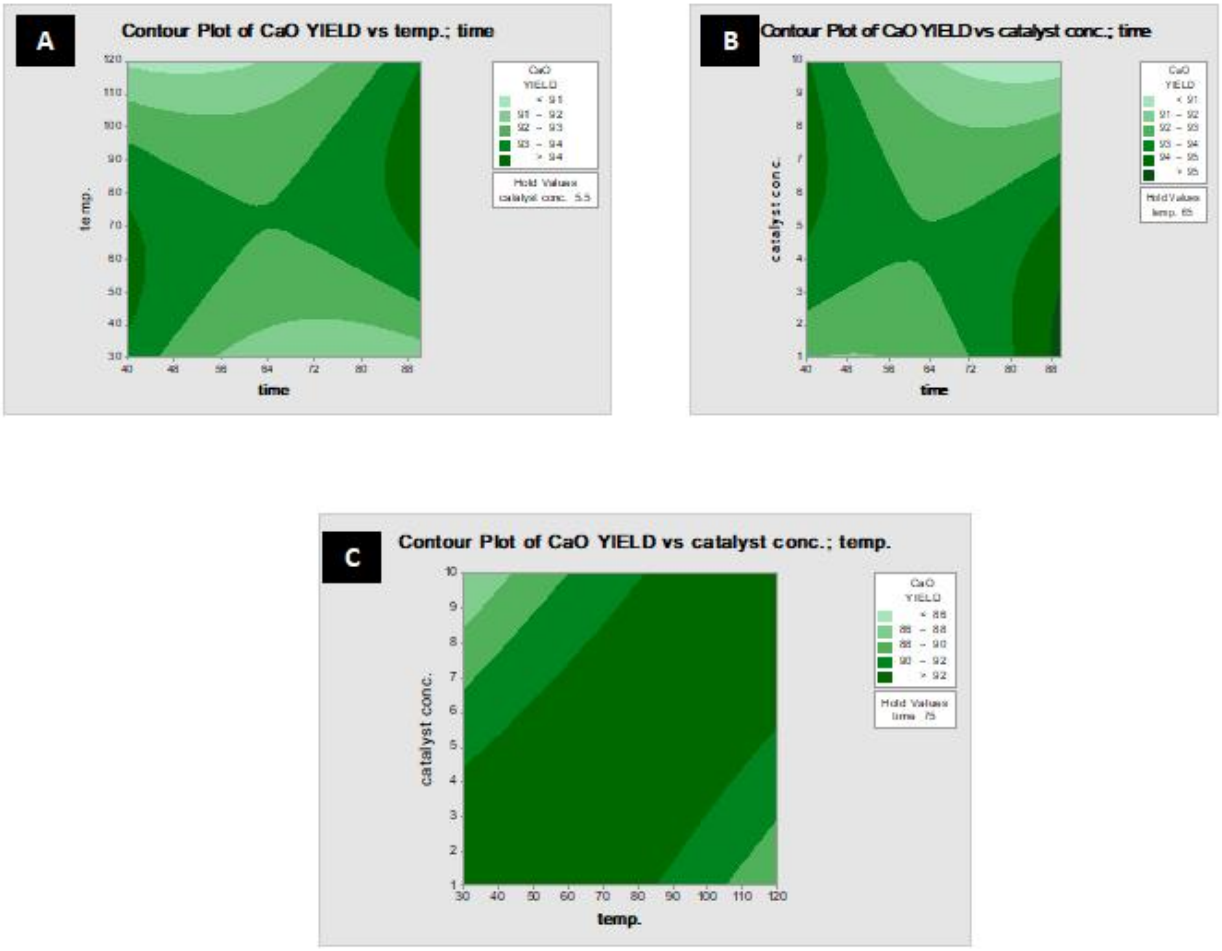

Figure 4.20: (A) Contour plots of Calcined SS Fame yield against catalyst concentration and time, at 65 °C. (B) Contour plot of CaO FAME yield against temperature and time, at 5.5 wt % catalyst concentration. (C) Contour plot of CaO FAME yield against catalyst concentration and temperature, at 75 min time.

Source: Field work, 2022.

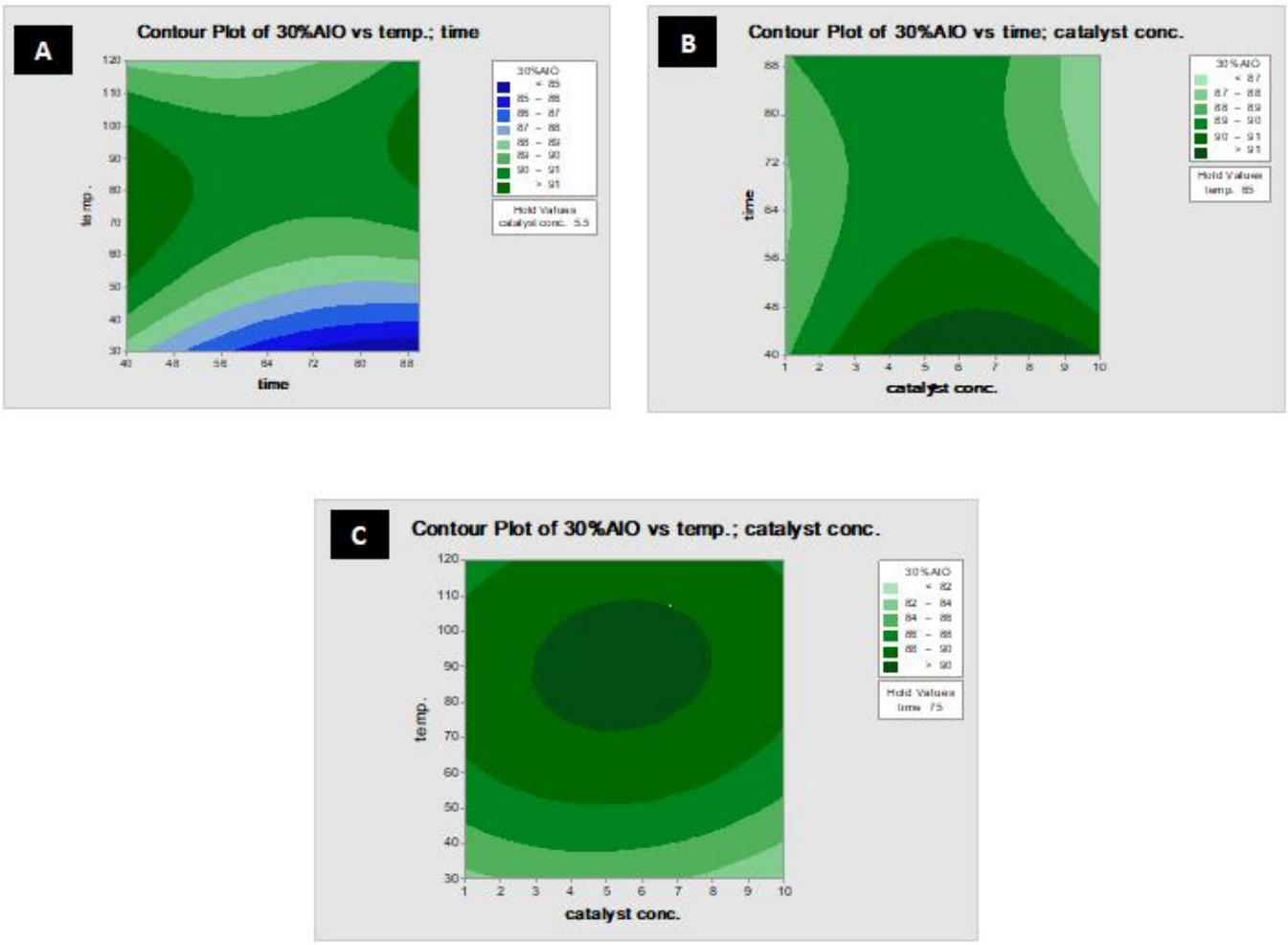

Figure 4.21: (A) Contour plot of 30%Al_2O_3/SS FAME yield against temperature and time, at 5.5 wt% catalyst concentration. (B) Contour plot of 30%Al_2O_3/CaO FAME yield against time and catalyst concentration, at 65 °C temperature. (C) Contour plot of 30%Al_2O_3/CaO FAME yield against temperature and catalyst concentration, at 75 min time.

Source: Field work, 2022.

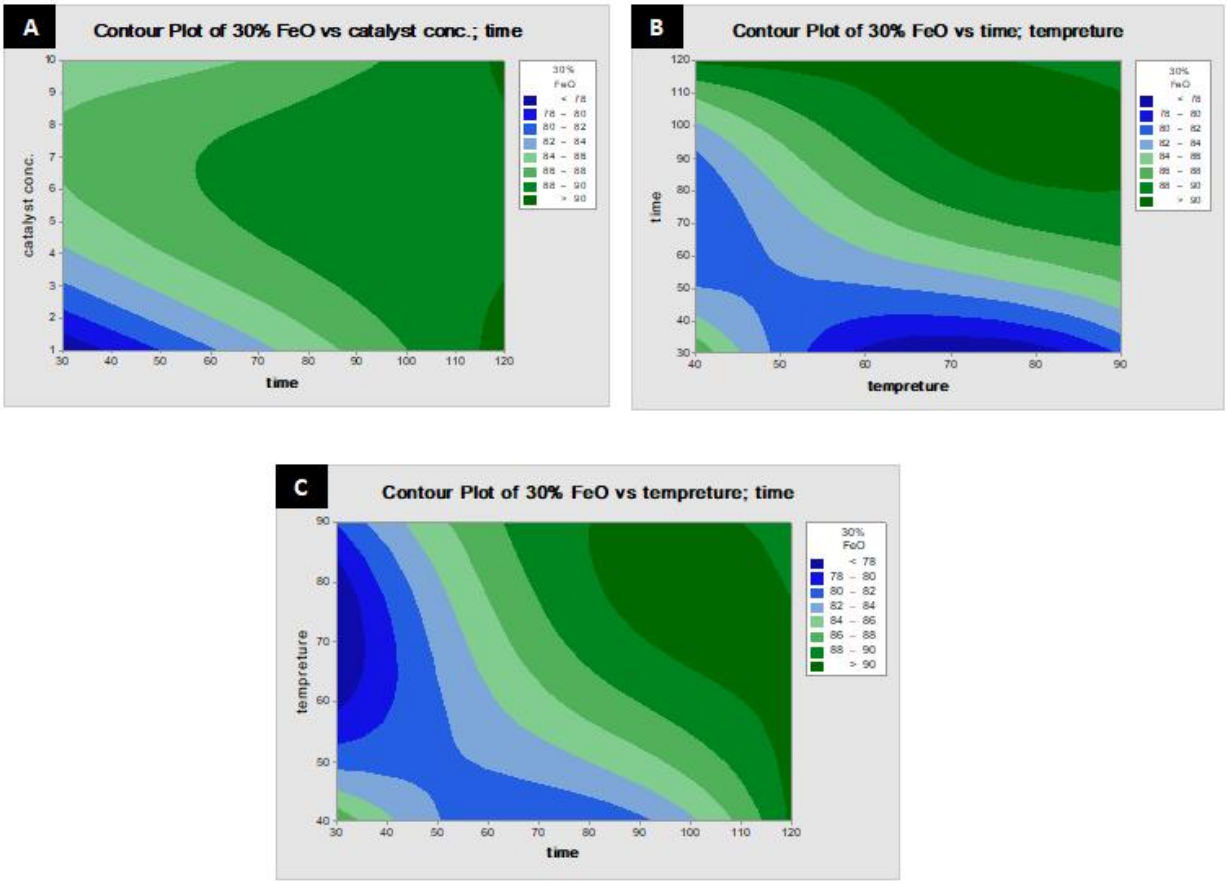

Figure 4.22: (A) Contour plot of 30%Fe_2O_3/CaO FAME yield against catalyst concentration and time. (B) Contour plot of 30%Fe_2O_3/SSFAME yield against time and temperature. (C) Contour plot of 30%Fe_2O_3/CaO FAME yield against temperature and time.

Source: Field work, 2022.

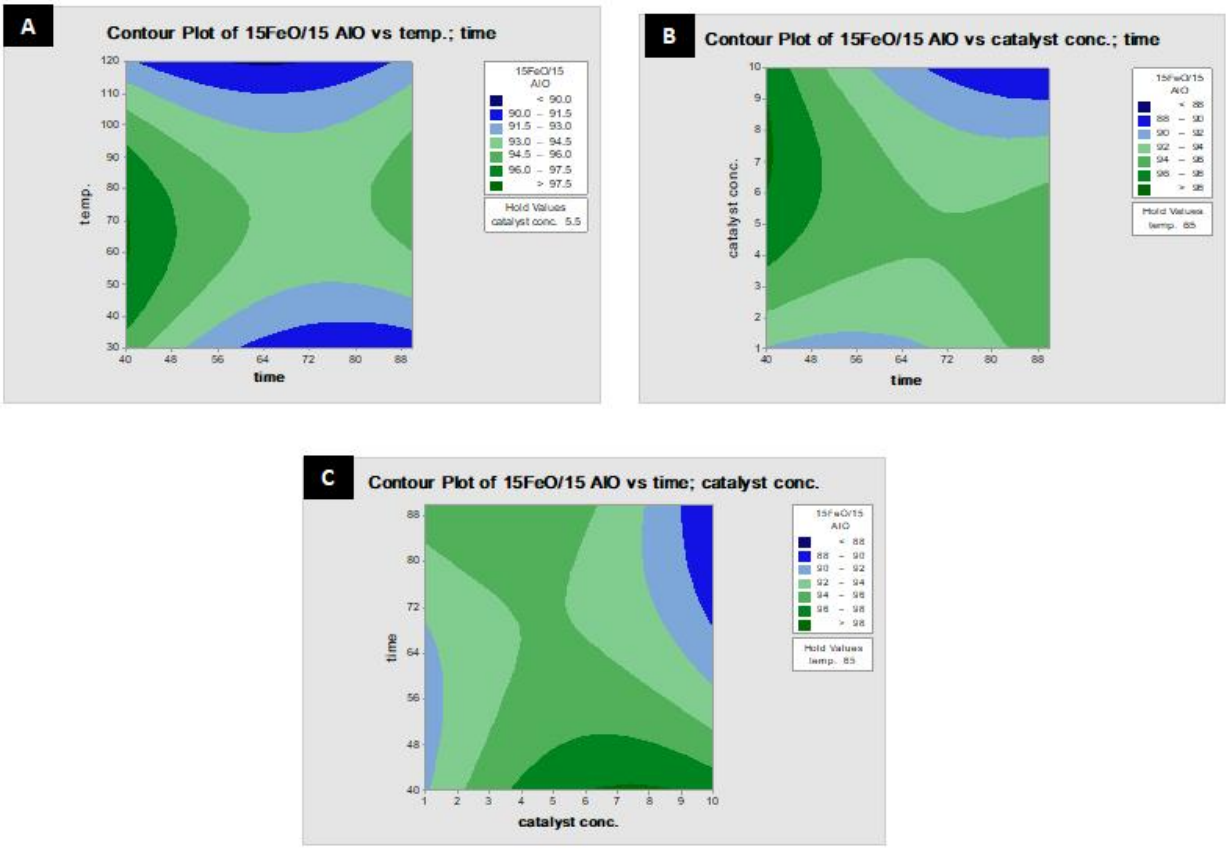

Figure 4.23: (A) Contour of 15%Al_2O_3/15%Fe_2O_3/CaO FAME yield against temperature and time, at 5.5 wt% catalyst concentrations. (B) Contour plot of 15%Al_2O_3/15%Fe_2O_3/CaO FAME yield against catalyst concentration and time, at 65 °C temperature. (C) Contour plot of 15%Al_2O_3/15%Fe_2O_3/CaO FAME yield against time and catalyst concentration, at 65 °C temperature.

Source: Field work, 2022.

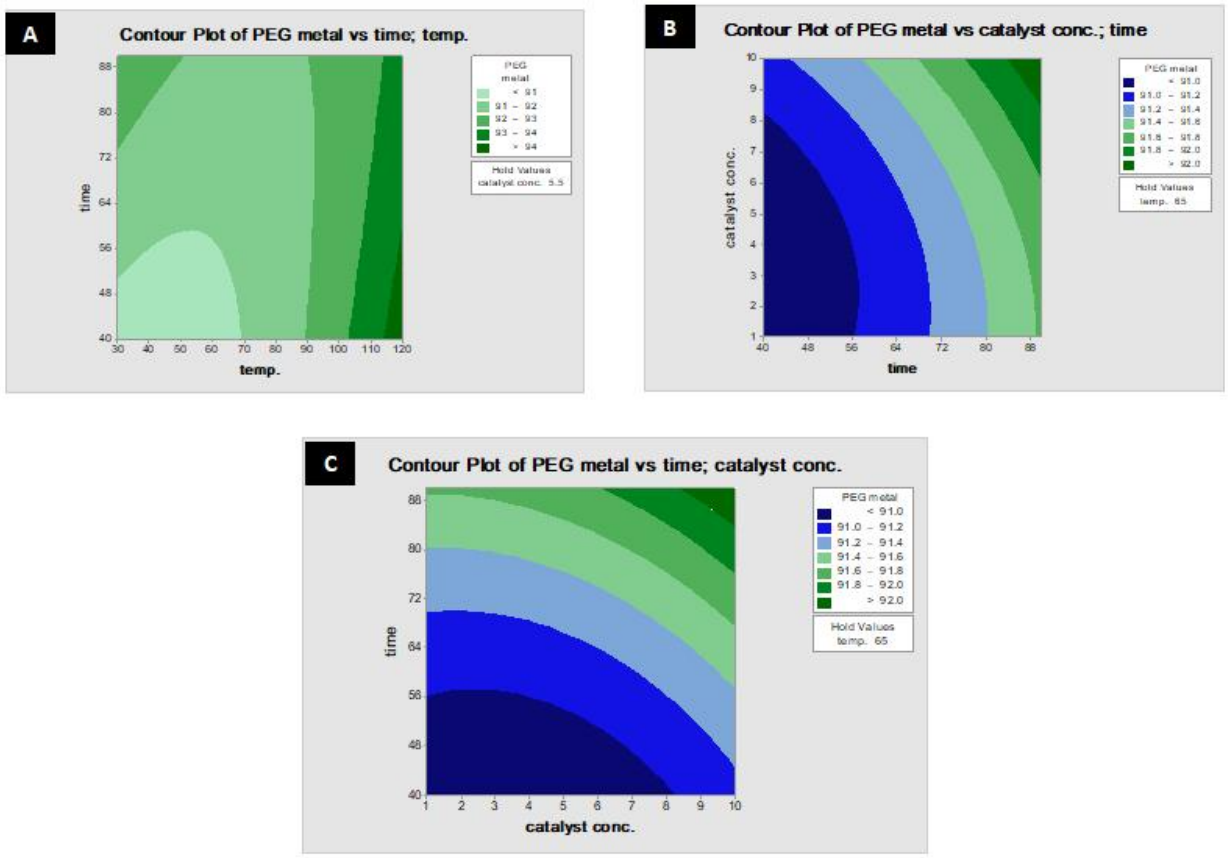

Figure 4.24: (A) Contour plot of PEGylated FAME yield against time and temperature, at 5.5 wt% catalyst concentration. (B) Contour plot of PEGylated FAME yield against catalyst concentration and time, at 65 °C temperature. (C) Contour plot of PEGylated FAME yield against time and catalyst concentration, at 65 °C temperature.

Source: Field work, 2022.

The contour plots of 15%Al_2O_3/15%Fe_2O_3/CaO FAME yield conversion were plotted against Y_3Y_2 (Figure 4.23A), Y_1Y_2 (Figure 4.23B) and Y_2Y_1 (Figure 4.23C). PEGylated FAME yield conversion was shown as a contour plot against $Y2Y_3$, Y_1Y_2, and Y_2Y_1 (Figure 4.24A, Figure 4.24B) (Figure 4.24C). One variable was kept constant while the other two were altered across their range to produce these charts.

The contour plots of the FAME yields obtained using calcined SS as nanocatalysts are shown in Figures 4.20A, B, and C, respectively. The reaction conditions were constant at 65 °C, 5.5 wt%,

and 75 minutes. With a catalyst present, the transesterification reaction will occur quickly. With a catalyst concentration of 1.17%, 1 minute of reaction can convert oil into biodiesel up to 50%[17]. Figure 4.24 shows the greatest FAME yields, which were 95% at 3 wt% catalyst loading and 88 min of reaction duration, 94% at 65 °C reaction temperature and 88 min of reaction, and 92% at 30 °C temperature (Figure 4.20C). Furthermore, where the p-value is greater than 5%, the interaction between catalyst concentration and reaction time on biodiesel production has no discernible impact. A catalyst concentration of 1% to 3% weight is used to produce biodiesel, and the process takes 88 minutes.

FAME yields increased as reaction temperature and time were raised to 65 °C and 88 min, respectively, as shown in Figure 4.20A&B. At 88 minutes of reaction time and 65 °C, the highest FAME yields were achieved at 95% and 94%. According to a research published, the transesterification reaction has produced 91% biodiesel at the optimal working temperature of 65 °C and a catalyst concentration of 1 wt%. For CaO catalysts to move transesterification reactions forward, this is the ideal circumstance[17].

According to Figure 4.21A, B, and C, the maximum biodiesel yield for 30% Al_2O_3/CaO catalyzed transesterification processes was 91% and 90% at constant reaction temperatures of 90 °C and 5.5 wt% at constant catalyst concentrations of 5.5 wt% and 75 min at constant reaction times[18]. The viscosity of fluids and surface tension are considerably reduced at higher temperatures, which facilitates cavitation. In addition to increasing the amount of liquid vapour present during the compression stage, extreme temps can also have an impact on cavitation activity[15]. There is no obvious relationship between reaction temperature and catalyst concentration and biodiesel yield. According to Figure 4.21A-C, a catalyst concentration range of 3–10% wt results in a FAME yield above 91% at reaction temperatures between 90 and

120 °C. According to a prior study, at low catalyst concentrations (3.7 wt% of CaO/MgO), raising the reaction temperature to 115.87 °C increased the biodiesel production (93.55%) because the higher temperature promoted catalyst dispersion in liquid media and improved mass transfer between the reactants[18].

Figure 4.22A, B, and C, respectively, show the contour plot of the 30% Fe_2O_3/CaO FAME yield against catalyst concentration and time, time and temperature, and temperature and time. Enhancing the transformation of oil to biodiesel is significantly influenced by the relationship between temperature and reaction time. The conversion increases as the reaction temperature rises, and the rate of the reaction likewise increases, shortening the reaction time. Because using high temps will hasten the reaction's transition to equilibrium. Conversely, a very long reaction time and a very high temperature can lower the conversion rate. This happens because as the methyl acetate evaporates and fills the reflux condenser, the contact between the oil and methyl acetate is diminished.

The contour plots all produced maximum biodiesel yield at 90% from 30%Fe_2O_3/CaO nanocatalyst. Increase in temperature 90 °C and reaction time 120 min increased the SVO biodiesel yield (Figure 4.22B&C). This is the most suitable condition for 30%Fe_2O_3/SS nanocatalysts for transesterification reaction to proceed in forward reaction. The FAME % increases due to increase in reaction time and reaction temperature; this has also been previously observed by other researchers[3,1].

At constant temperature at 65 °C and catalyst concentration of 5.5 wt% are shown in Figure 4.23A, B & C. Figure 4.23B & C show that as the catalyst concentration and reaction time were increased up to 6.5 wt% and 40 min ratio respectively, SVO FAME yields increased. Beyond

this, the yield started to decline. The higher biodiesel yields were obtained at 98% at 6.5 wt% catalyst concentrations and 40 min of reaction time. This is the most suitable condition for 15%Al_2O_3/15%Fe_2O_3/CaO catalysts for transesterification reaction to proceed in forward reaction. A similar observation was reported by researchers[19,20].

Increases in temperature (120 °C) and reaction time (40 min) in Figure 4.24A enhanced the formation of SVO FAME. At 40 minutes and 120 °C reaction temperature (5.5 wt% catalyst concentrations were constant), the highest biodiesel production of 94% was achieved. Figure 4.24B & C illustrates a drop in FAME yield of 92% for an increase in catalyst concentration of 10 wt% and a reaction period of 90 min (reaction temperature constant at 65 °C). Similar outcomes were seen while making biodiesel from soybean oil using leftover chicken eggshells[21].

4.7: Physicochemical Properties of FAME Produced

Table 4.15: Physicochemical properties of FAME produced

Properties	Test method	ASTM standard values	Calcined SS	30% Al_2O_3/ CaO	30% Fe_2O_3/CaO	15%Al_2O_3/ 15%Fe_2O_3/ CaO	PEGylated
Specific gravity at 15 °C kg/m^3	ASTM D1298	0.86-0.90	0.8003	0.8011	0.8042	0.8039	0.8006
Kinematic viscosity at 40 °C mm^2/s	ASTM D445	1.9 – 6.0	0.73	0.79	1.38	0.80	0.81
Flash point (°C)	ASTM D93	100-170	27	27	27	27	27
Moisture content (%)	ASTM D1123	0.05 max	0.03	0.03	0.02	0.02	0.02
Cloud point (°C)	ASTM D2500	-3 -12	-9	-10	-9	-7	-7
Pour point (°C)	ASTM D97	-5 -10	< -25	< -25	< -25	< -25	< -25
Acid Value (mg KOH/g)	ASTM D 974	0.5 max	0.44	0.43	0.49	0.43	0.42
Iodine value (gI_2/100g)	ASTM D93	< 120	117.11	123.73	125.61	120.53	118.35
Saponification value (mg/KOH)	ASTM D664	< 500	271.668	209.258	219.250	221.034	214.863

Source: Field work, 2022.

The physicochemical analyses which include specific gravity, kinematic viscosity, flash point, cloud point, pour point, acid value, iodine value and saponification value of the FAME were evaluated. The result of the products obtained using the following catalysts; SS, 30%Al_2O_3/CaO, 30%Fe_2O_3/CaO, 15%Al_2O_3/15%Fe_2O_3/CaO and PEGylated catalysts were compared with the ASTM value for FAME presented in Table 4.15.

Due to the volume metering nature of the fuel injection system in diesel engines, researches have demonstrated that the specific gravity of the fuel is crucial. For wasted vegetable oil methyl ester, specific gravity measurements were 0.800, 0.801, 0.804, 0.803, and 0.800 + 0.02 with corresponding densities of 800, 801, 804, 803 and 800 kg/m^3. These values are in line with significant requirements and are also reasonably close to the results of previous investigations[22].

Kinematic viscosity is a gauge of a fluid's resistance to flowing while being affected by gravity. The ability of the fuel to flow is indicated by viscosity, which has an impact on the performance of the fuel injection system, particularly at low temperatures[23]. Fuel spray atomization, flow capacity, spray penetration, and difficulty in cold weather are all impacted by biodiesel's increased kinematic viscosity. All of the nanocatalyst-produced biodiesel was found to have somewhat lower kinematic viscosity than the ASTM specifications. These values are in line with relevant criteria and are also fairly close to the results of previous investigations[24].

The temperature at which fuel will ignite when exposed to flame is known as the flash point. Because biodiesel fuels have higher flash points than fuels derived from petrochemicals, they enable safe fuel transportation and storage[25]. Low flash point values imply excessive volatility; they are also useful for categorizing fuels to lower handling and transportation risks. According to Table 4.15, none of the nanocatalyst-produced biodiesel's flash point values (130–170 °C) fall

within the ASTM range[28]. Because of the substantial risk involved in safely storing the fuel and transporting it, direct usage of the FAME produced may result in high volatility. As a result, the synthesized biodiesel can be blended with petroleum diesel or used as fuel without any further additions.

The presence of moisture in feedstock is unavoidable, and it has a substantial impact on the reaction conditions by preventing the synthesis of soap, which eventually lowers the catalyst's efficiency and lowers the yield of biofuels. The FAME generated has moisture content values that are below the ASTM requirement[26].

While the pour point is used to measure the sample's freezing point, the cloud point is the temperature upon which dissolved solids are no longer completely soluble and precipitate as a second phase, giving the fluid a hazy appearance. Table 4.15 shows that the biodiesel's cloud and pour point are both within ASTM requirements, and the outcome was identical[1]. As depicted in Table 4.15, all of the biodiesel's obtained pour point and cloud point values meet ASTM standards. The study's findings indicate that because the FAME generated met the ASTM requirement for pour and cloud point, it may be used as fuel at low temperatures[27].

The amount of potassium hydroxide needed to neutralize the amount of organic acids in one gram of fuel is used to determine the acid value[28]. One of the physiochemical traits carried over from the unprocessed oil utilized in the transesterification process to create biodiesel is acid value. High free fatty acid levels cause corrosion in fuel distribution pipes and channels when the acid value is high[28]. The FAME's produced acid values all fall within ASTM guidelines, which are also in line with published research[29]. All of the catalysts' saponification and iodine values were also determined, and they all meet ASTM standards[30].

4.8 Fatty Acid Composition of FAME

GC-MS analysis was determined to identify the composition of biodiesel for calcined SS, 30%Al_2O_3/CaO, 30% Fe_2O_3/CaO, 15%Al_2O_3/15%Fe_2O_3/CaO and PEGylated catalysts and the result of gas chromatography was shown in Figure 4.25 - 4.29. Table 4.16 to 4.20 provides a summary of the SVO biodiesel composition as determined by GC-MS with respect to retention time (RT). From the GC-MS results, it was discovered that the main FAMEs produced by calcined SS were Octanoic acid, methyl ester (R_T 9.37), Decanoic acid, methyl ester (R_T 11.59), Undecanoic acid, methyl ester (R_T 11.59), Tridecanoic acid, methyl ester (R_T 12.79), and 9,12-Octadecadienoic acid, methyl ester (R_T 13.50).

Figure 4.26 show the GC chromatograms of the FAME synthesized by 30%Al_2O_3-SS nanocatalyst. All five FAME components were identified as Dodecanoic acid, methyl ester (R_T 9.37), Undecanoic acid, 11-bromo-, methyl ester (R_T 11.55), Hexadecanoic acid, 15-methyl-, methyl ester (R_T 12.80), Chloromethyl 7-chlorododecanoate (R_T 13.54) and Hexadecanoic acid, 15-methyl-, methyl ester (R_T 13.62) as shown on Table 4.17.

The GC chromatograms of FAME synthesized by 30% Fe_2O_3/CaO is shown in Figure 4.27. The FAME components were identified as Octanoic acid, methyl ester (R_T 4.27), Decanoic acid, methyl ester (R_T 6.89), Dodecanoic acid, methyl ester (R_T 9.41) and Decanoic acid, methyl ester (R_T 11.57) as shown on Table 4.18.

From Figure 4.28, the GC-MS results of FAME synthesized by 15%Al_2O_3/15%Fe_2O_3/CaO nanocatalyst were identified as Octanoic acid, methyl ester (R_T 4.27), Decanoic acid, methyl ester(R_T 6.89), Dodecanoic acid, methyl ester (R_T 9.41) and Decanoic acid, methyl ester (R_T 11.57) on Table 4.19.

The GC chromatograms of FAME synthesized by PEGylated catalyst is shown in Figure 4.29. The FAME components were identified Octanoic acid, methyl ester ((R_T 4.28)), Decanoic acid, methyl ester (R_T 6.89), Dodecanoic acid, methyl ester (R_T 9.37), Undecanoic acid, 11-bromo-, methyl ester (R_T 11.55) and Hexadecanoic acid, 15-methyl-, methyl ester (R_T 12.79) as shown on Table 4.20. The presence of methyl esters was confirmed by the biodiesel chromatogram obtained from SVO. A chromatogram also verified the methyl ester's presence in the FAME.

4.9 FTIR of FAME

FTIR spectroscopy was used to examine the FAME produced calcined snail shell, 30%Al_2O_3/CaO, 30%Fe_2O_3/CaO, 15%Al_2O_3/15%Fe_2O_3/CaO and PEGylated catalysts. Figure 4.30 shows the spectra. Due to the presence of C=O in the samples, the peaks in the area between 1800 and 1700 cm^{-1} attributed to the stretching of C=O were seen in biodiesel. The signal at 1449 cm^{-1} in the biodiesel FTIR spectra is associated with the asymmetric stretching of -CH_3. The synthesis of biodiesel was confirmed by the absorbance peak at 1114 cm^{-1}, which was ascribed to the stretching of O-CH_3. This finding is consistent with the literature[31,32].

Table 4.16: Fatty acid composition of synthesized calcined SS

Retention time (min)	Identified compounds	Molecular formula	Molecule weight	Quality
9.37	Octanoic acid, methyl ester	$C_9H_{18}O_2$	158	45
11.55	Decanoic acid, methyl ester	$C_{11}H_{22}O_2$	186	47
11.59	Undecanoic acid, methyl ester	$C_{12}H_{24}O_2$	200	64
12.79	Tridecanoic acid, methyl ester	$C_{14}H_{28}O_2$	228	58
13.50	9,12-Octadecadienoic acid, methyl ester	$C_{19}H_{34}O_2$	294	76

Source: Field work, 2022.

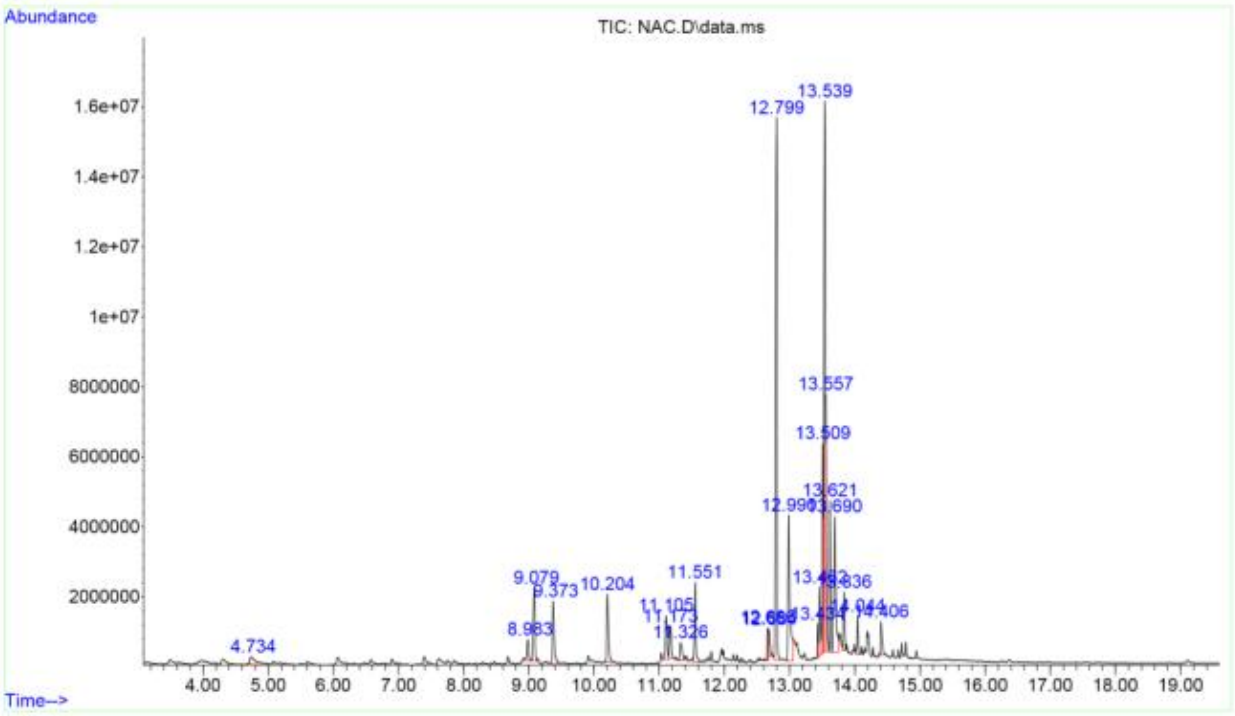

Figure 4.25: GC-MS analysis of biodiesel from spent vegetable oil synthesized by calcined SS.

Source: Field work, 2022.

Table 4.17: Biodiesel composition of synthesized 30%Al_2O_3/CaO

Retention time (min)	Identified compounds	Molecular formula	Molecule weight	Quality
9.37	Dodecanoic acid, methyl ester	$C_9H_{18}O_2$	214	91
11.55	Undecanoic acid, 11-bromo-, methyl ester	$C_{11}H_{22}O_2$	278	72
12.80	Hexadecanoic acid, 15-methyl-, methyl ester	$C_{12}H_{24}O_2$	284	87
13.54	Chloromethyl 7-chlorododecanoate	$C_{14}H_{28}O_2$	282	43
13.62	Hexadecanoic acid, 15-methyl-, methyl ester	$C_{19}H_{34}O_2$	284	86

Source: Field work, 2022.

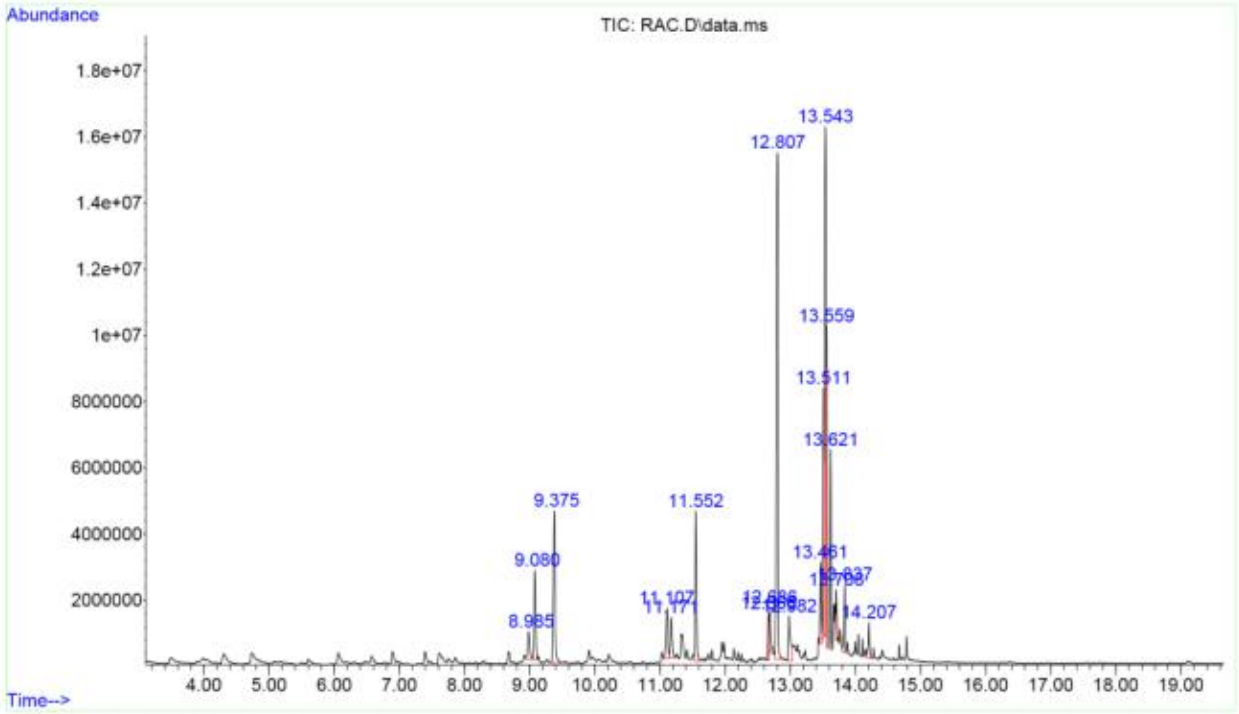

Figure 4.26: GC-MS analysis of biodiesel from spent vegetable oil synthesized by 30%Al_2O_3/CaO

Source: Field work, 2022.

Table 4.18: Biodiesel composition of synthesized 30% Fe_2O_3/CaO

Retention time (min)	Identified compounds	Molecular formula	Molecule weight	Quality
4.27	Octanoic acid, methyl ester	$C_9H_{18}O_2$	158	45
6.89	Decanoic acid, methyl ester	$C_{11}H_{22}O_2$	186	47
9.41	Dodecanoic acid, methyl ester	$C_{12}H_{24}O_2$	214	91
11.57	Decanoic acid, methyl ester	$C_{11}H_{22}O_2$	186	80

Source: Field work, 2022.

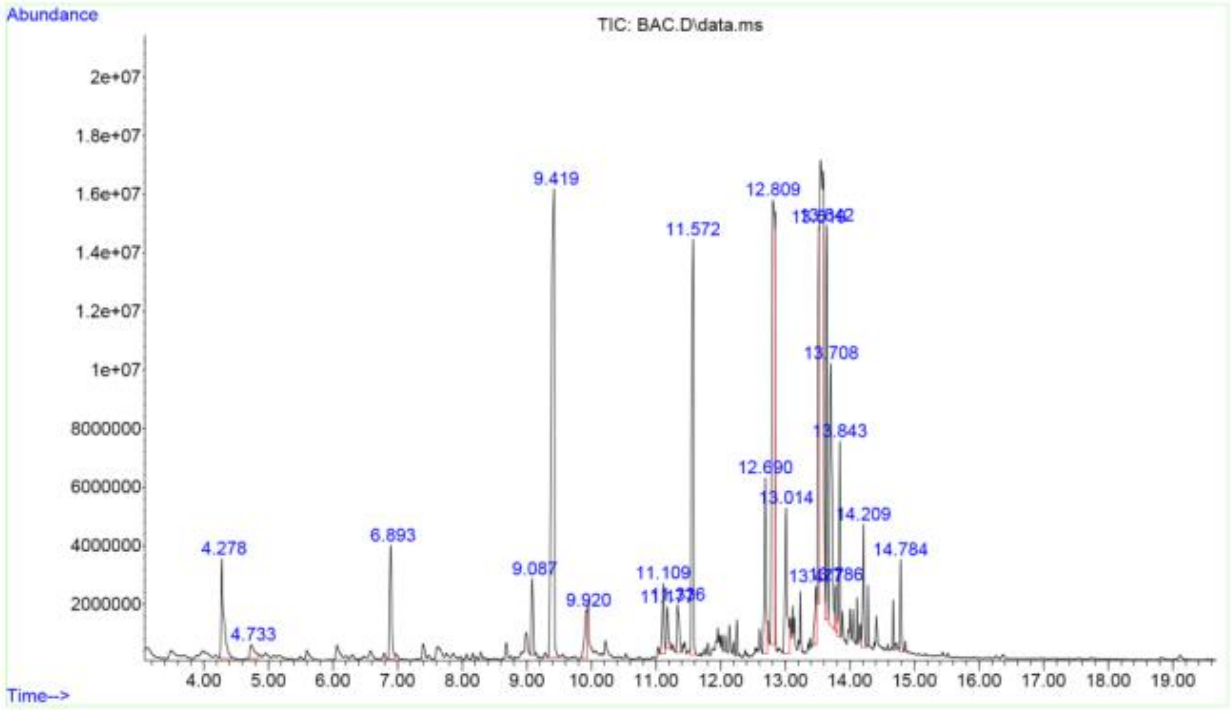

Figure 4.27: GC-MS analysis of biodiesel from spent vegetable oil synthesized by 30% Fe_2O_3/CaO.

Source: Field work, 2022.

Table 4.19: Biodiesel composition of synthesized 15%Al_2O_3/15%Fe_2O_3/CaO

Retention time (min)	Identified compounds	Molecular formula	Molecule weight	Quality
9.37	Octanoic acid, methyl ester	$C_9H_{18}O_2$	158	45
11.55	Decanoic acid, methyl ester	$C_{11}H_{22}O_2$	186	47
9.37	Undecanoic acid, methyl ester	$C_{12}H_{24}O_2$	200	64
12.79	Tridecanoic acid, methyl ester	$C_{14}H_{28}O_2$	228	58
13.50	9,12-Octadecadienoic acid, methyl ester	$C_{19}H_{34}O_2$	294	76
17.43	Pentadecanoic acid, methyl ester	$C_{16}H_{32}O_2$	256	66
20.33	Methyl tetradecanoate	$C_{15}H_{30}O_2$	242	76

Source: Field work, 2022.

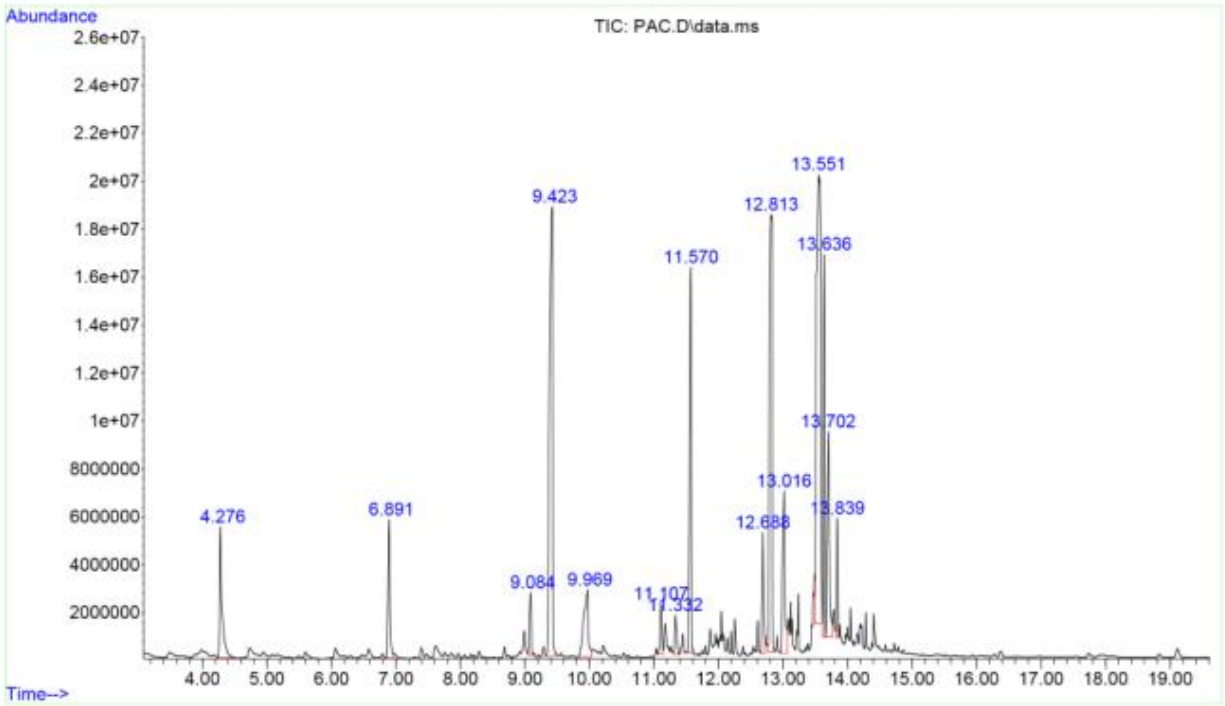

Figure 4.28: GC-MS analysis of biodiesel from spent vegetable oil synthesized by 15%Al_2O_3/15%Fe_2O_3/CaO.

Source: Field work, 2022.

Table 4.20: Biodiesel composition of synthesized PEGylated catalyst.

Retention time (min)	Identified compounds	Molecular formula	Molecule weight	Quality
4.28	Octanoic acid, methyl ester	$C_9H_{18}O_2$	158	91
6.89	Decanoic acid, methyl ester	$C_{11}H_{22}O_2$	186	97
9.37	Dodecanoic acid, methyl ester	$C_{12}H_{24}O_2$	214	91
11.55	Undecanoic acid, 11-bromo-, methyl ester	$C_{14}H_{28}O_2$	278	72
12.79	Hexadecanoic acid, 15-methyl-, methyl ester	$C_{19}H_{34}O_2$	284	87

Source: Field work, 2022.

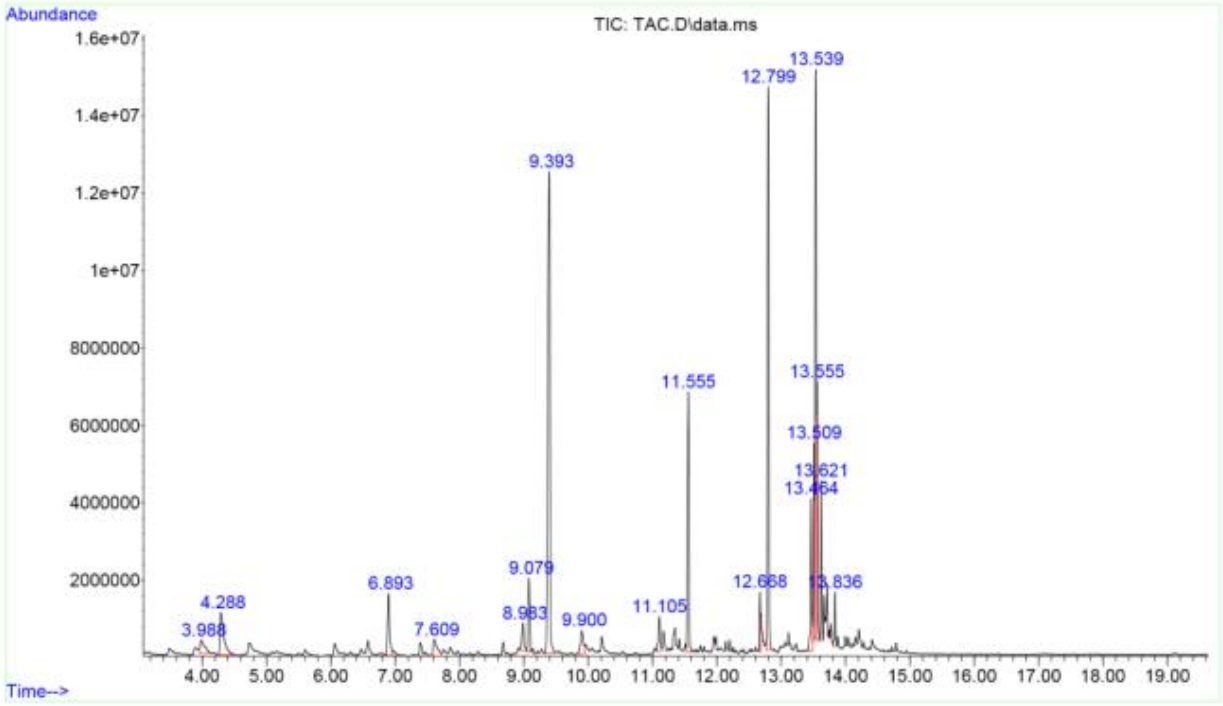

Figure 4.29: GC-MS analysis of biodiesel from spent vegetable oil synthesized by PEGylated catalyst.

Source: Field work, 2022.

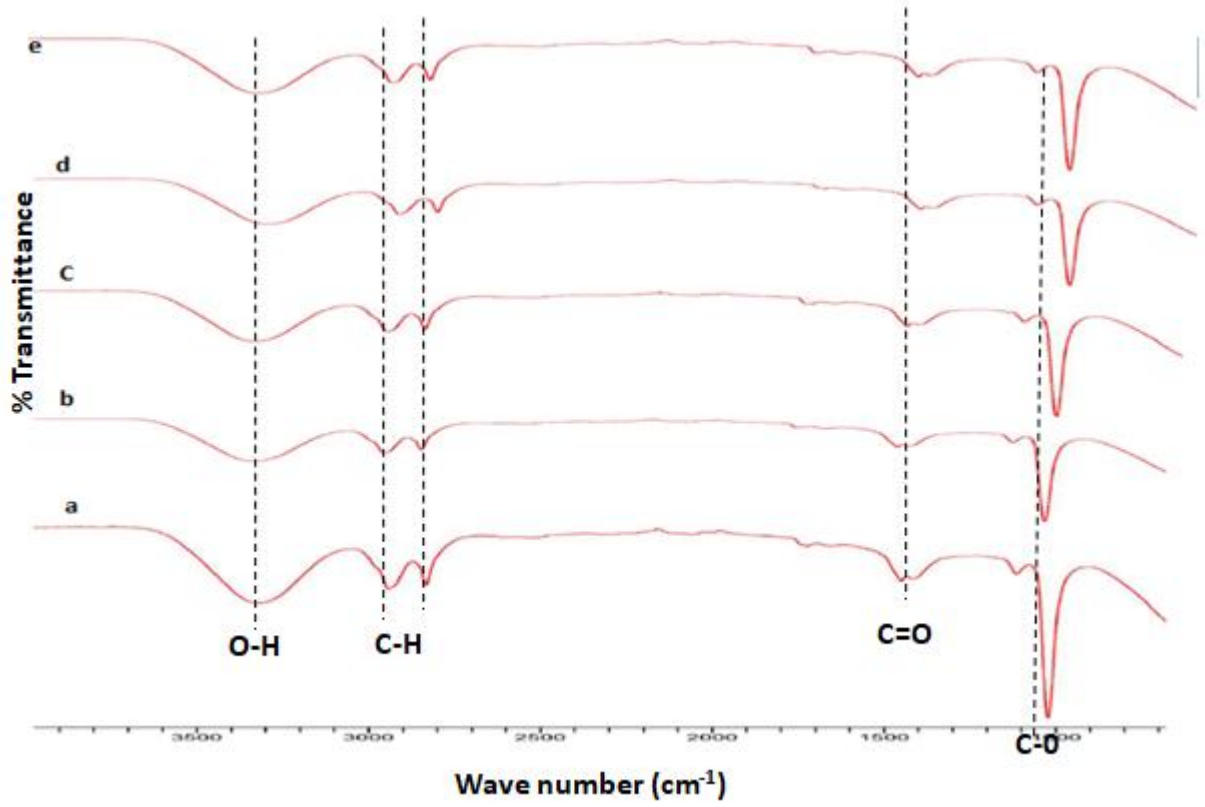

Figure 4.30: FT-IR spectra of (a) calcined SS, (b) 30%Al_2O_3/CaO, (c) 30%Fe_2O_3/CaO, (d) 15%Al_2O_3/15%Fe_2O_3/CaO and (e) PEGylated biodiesel.

Source: Field work, 2022.

Endnotes

1. N. Mansir, S. H. Teo, I. Rabiu & Y. H. Taufiq-Yap. *Effective biodiesel synthesis from waste cooking oil and biomass residue solid green catalyst.* **Chem. Eng. J.** 347, 2018, 137−144.

2. S. H Teo, A. Islam, E. S. Chan, S. Thomas Choong, N. H. Alharthi, Y. H. Taufiq-Yap & M. R. Awual. *Efficient biodiesel production from jatropha curcus using $CaSO_4/Fe_2O_3$-SiO_2 core-shell magnetic nanoparticles.* **J. Cleaner Prod.** 208, 2019, 816−826.

3. K. N. Krishnamurthy, S. N. Sridhara & C. S. Ananda Kumar. *optimization and kinetic study of biodiesel production from hydnocarpus wightiana oil and dairy waste scum using snail shell cao nano catalyst.* ***Renewable Energy*** 146: 2020, 280–296.

4. J. M Borah, A. Das, .V. Das, N. Bhuyan & D. Deka. *Transesterification of waste cooking oil for biodiesel production catalyzed by Zn substituted waste egg shell derived CaO nanocatalyst.* **Fuel,** 242, 2019, 345–354.

5. G. Enguilo, R. Romero, R. Gómez-Espinosa, A. Romero, S. Martínez & R. Natividad. *Biodiesel production from waste cooking oil catalyzed by a bifunctional catalyst*. **ACS omega,** *6*(37), 2021, 24092-24105.

6. A. A. Ayodeji, O. E. Modupe, B. Rasheed & J. M. Ayodele. *Data on CaO and eggshell catalysts used for biodiesel production.* **Data Br.** 19, 2018, 1466–1473.

7. I. B. Laskar, T. Deshmukhya, P. Bhanja, B. Paul, R. Gupta & S. Chatterjee. *Transesterification of soybean oil at room temperature using biowaste as catalyst; an experimental investigation on the effect of co-solvent on biodiesel yield.* **Renewable Energy,** 162, 2020, 98-111.

8. A. A. Otori, M. Mann, A. T. Suleiman & E. C. Egwim. *Optimization of biodiesel production from daniella oliveri oil seed using waste snail shell as heterogeneous catalyst.* **AU eJournal of Interdisciplinary Research (ISSN: 2408-1906)**, 4(1), 2019, 22-33.

9. G. Khoobbakht, K. Kheiralipour, H. Rasouli, M. Rafiee, M. Hadipour & M. Karimi. *Experimental exergy analysis of transesterification in biodiesel production.* **Energy,** 196, 2016, 117092.

10. J. Dantas, E. Leal, D.R. Cornejo, R.H.G.A. Kiminami & A.C.F.M. Costa. *Biodiesel production evaluating the use and reuse of magnetic nanocatalysts Ni0. 5Zn0. 5Fe_2O_4 synthesized in pilot-scal.,* **Arabian Journal of Chemistry** 13, 1, 2020, 3026–3042.

11. H.S. Kusuma, A. Ansori, S. Wibowo, D. Bhuana & M. Mahfud. *Optimization of transesterification process of biodiesel from nyamplung (Calophyllum Inophyllum Linn)*

using microwave with CaO catalyst. **Korean Chemical Engineering Research,** 56(4), 2018, 435–440.

12. M. Bahadi, M.F. Yusoff, J. Salimon & D. Derawi. *Optimization of response surface methodology by D-optimal design for synthesis of food-grade palm kernel based biolubricant.* **Industrial Crops and Products**, 139, 2019, Article number: 111452.

13. A. Endut, S.H. Abdullah, N.H. Hanapi, S.H. Hamid, F. Lananan, M.K. Kamarudin. *Optimization of biodiesel production by solid acid catalyst derived from coconut shell via response surface methodology.* **Int Biodeterior Biodegrad,** 124:2017, 250–7.

14. A. Ahmad, K. Alkharfy, T. Wani, M. Raish. *Application of Box-Behnken design for ultrasonic-assisted extraction of polysaccharides from Paeonia emodi.* **International Journal of Biological Macromolecules,** 72, 2015, 990–997.

15. A. Ansori, S. Wibowo, H. S. Kusuma, D. S. Bhuana & M. Mahfud. *Production of biodiesel from Nyamplung (Calophyllum inophyllum L.) using microwave with CaO catalyst from eggshell waste: optimization of transesterification process parameters.* **Open Chemistry,** 17(1), 2019, 1185–1197.

16. S. S Kashyap, P. R. Gogate & S. M. Joshi. *Ultrasound assisted synthesis of biodiesel from karanja oil by interesterification: Intensification studies and optimization using RSM.* **Ultrasonics Sonochemistry**, 50, 2019, 36–45.

17. A. M. Medeiros, E. R. Santos, S. H. Azevedo, A. A. Jesus, H. N. Oliveira & M.B. Sousa. *Chemical interesterification of cotton oil with methyl acetate assisted by ultrasound for biodiesel production.* **Brazilian Journal of Chemical Engineering,** 35(3), 2018, 1005–1018.

18. S. Niju, & M. Balajii. *Waste Sea shells for biodiesel production–current status and future perspective.* **Biochemical and Environmental Bioprocessing,** 2019, 53-86.

19. S. Douvartzides, D. Charisiou, N. Papageridis and M. Goula. *Green diesel: biomass feedstocks, production technologies, catalytic research, fuel properties and performance in compression ignition internal combustion engines.* **Energies,** 12, 2019, 809.

20. Y. Huang, F. Li, G. Bao, W. Wang & H. Wang. *Estimation of kinematic viscosity of biodiesel fuels from fatty acid methyl ester composition and temperature.* **J. Chem. Eng. Data** 65, 2020, 2476–2485.

21. J. Goli, and O. Sahu. *Development of heterogeneous alkali catalyst from chicken eggshell for biodiesel production. Renew.* **Energy,** 2018.
22. H. Mazaheri, H. Chyuan, Z. Amini, H. H. Masjuki, H. S. Chia, A. B. Irfan & T. M. Khan. *An overview of biodiesel production via calcium oxide based catalysts: current state and perspective*. **Energies 14,** no. 13, 2021, 3950.

23. H. Ong, M. Mofiju, A. Silitonga, D. Gumilang, F. Kusumo & T. Mahlia. *Physicochemical properties of biodiesel synthesised from grape seed, Philippine tung, Kesambi, and palm oils.* **Energies** 13, 2020, 1319.

24. N. F. Nasir & M. M. Hazri. *Calcium oxide from waste shells as potential green catalyst for biodiesel production.* **Research progress in mechanical and manufacturing engineering,** 1, 2020, 44-55.

25. X. Han, D. Zhang, J. Yan, S. Zhao & J. Liu. *Process development of flue gas desulphurization wastewater treatment in coal-fired power plants towards zero liquid discharge: energetic, economic and environmental analyses.* **J. Clean. Prod.** 261, 2020, 121144.

26. J. Gardy, A. Osatiashtiani, O. Céspedes, A. Hassanpour, X. Lai & A. Lee. *Applied Catalysis B: environmental A magnetically separable SO4/Fe-Al-TiO2 solid acid catalyst for biodiesel production from waste cooking oil.* **Appl. Catal. B Environ.** 234, 2018, 268–278.

27. D. Singh, D. Sharma, S. Soni, S. Sharma & D. Kumari. *Chemical compositions, properties, and standards for different generation biodiesels.* **A review. Fuel,** 253, 2019, 60-71.

28. R. Sakthivel, K. Ramesh, R. Purnachandran & P. Mohamed Shamee. *A review on the properties, performance and emission aspects of the third generation biodiesels.* **Renew. Sustain. Energy Rev**. 82, 2018, 2970-92.

29. T. Ahmad, M. Danish, P. Kale, B. Geremew, S. Adeloju, M. Nizami. *Optimization of process variables for biodiesel production by transesterification of flaxseed oil and produced biodiesel characterizations.* **Renew. Energy,** 139, 2019, 1272–1280.

30. A. Bassam, M. Abatal, O. Tzuc, L. Pedro and C. Aguilaruc. *Physical and chemical properties of biodiesel obtained from amazon Sailfin Catfish (Pterygoplichthys pardalis) biomass oil.* **J. Chem.,** 2019, 7829630.

31. A. C. Ugbede, E. E. Jumoke & M. A. Abdullahi. *Development and application of heterogeneous catalyst from snail shells for optimization of biodiesel production from moringa oleifera seed oil.* **American Journal of Chemical Engineering**, 9(1), 2021, 1-17.

32. T. Anbessie, T. Mamo and Y. Mekonnen. *Optimized biodiesel production from waste cooking oil (WCO) using calcium oxide (CaO) nano- catalyst.* **Sci. Rep.,** 9, 2019, 18982.

Chapter Five

Conclusion

5.1 Summary of Findings

In present work, five different types of eco-friendly, economical, nontoxic, biodegradable and reusable solid catalyst from SS were successfully prepared namely; SS, 30%Al_2O_3-CaO, 30% Fe_2O_3-CaO, 15%Al_2O_3-15%Fe_2O_3-CaO and PEGylated 15%Al_2O_3-15%Fe_2O_3-CaO catalysts calcined at 800 °C by wet impregnation method. Thus prepared nanocatalysts were investigated by FTIR, XRD and SEM analysis.

Given the well-known hygroscopic nature of Ca-O and the fact that calcining the SS confirmed the decomposition of $CaCO_3$ to CaO, the presence of sharp peaks in the calcined SS and other catalysts, such as the Al_2O_3-FeO doped SS and PEGylated spectrum, can be attributed to stretching vibration of hydroxides (OH). The observed positions of the diffraction peaks of the calcined SS, 30%Al_2O_3/CaO, 30%Fe_2O_3/CaO, 15%Al_2O_3-15%Fe_2O_3/CaO and PEGylated nanocatalysts are in complete agreement with the corresponding values reported for CaO (JCPDS, Card No. 028-0775), calcium ferrate (JCPDS, Card No. 032-0168), and magnetite (JCPDS, Card No.13-534) which suggests that doping metals and PEG with calcined SS have a strong effect on the crystallinity and showed the strong evidence for the formation of bimetallic and PEGylated catalysts. The morphology of prepared catalysts revealed that all catalysts contained mixture of particles with different sizes and aggregation which induced the porous agglomerate structures from SEM analysis. The synthesized catalysts were then applied in transesterification of biodiesel production.

Response surface approach and a central composite design with a three-level, three-factors were used to optimize transesterification for the synthesis of biodiesel from used vegetable oil. In order to optimize the transesterification parameters and assess the combined impacts of the three components, Box-Behnken Design (BBD) was used to construct a total of 15 tests using the three

operating parameters catalyst concentration, reaction time, and reaction temperature. The pristine (calcined SS), synthesized mixed metal oxide and PEGylated catalysts were used for the transesterification of SVO to produce FAME. The calcined SS catalyst achieved 96.17% FAME yield under the catalyst loading of 1 wt%, reaction temperature of 48.18 °C and reaction time of 90 min. 30%Al_2O_3/CaO recorded biodiesel yield of 91.21% at (7 wt% , 40 min & 77.27 °C). 30%Fe_2O_3/CaO achieved 94.13% FAME yield at (9.18wt%, 40 min & 99.09 °C) while 15%Al_2O_3/15%Fe_2O_3/CaO recorded biodiesel yield of 98.11% at (10 wt%, 40 min & 95.45 °C). PEGylated catalyst achieved FAME yield of 97.29% at (1 wt%, 40 min & 120 °C). The order of activity of the synthesized catalysts for FAME production is 15%Al_2O_3/15%Fe_2O_3/CaO > PEGylated > calcined SS > 30%Fe_2O_3/CaO > 30%Al_2O_3/CaO. 15%Al_2O_3/15%Fe_2O_3/CaO catalyst had a higher conversion rate when compared to other catalysts. The greater surface area is likely responsible for the higher conversion.

The physicochemical properties of the produced FAME show that the spent vegetable oil may be used in a diesel engine with little modification or maybe use as an additive to conventional diesel. GC-MS analysis was determined to identify the composition of FAME produced for all nanocatalysts. The chromatogram of biodiesel obtained from SVO confirmed the presence of methyl esters. FAME produced synthesized by all the catalysts were investigated by FTIR spectroscopy. The absorbance peaks and spectra confirmed the formation of biodiesel.

5.2 Conclusion

SS may be recycled into valuable products like biodiesel, which has considerable positive effects on the environment and catalytic activity. These kinds of eco-friendly waste material-derived compounds have the potential to be effective reagents and catalysts for a variety of chemical transformations in addition to the synthesis of biodiesel. The study's findings demonstrated that all synthesized catalysts made from snail shells had excellent catalytic activity, were simple to separate during the transesterification reaction, and could be used to make heterogeneous catalysts from used shell, which could lower the cost of producing biodiesel. It has been established that used vegetable oil is a possible feedstock for industrial use.

5.3 Recommendations

i. It is necessary to conduct more study on the combination of different feedstocks for the synthesis of biodiesel.
ii. Future research on catalyst regeneration and improvement of renewability is advised.
iii. The industrial uses of the biodiesel purification process, washing water, and glycerol should be the subject of further study.

5.4 Contribution to Knowledge

The thesis as presented has made specific contributions to knowledge in the following areas:

i. Biodiesel yield obtained from the transesterification of SVO using bimetallic catalyst (15%Al_2O_3/15%Fe_2O_3/CaO) is higher than the yield obtained from PEGylated 15%Al_2O_3/15%Fe_2O_3/CaO, calcined SS, 30%Fe_2O_3/CaO and 30%Al_2O_3/CaO catalyzed transesterification process, under the different reaction conditions. Bimetallic catalyst (15%Al_2O_3/15%Fe_2O_3/CaO) is thus a preferred catalyst in the transesterification of spent vegetable oil for biodiesel production.

ii. Optimum conditions at different reaction temperature, catalyst concentration and reaction time have been established.

iii. ANOVA model for the prediction of biodiesel has been introduced. This new approach will reduce biodiesel production costs, for the conventional method involves the use of complex and costly equipment.

iv. Optimization of biodiesel from Spent Vegetable Oil (SVO) has been achieved. This will assist greatly in decision/policy making on biodiesel in Nigeria. Quantifiable results from the biodiesels are a much needed baseline for future works and related applications.

5.5 Suggested Areas for Further Studies

Proper characterization of catalyst was not done completely due to the limitation of instrumental facilities such as Transmission electron microscope (TEM) and Thermogravimetric analysis (TGA). Further works on characterization of catalyst can be done.

Bibliography

Book

Hu, Y., Chen, Q., Feng, S., & Zuo, C. *Microscopic fringe projection profilometry: A review*. Opt. Lasers Eng., 106192, 135, 2020, 106192.

Kashyap, S. S., Gogate, P. R., & Joshi, S. M. *Ultrasound assisted synthesis of biodiesel from karanja oil by interesterification: Intensification studies and optimization using RSM.* Ultrasonics Sonochemistry, 50, 2019, 36–45.

Zhang, J., Sun, J., Chen, Q., & Zuo, C. *Resolution analysis in a lens-free on-chip digital holographic microscope*. IEEE Trans. Comput. Imag, 6, 2020, 697-710.

Conference Proceeding

Amirthavalli, V. & Warrier, A. R. *Production of biodiesel from waste cooking oil using MgO nanocatalyst.* **AIP Conf. Proc.,** 2115, 2019, 030609.

Ansori, A., Wibowo, S., Kusuma, H. S., Bhuana, D. S., & Mahfud, M. *Production of biodiesel from Nyamplung (Calophyllum inophyllum L.) using Microwave with CaO catalyst from eggshell waste: Optimization of transesterification process parameters.* **Open Chemistry,** 7(1), 2019, 1185–1197.

Journal

Abukhadra, M. R., Ibrahim, S. M., Yakout, S. M., El-zaidy, M. E., & Abdeltawab, A. A. *Synthesis of Na^{+} trapped bentonite/zeolite-P composite as a novel catalyst for effective production of biodiesel from palm oil; Effect of ultrasonic irradiation and mechanism.* **Energy Convers. Manag.** 196, 2019, 739–750.

Ahmad, T., Danish, M., Kale, P., Geremew, B., Adeloju, S. B., & Nizami, M. *Optimization of process variables for biodiesel production by transesterification of flaxseed oil and produced biodiesel characterizations.* **Renew. Energy,** 139, 2019, 1272–1280.

Ahmad, A., Alkharfy, K., Wani, T., & Raish, M. *Application of box-behnken design for ultrasonic-assisted extraction of polysaccharides from Paeonia emodi.* **International Journal of Biological Macromolecules,** 72, 2015, 990–997.

Alam, Z., Zhang, C., & Samali, B. *The role of viscoelastic damping on retrofitting seismic performance of asymmetric reinforced concrete structures.* **Earthq. Eng. Eng. Vib** 19, (1), 2020, 223-237.

Alam, Z., Sun, L., Zhang, C., Su, Z., & Samali, B. *Experimental and numerical investigation on the complex behaviour of the localised seismic response in a multi-storey plan-Asymmetric structure.* **Struct. Infrastruct. Eng,** 17 (1), 2021, 86-102.

Al Tawaha, A. R., & Le, V. V. *Measurement and prediction of the density and viscosity of biodiesel blends.* **Internat. J. Technol**., 9, 2018, 1015.

Ambat, I., Srivastava, V., Haapaniemi, E., & Sillanpapa, M. *Nano-magnetic potassium impregnated ceria as catalyst for the biodiesel production.* **Renew. Energy,** 39, 2019, 1428-1436.

Anbessie, T., Mamo, T., & Mekonnen, Y. *Optimized biodiesel production from waste cooking oil (WCO) using calcium oxide (CaO) nanocatalyst.* **Sci. Rep.** 9, 2019, 18982.

Ayodeji, A. A., Modupe, O. E., Rasheed, B., & Ayodele, J. M. *Data on CaO and eggshell catalysts used for biodiesel production.* **Data Br.** 19, 2018, 1466–1473.

Bahadi, M., Yusoff, M. F., Salimon, J., & Derawi, D. *Optimization of response surface methodology by D-optimal design for synthesis of food-grade palm kernel based biolubricant.* **Industrial Crops and Products,** 139, 2019, Article number: 111452, 2019.

Bano, S. *Fabrication and optimization of nanocatalyst for biodiesel production: An Overview.* **Frontiers in Energy Research 8.,** 2020.

Bassam, A., Abatal, M., Tzuc, O., Pedro, L. C., & Aguilar-uc, C. *Physical and chemical properties of biodiesel obtained from amazon sailfin catfish (Pterygoplichthyspardalis) biomass oil.* **J. Chem.,** 2019, 7829630.

Borah, J. M., Das, A., Das, V., Bhuyan, N., & Deka, D. *Transesterification of waste cooking oil for biodiesel production catalyzed by Zn substituted waste egg shell derived CaO nanocatalyst.* **Fuel,** 242, 2019, 345–354.

Cercado, A. P., Ballesteros, F. C., & Capareda, S. C. *Biodiesel from three microalgae transesterification processes using different homogenous catalysts.* **Int. J. Technol,** 4, 2018, 645-651

Changmai, B., Vanlalveni, C., Ingle, A .P., Bhagat, R., & Rokhum, S. L. *Widely used catalysts in biodiesel production: a review.* **RSC advances.** 10(68): 2020; 41625-79.

Chen, S., Hassanzadeh-Aghdam, M. K., & Ansari, R. *An analytical model for elastic modulus calculation of SiC whisker-reinforced hybrid metal matrix nanocomposite containing SiC nanoparticles.* **J. Alloys Compd.** 767, 2018, 632-641.

Chozhavendhan, S., Vijay, M., Fransila, B., Praveen, R., & Karthiga, G. *A review on influencing parameters of biodiesel production and purification processes*. **Current Res. Green Sust. Chem**., 1–2, 2020: 1–6.

Dantas, J., Leal, E., Cornejo, D., Kiminami R., & Costa, A. *Biodiesel production evaluating the use and reuse of synthesized in pilot-scale.* **Arabian J. Chem.,** 13 (1) 2020: 3026–3042.

Degfie, T. A., Mamo, T. T., & Mekonnen, Y. S. *Optimized Biodiesel production from Waste cooking oil (WCO) using calcium oxide (CaO) nano-catalyst*. **Sci. Rep**. 9, 2019, 18982.

Douvartzides, S., Charisiou, D., Papageridis, N., & Goula, M. *Green diesel: biomass feedstocks, production technologies, catalytic research, fuel properties and performance in compression ignition internal combustion engines.* **Energies,** 12, 2019: 809.

Duan, Z., Yin, Q., Li, C., Dong, L., Bai, X., Zhang C., Yang, M., Jia, D., Li, R., & Liu, Z. *Milling force and surface morphology of 45 steel under different Al_2O_3 nanofluid concentrations.* **Int. J. Adv. Manuf. Technol.,** 107 (3) 2020, 1277-1296.

Efavi, J. K., Kanbogtah, D., Apalangya, V., Nyankson, E., Tiburu, E., Dodoo-Arhin, D., Onwona-Agyeman, B., & Yaya, A. *The effect of NaOH catalyst concentration and extraction time on the yield and properties of Citrullus vulgaris seed oil as a potential biodiesel feedstock.* **S. Afr. J. Chem. Eng.,** 25, 2018, 98-102.

Endut, A., Abdullah, S. H., Hanapi, N. H., Hamid, S. H., Lananan, F., & Kamarudin, M. K. *Optimization of biodiesel production by solid acid catalyst derived from coconut shell via response surface methodology.* **Int Biodeterior Biodegrad,** 124, 2017: 250–7.

Enguilo Gonzaga, V., Romero, R., Gómez-Espinosa, R. M., Romero, A., Martínez, S. L., & Natividad, R. *Biodiesel production from waste cooking oil catalyzed by a bifunctional catalyst.* **ACS omega,** 6(37) 2021, 24092-24105.

Faisal, A., Priji, P., Unni, P., Nair, K., & Kulangara, M. *Optimization of parameters for the production of biodiesel from rubber seed oil using onsite lipase by response surface methodology*. **Biotech.,** 8 (11) 2018, 459.

Farooq, M., Ramli, A., & Naeem, A. *Biodiesel production from low FFA waste cooking oil using heterogeneous catalyst derived from chicken bones.* **Renew. Energy,** 76, 2015, 362-368

Gardy, J., Osatiashtiani, A., Céspedes, O., Hassanpour, X., & Lee, A. *Applied Catalysis B: environmental A magnetically separable SO4/Fe-Al-TiO_2 solid acid catalyst for biodiesel production from waste cooking oil*. **Appl.Catal. B Environ.,** 234, 2018, 268–278.

Gardy, J., Rehan, M., Hassanpour, A., Lai, X., & Nizami, A. *Advances in nano-catalysts based biodiesel production from non-food feedstocks*. **J. Environ. Manag**., 2019, 249, 109316.

Gardy, J., Nourafkan, E., Osatiashtiani, A., Lee, A. F., Wilson, K., Hassanpour, A., & Lai, X. *A core-shell SO4/Mg-Al-Fe3O4 catalyst for biodiesel production*. **Appl. Catal., B,** 259, 2019, 118093.

Ghalandari, A., Taghizadeh, M., & Rahmani, M. *Statistical optimization of the biodiesel production process using a magnetic core-mesoporous shell KOH/Fe3O4@g-Al2O3 nanocatalyst.* **Chem. Eng. Technol.** 42, 2019.

Giakoumis E. G., & Sarakatsanis, C. K. *Estimation of biodiesel cetane number, density, kinematic viscosity and heating values from its fatty acid weight composition.* **Fuel,** 222, 2018, 574–585.

Goli, J., & Sahu, O. *Development of heterogeneous alkali catalyst from chicken eggshell for biodiesel production. Renew.* **Energy,** 2018.

Gupta, A. R., & Rathod, V. K. *Waste cooking oil and waste chicken eggshells derived solid base catalyst for the biodiesel production: optimization and kinetics.* **Waste Manag.,** 2018, 79169-178.

Han, X., Zhang, D., Yan, J., Zhao, S., & Liu, J. *Process development of flue gas desulphurization wastewater treatment in coal-fired power plants towards zero liquid discharge: energetic, economic and environmental analyses.* **J. Clean. Prod.,** 261, 2020, 121144.

Helwani, Z., Ramli, M., Saputra, E., Bahruddin, B., Yolanda, D., Fatra, W., Idroes, G., Muslem, M., Mahlia, T. M., & Idroes, R. *Impregnation of CaO from eggshell waste with magnetite as a solid catalyst (Fe_3O_4/CaO) for transesterification of palm oil off-grade.* **Catalysts,** 10, 2020, 164.

Hossain, N., Mahlia, T. M., & Saidur, R. *Biotechnology for biofuels latest development in microalgae-biofuel production with nano-additives.* **Biotechnol. Biofuels 12, 125.,** 2019.

Huang, Y., Li, F., Bao, G., Wang, W., & Wang, H. *Estimation of kinematic viscosity of biodiesel fuels from fatty acid methyl ester composition and temperature.* **J. Chem. Eng. Data,** 65, 2020, 2476–2485.

Ibrahim, M., Adlina, A., Islam, A., Rashid, U., Ibrahim, S., & Mashuri, S. *Preparation of Na_2O supported CNTs nanocatalyst for efficient biodiesel production from waste-oil.* **Energy Convers. Manag.** 205, 2020, 112445.

Ilic, I. B. B., Miladinovic, M. R., Stamenkovic, O. S., & Veljkovic, V. B. *Application of nano CaO-based catalysts in biodiesel synthesis.* **Renew. Sust. Energy Rev.** 72, 2017, 746–760.

Jeyakumar, N., & Narayanasamy B. *Environmental effects optimization of used cooking oil methyl ester production using response surface methodology*. Energy **Sources, Part Recov., Util. Environ. Eff**., 41 (19), 2019, 2313–2325.

Junior, E. G., Perez, V. H., Reyero, I., Serrano-Lotina, A., & Justo. O. R. *Biodiesel production from heterogeneous catalysts based K_2CO_3 supported on extruded γ-Al_2O_3.* **Fuel,** 241, 2019, 311-318.

Karmakar, R., Kundu, K., & Rajor, A. *Fuel properties and emission characteristics of biodiesel produced from unused algae grown in India.* **Petrol. Sci.,** 15 (2), 2018, 385–395.

Kayode, B., & Hart, A. *An overview of transesterification methods for producing biodiesel from waste vegetable oils*. **Biofuels,** 10 (3), 2019, 419-437.

Kazemifard, S., Nayebzadeh, H., Saghatoleslami, N., & Safakish, E. *Assessment the activity of magnetic KOH/Fe_3O_4 @Al_2O_3 core–shell nanocatalyst in transesterification reaction: effect of Fe/Al ratio on structural and performance.* **Environ. Sci. Pollut. Res**., 25, 2018, 32811–32821.

Kelarijani, A. F., Zanjani, N. G., & Pirzaman, A. K. *Ultrasonic assisted trans- esterification of rapeseed oil to biodiesel using nano magnetic catalysts.* **Waste Biomass Valorization,** 11, 2020, 2613-2621.

Khan, O., Yadav, A. K., Khan, M. E., & Parvez, M. *Characterization of bioethanol obtained from Eichhornia Crassipes plant; its emission and performance analysis on CI engine.* **Energy Sources, Part A: recovery, Util., Environ. Eff**., 2021, 1–11.

Khatibi, M., Khorasheh, F., & Larimi, A. *Biodiesel production via transesterification of canola oil in the presence of Na–K doped CaO derived from calcined eggshell.* **Renewable Energy,** 163, 2021, 1626-1636.

Khoobbakht, G., Kheiralipour, K., Rasouli, H., Rafiee, M., Hadipour, M., & Karimi, M. *Experimental exergy analysis of transesterification in biodiesel production.* **Energy,** 196, 2016, 117092.

Kirubakaran, M., & Selvan, V. *A comprehensive review of low cost biodiesel production from waste chicken fat.* **Renew. Sust. Energy Rev.** 82 (1), 2018, 390-401.

Krishnamurthy, K. N., Sridhara, S. N., & Ananda Kumar, C. S. *Optimization and kinetic study of biodiesel production from Hydnocarpus Wightiana oil and dairy waste scum using snail shell cao nano catalyst.* **Renewable Energy,** 2020, 146: 280–296.

Kurniawan, E., & Perdana, F. *Biodiesel production of waste cooking oil catalyzed by cao derived from snail (achatina fulica) shell waste.* **Journal of Chemical Process and Material Technology,** 1(1), 2022, 1-7.

Kusuma, H. S., Ansori, A., Wibowo, S., Bhuana, D., & Mahfud, M. *Optimization of transesterification process of biodiesel from nyamplung (calophyllum inophyllum linn) using microwave with cao catalyst.* **Korean Chemical Engineering Research,** 56(4), 2018, 435–440.

Laskar, I. B., Rajkumari, K., Gupta, R., Chatterjee, S., Paul, B., & Rokhum, S. L. *Waste snail shell derived heterogeneous catalyst for biodiesel production by the transesterification of soybean oil.* **RSC advances**, 8(36), 2018, 20131-20142.

Laskar, I. B., Deshmukhya, T., Bhanja, P., Paul, B., Gupta, R., & Chatterjee, S. *Transesterification of soybean oil at room temperature using biowaste as catalyst; an experimental investigation on the effect of co-solvent on biodiesel yield.* **Renewable Energy,** 162, 2020, 98-111.

Li, X., Zhang, R., Zhang, X., Zhu, P., & Yao, T. *Silver-catalyzed decarboxylativeallylation of difluoroarylacetic acids with allylsulfones in water*. **Chem. Asia J,** 15 (7), 2020, 1175-1179.

Mahesh, S. E., Ramanathan, A., Begum, K. M., & Narayanan, A. *Biodiesel production from waste cooking oil using KBr impregnated CaO as catalyst.* **Energy Convers. Manage,** 2015, 91, 442-450.

Mamo, T. T. *Microwave-assisted biodiesel production from microalgae, scenedesmus species, using goat bone: made nano-catalyst.* **Appl. Biochem. Biotechnol.,** 2020.

Mansir, N., Teo, S. H., Mijan, N. A., & Taufiq-Yap, Y. H. *Efficient reaction for biodiesel manufacturing using bi-functional oxide catalyst.* **Catalysis Communications,** *149*, 2018, 106201.

Marinković, D.M, Miladinović, M.R., Avramović, J.M., Krstić, I.B., Stanković, M.J., Stamenković, O.S., Jovanović, D.M., & Veljković, V.B. *Kinetic modeling and optimization of sunflower oil methanolysis catalyzed by spherically-shaped CaO/γ-Al2O3 catalyst*. **Energy Convers. Manage.,** 163, 2018, 122−133

Marwaha, A., Dhir, A., Mahla, S., & Mohapatra, S. *An overview of solid base heterogeneous catalysts for biodiesel production.* **Catal. Rev.,** 60 (4), 2018, 594–628.

Mazaheri, H., Chyuan, H., Amini, Z., Masjuki, H. H., Chia H. S., Irfan A. B., & Khan T. M. *An overview of biodiesel production via calcium oxide based catalysts: current state and perspective*. **Energies,** 14(13), 2021, 3950.

Medeiros, A.M., Santos, E.R., Azevedo, S.H., Jesus, A.A., Oliveira, H.N., & Sousa, M.B. *Chemical interesterification of cotton oil with methyl acetate assisted by ultrasound for biodiesel production.* **Brazilian Journal of Chemical Engineering,** 35(3), 2018, 1005–1018.

Mohamed, M., Bayoumy, W., El-Faramawy, H., El-Dogdog, W., & Mohamed, A. *Novel α-Fe2O3/AlOOH(γ-Al_2O_3) nanocatalyst for efficient biodiesel production from waste oil: Kinetic and thermal studies.* **Renewable Energy,** 160, 2020, 450−464.

Mokhatr, M., Mohamed, M., & El-Faramawy, H. *An innovative nanocatalyst α Fe_2O_3/AlOOH processed from gibbsite rubbish ore for efficient biodiesel production via utilizing cottonseed waste oil.* **Fuel,** 297, 2021, 120741.

Nasir, N. F., & Hazri, M. M. *Calcium oxide from waste shells as potential green catalyst for biodiesel production.* **Research progress in mechanical and manufacturing engineering,** 1(1), 2020, 44-55.

Nguyen, H. C., Nguyen, M. L., Su, C. H., Ong, H. C., Juan, H. Y., & Wu, S. J. *Bio-derived catalysts: a current trend of catalysts used in biodiesel production.* **Catalysts,** 11(7), 2021, 812.

Niju, S., & M. Balajii. *Waste Sea shells for biodiesel production–current status and future perspective.* **Biochemical and Environmental Bioprocessing,** 2019, 53-86.

Nurun, N., Mostafizur, R., Muhammaad, A. I., Farhad, M. H., Peter, B., William, N. R., John, T., Zoran, D. R., & Richard, J. B. *Fuel characterization, engine performance, combustion and exhaust emissions with a new renewable Licella biofuel*. **Energy Convers. Manage.,** 96, 2015, 588–598.

Okonkwo, Chinwe, P., Ajiwe, V. I. E., Obiadi, M. C., Odidika, C. C., & Okwu, M. *Kinetics and Transesterification of the Oil Obtained from Cussonia bateri (Jansa Seed) as a Step in Biodiesel Production Using Natural Heterogeneous Catalyst.* **American Journal of Applied Chemistry,** 9(5): 2021, 164-171.

Ong, H. C., Mofiju, M., Silitonga, A.S., Gumilang, D., Kusumo F., & Mahlia, T. M. I. *Physicochemical properties of biodiesel synthesized from grape seed, Philippine tung, Kesambi, and palm oils.* **Energies,** 13, 2020, 1319.

Otori, A. A., Mann, M., Suleiman, A. T., & Egwim, E. C. *Synthesis of heterogeneous catalyst from waste snail shells for biodiesel production using Afzelia africana seed oil.* **Nigerian Journal of Chemical Research,** 23(1), 2018, 35-51.

Otori, A. A., Mann, M., Suleiman, A. T., & Egwim, E. C. *Optimization of biodiesel production from daniella oliveri oil seed using waste snail shell as heterogeneous catalyst.* **AU eJournal of Interdisciplinary Research (ISSN: 2408-1906),** 4(1), 2019.

Ozkan S., Puna, J. F., Gomes, J., Cabrita, T., Palmeira, J. V., & Santos, M. T. *Preliminary study on the use of biodiesel obtained from waste vegetable oils for blending with hydrotreated kerosene fossil fuel using calcium oxide (CaO) from natural waste materials as heterogeneous catalyst.* **Energies,** 12(22), 2019: 4306.

Pan, H., Li, H., Zhang, H., Wang, A., & Yang, S. *Acidic ionic liquid- functionalized mesoporous melamine-formaldehyde polymer as heterogeneous catalyst for biodiesel production.* **Fuel,** 239, 2019, 886–895.

Pandit, P. R., & Fulekar, M. H. *Egg shell waste as heterogeneous nanocatalyst for biodiesel production: optimized by response surface methodology.* **J. Environ. Manag.** 2017, 198-319-329.

Peng, Y. P., Amesho, K. T., Chen, C. E., Jhang, S. R., Chou, F. V., & Lin, Y. C. *Optimization of biodiesel production from waste cooking oil using waste eggshell as a base catalyst under a microwave heating system*. **Catalysts,** 8(2), 2018, 81.

Rahimi, T., Kahrizi, D., Feyzi, M., Ahmadvandi, H., & Mostafaei, M. *Catalytic performance of MgO /Fe_2O_3-SiO_2 core-shell magnetic nanocatalyst for biodiesel production of Camelina sativa seed oil: Optimization by RSM-CCD method.* **Ind. Crops Prod.,** 159, 2021, 113065.

Roschat, W. *The kinetic study of transesterification reaction for biodiesel production catalyzed by CaO derived from eggshells.* **Journal of Materials Science and Applied Energy**, 8(1), 2019: 358-364.

Sakthivel, R., Ramesh, K., Purnachandran, R., & Mohamed, S. P. *A review on the properties, performance and emission aspects of the third generation biodiesels.* **Renew. Sustain. Energy Rev.,** 82, 2018, 2970-92.

Singh, D., Sharma, D., Soni, S., Sharma, S., & Kumari, D. *Chemical compositions, properties, and standards for different generation biodiesels.* **A review. Fuel,** 253, 2019, 60- 71.

Sulaiman, & Fatin, N. *Transition metal oxide (NiO, CuO, ZnO)-doped calcium oxide catalysts derived from eggshells for the transesterification of refined waste cooking oil.* **RSC advances,** 11.35, 2021: 21781-21795.

Tamjidi, S., & Esmaeili, H. *Chemically modified CaO/Fe_3O_4 nanocomposite by Sodium dodecyl sulfate for Cr (III) removal from water.* **Chem. Eng. Technol.,** 42 (3), 2019, 607-616.

Teo, S. H., Islam, A., Chan, E. S., Thomas, S., Choong, S., Alharthi, N. H., Taufiq-Yap, Y. H., & Awual, M. R. *Efficient biodiesel production from jatropha curcus using $caso_4/fe_2o_3$-sio_2 core-shell magnetic nanoparticles.* **J. Cleaner Prod.** 208, 2019, 816−826.

Thangaraj, B., Solomon, P., Muniyandi B., & Ranganathan, S. *Catalysis in biodiesel production.* **Chem. Eng. Technol.,** 2019.

Trejo-Zarraga, F., Jesús, L., Chavarría-Hernandez, J., & Sotelo-Boyas, R. *Kinetics of transesterification processes for biodiesel production. Biofuels: state of development.* **Chem. Asia J.,** 2018, 149-179.

Ugbede, A. C., Jumoke, E. E., & Abdullahi, M. A. *Development and application of heterogeneous catalyst from snail shells for optimization of biodiesel production from moringa oleifera seed oil.* **American Journal of Chemical Engineering**, 9(1), 2021, 1-17.

Vinoth, A., & Raj, J. *Biodiesel production from Microalgae Nannochloropsis Oculat using heterogeneous Poly Ethylene Glycol (PEG) encapsulated $ZnOMn^{2+}$ nanocatalyst.* **Bioresource Technology,** 282, 2019: 348–352.

Wang, M., Hu, M., Li, Z., He, L., Song, Y., Jia, Q., Zhang, Z., & Du, M. *Construction of Tb-MOF-on-Fe-MOF conjugate as a novel platform for ultrasensitive detection of Carbohydrate antigen 125 and living cancer cells. Biosens.* **Bioelectron.,** 142, 2019, 111536.

Wang, A., Sudarsanam, P., Xu, Y., Zhang, H., Li, H., & Yang, S. *Functionalized magnetic nanosized materials for efficient biodiesel synthesis via acidebase/ enzyme catalysis.* **Green Chem.** 22 (10), 2020, 2977-3012.

Wei, Z., Chen, W., Wang, Z., Li, N., Zhang, P., Zhang, M., & Qiang, Q. *High-temperature persistent luminescence and visual dual-emitting optical temperature sensing in self-activated $CaNb_2O_6$: $Tb_3þ$ phosphor*. **J. Am. Ceram. Soc.,** 104 (4), 2021, 1750-1759

Zheng, J., Zhang, C., & Li, A. *Experimental investigation on the mechanical properties of curved metallic plate dampers.* **Appl. Sci**., 10(1), 2019, 269.

Bio-data

A. PERSONAL DATA

Full Names	**Shakirudeen Modupe, ABATI**
Permanent Home Address	4c, Temitope Street, Boluwaji, Ibadan, Oyo State.
E-mail Address	abatiedwin@gmail.com
Phone Number	08157070839
Date of Birth	4th June, 1994
Place of Birth	Oyo
Nationality	Nigerian
Next of kin	Mrs. Abati Adeshola

B. EDUCATION BACKGROUND

Educational Institutions Attended with Dates and Qualifications

- Lead City University, {***MSc. Industrial Chemistry***} 2021 – till date
- Moshood Abiola Polytechnic, {***HND in Chemistry***} 2016-2019
- Abraham Adesanya Polytechnic, {***ND in Science Lab. Tech.***} 2011-2013
- Achievers' Model College, Ijebu-Igbo, Ogun State
  (***Senior Secondary School Certificate***) 2005-2011
- Mercy Model School, Ijebu-Igbo, Ogun State
  (***Primary school leaving certificate***) 1996-2005

C. WORK EXPERIENCE WITH DATES

- Nigerian Bottling Company December, 2012- June, 2013
- Masterstroke Packages Limited June, 2015- June, 2016
- Federal Airports Authority of Nigeria December, 2019- October, 2020

D. PUBLICATION: Thesis and Dissertation

1. Storage Stability Analysis of Multi Biodiesel Blend with Petroleum Diesel, Kerosene and Ethanol

E. REFEREES

1. Dr. A. O. Bamisaye
   Department of Chemical Sciences
   (*Industrial Chemsitry, Chemistry Unit*)

Lead City University,

Ibadan, Oyo State.

2. Dr. O. K. Oderinde

Department of Chemical Sciences

(*Industrial Chemsitry, Chemistry Unit*)

Lead City University,

Ibadan, Oyo State.

The University Compliance Certification

This is to certify that this Thesis written by Shakirudeen ABATI with matriculation number LCU/PG/002380 in the Department of Chemical Science, Faculty of Applied Sciences, Lead City University, Ibadan, Oyo State is in full compliance with approved University format and style.

---------- ----------

Signature **Date**